THE UNFOLDED PROTEIN RESPONSE IN RELATION TO MITOCHONDRIAL BIOGENESIS IN SKELETAL MUSCLE CELLS

ZAHRA S. MESBAH MOOSAVI

A THESIS SUBMITTED TO THE FACULTY OF GRADUATE STUDIES IN PARTIAL FULFILLMENT OF THE REQUIREMENTS FOR THE DEGREE OF

MASTER OF SCIENCE

GRADUATE PROGRAM IN KINESIOLOGY AND HEALTH SCIENCE

YORK UNIVERSITY
TORONTO, ONTARIO

OCTOBER 2016

ABSTRACT

Mitochondrial biogenesis involves nuclear- and mitochondrial-derived proteins to be integrated into functional organelles. Muscle development and chronic exercise are two physiological stimuli that trigger the production of mitochondrial components to produce more mitochondria. However, the synthesis of new proteins can induce cellular stress. Thus, the unfolded protein response (UPR), which takes place in the mitochondria or the endoplasmic reticulum, ensures correct protein handling. Whether the UPR must precede mitochondrial biogenesis is unknown. We used two models of mitochondrial biogenesis, skeletal muscle differentiation and chronic exercise of muscle cells in culture, and examined UPR activation. We partially inhibited one branch of the UPR involving the protein CHOP, with either a drug (TUDCA) or gene knockdown. Our results indicate that mitochondrial biogenesis occurs independently of stress-induced CHOP, and reducing ER stress may further augment mitochondrial content.

ACKNOWLEDGEMENTS

"Whoever does not thank the one who does him a favour from among Allah's creatures has not thanked Allah either."
-Imam Ali Al-Ridha (peace be upon him)

Of course, all my thanks go to God, for nothing would be possible without His mercy. Nevertheless, this thesis would not have been complete without certain individuals in my life that I would like to acknowledge:

First and foremost, my infinite thanks and gratitude go to my loving parents who without their support and prayers I never would have gotten this far. Thank you for putting up with my absences at family gatherings and my long days at the lab. I wish I could have been around more and just say how much I really do love you. I'm sorry for making the both of you chase my car down the driveway with my breakfast every single morning and making sure I remember to feed myself when I was just too busy to care. I dedicate this thesis to you.

To my soulmate, Mehrdadam, though we were miles apart, you never failed to be by my side every step of the way and hold my hand when times seemed bleak, no matter what. I couldn't have done it without you. I love you.

To my sisters, I love you all. Laila, thanks for making my late night meals. I'll eventually learn to be just as great of a cook. Zohreh, your long-distant messages were heartwarming, but we're finally reuniting. And finally to my older sister Shima, and brother, Saman, I am sorry for not being available for you as much as I would have liked. You know how much I cherish spending time with you and the adorable munchkins. Shima, I will miss you and how you always tried sneaking into my room for a little chat. You never failed to offer your support and love, though I had none to give. I wish I could be as kind as you.

And to my best minion and loyal friend, Claudia Tran. Though we worked by each other for a short period, without your help, I probably would still be writing my thesis! Thank you for the good memories. I wish you the best!

To my lab mates, I have enjoyed my time working alongside all of you. I sincerely wish you all success!

And last, but definitely not least, to my supervisor and mentor, Dr. Hood. I would like to express my gratitude in giving me the opportunity to work alongside you. Your guidance, patience, and expertise have made me stronger as both an individual and academic. I have learned so much from you. For that, I owe this thesis to you.

TABLE OF CONTENTS

LIST OF TABLES

CHAPTER 2: MANUSCRIPT

APPENDIX B: DATA AND STATISTICAL ANALYSIS

LIST OF FIGURES

CHAPTER 1: REVIEW OF LITERATURE

CHAPTER 2: MANUSCRIPT

APPENDIX B: ADDITIONAL DATA

LIST OF ABBREVIATIONS

ADP	Adenosine diphosphate
Akt	Serine/threonine protein kinase Akt
AMP	Adenosine monophosphate
AMPK	AMP-activated protein kinase
ANOVA	Analysis of variance
AP-1	Activator protein 1
ASK-1	Active apoptosis-signaling kinase 1
ATF	Activating transcription factor
ATFS-1	Activating transcription factor associated with stress-1
ATP	Adenosine triphosphate
Bax	Bcl-2 associated X protein
Bcl-2	B-cell lymphoma 2
Bim	Bcl-2 like protein 11
BiP	Binding immunoglobulin protein
bZIP	Basic leucine zipper
C/EBP	CCAAT-enhancer binding protein
Ca^{2+}	Calcium ion
CaMK	Ca^{2+}/calmodulin-dependent protein kinase
cAMP	Cyclic AMP
CCA	Chronic contractile activity
CHOP	C/EBP homologous protein
ClpP	ATP-dependent Clp protease proteolytic subunit
ClpX	ATP-dependent Clp chaperone
ClpXP	ATP-dependent Clp protease complex
COX	Cytochrome c oxidase
CPN10	mitochondrial chaperonin 10
CRE	cAMP response element
DNA	Deoxyribonucleic acid
eIF2α (-P)	Eukaryotic translation-initiation factor-2 alpha
ER	Endoplasmic reticulum
ERAD	ER-associated degradation machinery
ERO1α	ER oxidase-1 alpha
ERSE-I/-II	ER stress response elements –I and -II
ERα	Estrogen receptor alpha
ETC	Electron transport chain
FOXO3	Forkhead box O 3
FTW	Fast-twitch white
GADD	Growth arrest and DNA damage-inducible

HAF-1	ABC (ATP Binding Cassette) transporter
IMM	Inner mitochondrial membrane
IMS	Intermembrane space
IP3R1	Inositol triphosphate receptor-1
IRE1	Inositol-requiring enzyme-1
JNK	c-jun N-terminal kinase
MAM	Mitochondrial-associated membrane
MAPK	Mitogen-activated protein kinase
Mcl-1	Myeloid cell leukemia sequence
MEF	Mouse embryonic fibroblast
Mfn2	Mitofusin-2
MHC	Myosin heavy chain
mRNA	Messenger RNA
mtDNA	Mitochondrial DNA
mtHSP60	60 kDA mitochondrial heat shock protein
mtHSP70	75 kDA mitochondrial heat shock protein
mTOR	Mammalian/mechanistic target of rapamycin
PTP	Mitochondrial permeability transition pore
MURE	UPR^{mt} response element
NAD	Nicotinamide adenine dinucleotide
NRF-1/-2	Nuclear respiratory factor-1 and -2
NUGEMPs	Nuclear genes encoding mitochondrial proteins
Nrf2	Nuclear factor (erythroid-derived 2)-like 2
OMM	Outer mitochondrial membrane
OXPHOS	Oxidative phosphorylation
PAM	Presequence translocase-associated import-motor complex
PBA	4-phenylbutrate
PDI	Protein disulfide isomerase
PERK	PKR-like ER kinase
PGC-1α	Peroxisome proliferator activator receptor (PPAR) γ coactivator 1 alpha
PKR	Protein kinase RNA-activated
PQC	Protein quality control
PUMA	p53 upregulate modulator of apoptosis
RIDD	Regulated IRE1-dependent decay
RNA	Ribonucleic acid
RNase	Endoribonuclease
ROS	Reactive oxygen species
S1P	Site-1 protease
S2P	Site-2 protease
SDS-PAGE	Sodium dodecyl sulfate polyacrylamide gel electrophoresis

Sirt3	Sirtuin-3
SR	Sarcoplasmic reticulum
Tfam	Mitochondrial transcription factor A
TIM	Translocase of the inner mitochondrial membrane
TNF	Tumor necrosis factor
TOM	Translocase of the outer mitochondrial membrane
TRAF-2	TNF receptor-associated factor 2
TUDCA	Tauroursodeoxycholic acid
UPR	Unfolded protein response
UPR^{ER}	Endoplasmic reticulum UPR
UPR^{MT}	Mitochondrial UPR
WBP1	WW binding protein 1
XBP1	X-box binding protein 1
XBP1s	Spliced XBP1

CHAPTER 1: REVIEW OF LITERATURE

1.0. Mitochondria

Early in eukaryotic evolution, mitochondria originally descended from an engulfed endosymbiotic bacterium similar to modern-day α-proteobacteria (5, 29). Mitochondria, commonly known as the "powerhouses of the cell," provides energy in the form of adenosine triphosphate (ATP) and assist in the maintenance of metabolic homeostasis (216). In addition, alternative roles in regulatory cellular function include autophagy (organelle degradation) (66, 106, 183), apoptosis (programmed cell-death) (111, 142, 213, 234), and calcium homeostasis (63, 76, 122). Being dynamic in nature, they can actively travel within the cell, divide, fuse, or form reticular structures (43). Mitochondria comprises of four compartments: 1) the outer mitochondrial membrane (OMM), 2) the inner mitochondrial membrane (IMM), 3) the intermembrane space (IMS) and 4) the matrix.

Mammalian mitochondria contain their own set of genomes which encodes a total of 13 proteins that are core components of oxidative phosphorylation (OXPHOS) (156, 240). The remaining ~99% of the 1158 proteins (29) are nuclear-encoded precursor proteins produced on cytosolic ribosomes which are then imported through the mitochondrial protein import machinery (44, 156, 177). The common entry gate of the nascent proteins is through the multi-subunit complex, the translocase of the outer membrane (TOM complex) embedded within the OMM (13, 91, 115). The OMM is permeable to small metabolites and solutes, however upon cell death, the OMM permeability increases, allowing for the release of soluble proteins that are usually retained within the IMS (113, 215, 216). The IMM which functions as the energy-transducing membrane of the mitochondria (130), consists of the electron transport chain (ETC) in which the transport of electrons along a series of complexes facilitate the production of water

and ATP (7, 130). Extended membrane invaginations, termed cristae, characterize the IMM (43, 91). The space between the IMM and OMM, termed the IMS, allows for the compartmentalization of protons necessary for the formation of an electrochemical gradient required for ATP synthesis (130). Lastly, the matrix is a protein-rich core (130) where the citric acid cycle occurs, as well as the proteolytic processing of imported hydrophilic preproteins (91).

1.1. Regulation of Mitochondrial Biogenesis in Skeletal Muscle

Basal levels of skeletal muscle have very low mitochondrial content. With a physiological stimulus, such as exercise, the plasticity of skeletal muscle allows for the expansion of the mitochondrial network (64, 84, 88). The dynamic processes involved in the growth of mitochondria in number and size via fusion, fission, and reticular formation, is termed mitochondrial biogenesis (85, 103). The exercising skeletal muscle generates action potentials to trigger Ca^{2+} release from the sarcoplasmic reticulum (SR), a specialized form of the endoplasmic reticulum (ER) found specifically in skeletal muscle. The released calcium facilitates actin and myosin cross-bridging to occur to allow muscular contraction (86).

There are four main signaling molecules triggered with continuous contractile activity: 1) intracellular calcium (Ca^{2+}) accumulation sensed by calcium/calmodulin-dependent protein kinase (CaMK) (162, 246, 248); 2) phosphorylation of p38 mitogen-activated protein kinase (MAPK) (62, 126, 247); 3) phosphorylation of AMP-activated protein kinase (AMPK) in response to alterations in adenosine diphosphate (ADP) to ATP ratio (62, 161, 245, 266); and 4) production of reactive oxygen species (ROS) (95, 118). The signal transduction pathways activate the master regulator of mitochondrial biogenesis, transcription coactivator peroxisome proliferator-activated receptor gamma (PGC-1α), along with transcription factor nuclear respiratory factor-1 and -2 (NRF-1 and NRF-2) (51, 197, 233) to transcribe nuclear genes-

encoding mitochondrial proteins (NUGEMPs) (162, 198). The mitochondrion itself has a circular mitochondrial DNA (mtDNA) transcribed by the nuclear-encoded mitochondrial transcription factor A (TFAM), and is imported via the protein import machinery of the organelle (36, 198). It is the timely and coordinated expression of nuclear and mitochondrial genomes that facilitates mitochondrial biogenesis (45, 244).

1.2. Exercise Training and Mitochondrial Biogenesis

Endurance training leads to a production of nuclear- and mitochondrial-encoded proteins that assemble into OXPHOS components of the ETC (243, 244). Endurance training can range from several minutes to hours at various intensities, consisting of repetitive, low-resistance exercise, such as running (48). An exercise regimen employing the appropriate duration, frequency, and submaximal intensity can increase mitochondrial content, usually ranging from 50 to 100% within ~6 week period, directly resulting in augmented endurance capacity (40, 56, 85). Conversely, resistance training has no impact on total content, rather, it has been found to enhance the quality of mitochondrial function or respiration, as well as morphology (100, 133, 140, 175, 212, 220, 265). To date, the signals preceding exercise-induced mitochondrial adaptations have not yet been fully elucidated. Nevertheless, endurance exercise has been recommended as a means to enhance motor coordination and quality of life in skeletal muscle diseases such as such as Parkinson's disease (37, 176, 208) and mitochondrial myopathy (101, 217).

1.3. Models of Mitochondrial Biogenesis

Mitochondrial biogenesis associated with endurance training can be stimulated using artificial modes of exercise such as electrically stimulating cells in culture or the motor nerve of an animal to induce CCA. These models have the advantage of producing large changes in

mitochondrial content within a short period (84, 128, 219). An *in vivo* experimental design would involve exercising the rodent under study based on a specified protocol and extracting the muscle for subsequent analysis (96, 173, 219). An electrical stimulator can also be used to mimic muscular contractions in animals, first introduced by Williams and coworkers (242, 244). Another powerful means of inducing mitochondrial biogenesis can be via cell culture. Cultivating and harvesting skeletal muscle cells is an effective means of studying molecular mechanisms in an isolated environment without introducing the whole-body effect variable in the experiment. Knockout animals can cause pathological conditions and may not be viable past development, in which cell culture can eliminate the pathological aspect. The following sections will discuss the two models of mitochondrial biogenesis *in vitro*.

1.3.1. Differentiation-induced Mitochondrial Biogenesis

Muscle development involves mitotically quiescent stem cells residing along the basal lamina of myofibers activated upon trauma to their surrounding environment. They begin to proliferate as myogenic progenitor cells denoted as myoblasts (201). Subsequently, myoblasts undergo myogenesis or differentiation, a process involving the fusion of progenitors into multinucleated myotubes that express contractile properties (194). Myogenesis requires an adequate energy source to meet the high demands of myogenic programming in which regulatory and biosynthetic pathways are activated. Differentiation of myoblasts to myotubes is a well-established model for mitochondrial biogenesis, as the process involves a rise in mitochondrial content (36). Interestingly, differentiation appears to depend on mitochondrial function (47). Respiration-deficient myoblasts lacking mtDNA, despite their ability to continue to proliferate, had impaired myotube formation (81). Similarly, blocking mitochondrial protein synthesis with the inhibitor chloramphenicol abrogated differentiation (68, 112). Taken together, these studies

convey the importance of functional mitochondrial biosynthetic pathways in myogenic differentiation.

During the early days of myoblast fusion, mitochondrial contents decrease as they are being cleared, in order to re-establish new mitochondrial networks that are better primed for OXPHOS and are more tightly coupled (204). Upon induction of differentiation, mitochondria undergo clearance via mitophagy, a process targeting mitochondria for degradation, prior to the formation of new mitochondria (204). Mitophagy must precede mitochondrial biogenesis in order for myogenic differentiation to occur (57, 204). Furthermore, the mitochondria found in myoblasts are metabolically different than those found in myotubes. Contrary to myoblasts, myotubes have a greater reliance on glucose oxidation than glycolysis (116, 132, 204). Upon terminal differentiation, the ETC complex subunits are augmented, indicative of increased mitochondrial content (36, 57, 132, 149, 204). In conclusion, differentiation-induced mitochondrial biogenesis is a well-established model used in cell culture.

1.3.2. CCA-induced Mitochondrial Biogenesis

An alternative model for mitochondrial biogenesis is electrically-induced chronic contractile activity (CCA) (38, 87, 244). Motor neuron activation during training can be mimicked both *in vivo* and *in vitro* via electrical stimulation. *In vivo* stimulation involves the implantation of two wire electrodes spanning the common peroneal nerve of the rodent under study to deliver electrical impulses at a fixed setting, thus, contracting the muscle of the innervated leg (46, 87, 128, 218, 219). *In vitro* stimulation of myotubes in culture incorporates a similar concept by inputting parallel platinum wires in cell plates attached to an external stimulator (28, 38). Mitochondrial adaptations in a cell culture model can be induced with 3 h stimulation per day for a total of 4 days (38, 226). The cell culture model has the advantage of

working within an isolated system where variables are under greater control without the systematic bodily influence, hence being a powerful tool in mimicking the physiological stimuli of endurance exercise.

Both models stimulate action potentials to travel along the sarcolemma of the skeletal muscle to release Ca^{2+} from the sarcoplasmic reticulum (33, 120, 128, 174, 209). The accumulation of Ca^{2+} activates Ca^{2+}-sensitive signaling pathways, namely CaMK, and thus inducing mitochondrial biogenesis (162, 246, 248). Similar to traditional exercise, CCA augments PGC-1α levels, cytochorome c oxidase (COX) activity, as well as the import of NUGEMPs into the mitochondria such as Tfam, to facilitate mitochondrial biogenesis (65, 96).

2.0. The Mammalian Unfolded Protein Response

As aforementioned, mitochondrial biogenesis is an intricate process that involves the synthesis and import of several hundred nuclear encoded proteins to the mitochondria (29). Due to the high volume of protein synthesis and import concurrent with mitochondrial biogenesis, maintenance of protein homeostasis, or proteostasis (12), becomes of crucial importance as any malformed proteins can hinder or alter the biosynthetic processes involved (160). Mitochondria, as well as the endoplasmic reticulum (ER), play vital roles in protein translation, modification, and processing. Protein folding is the most error prone step in gene expression (195). As part of the protein quality control (PQC) system, the unfolded protein response (UPR) is activated under certain pathological or physiological conditions that can compromise protein folding efficiency (80). The UPR is a transcriptional induction program coupled with ER or mitochondrial retrograde (organelle to nucleus) signaling, in an attempt to restore proteostasis (158, 190) by reducing accumulation of unfolded proteins via: 1) decreasing global protein translation while selectively increasing translation of chaperones (which assist in protein folding) and proteases

(that degrade excess proteins) to augment folding capacity; 2) breakdown misfolded proteins; 3) or, if proteostasis still cannot be attained, induce apoptosis of the cell (199).

The prototype of the UPR was first discovered in the mid-1970s in mammalian cultured cells (144). It was not until 1989 that the UPR was reported to exist in yeast (158, 190). During the 1990s, the UPR was more extensively studied in lower order organisms, such as yeast and flies, due to its relative simplicity in contrast to mammals thus allowing for better comprehension of the molecular mechanisms involved (144).

The establishment of the yeast UPR in the mid-1990s shed light upon the mechanisms of mammalian UPR. To date, numerous studies regarding the UPR in different tissues have been conducted. Skeletal muscle is of particular interest due to its specialized form of the ER, the SR. In both physical and functional terms, the mitochondria and the ER coexist as tightly connected organelles (232). Since mitochondria are critical to skeletal muscle integrity, how they co-function with the ER is of interest. A separate UPR emanating from the mitochondria is also captivating, as mitochondria require precise stoichiometry in the synthesis of both nuclear and mitochondrial encoded proteins.

2.1. Unfolded Proteins

Proteins are the prime building blocks of cellular structure. Its synthesis is one of the most important events for a cell as proteins not only form its structural components, but also constitutes enzymes involved in catalytic reactions necessary for life (78). According to Anfinsen's dogma, a protein's structure and folding pathways are primarily determined by its amino acid sequence (6, 145, 199). As configuration of a protein determines its function, correct protein folding becomes a vital step in protein synthesis. Maintenance of proteostasis requires molecular chaperones and foldases, which assist in promoting a functional protein-folding

environment by preventing the aggregation of newly synthesized, imported or denatured proteins (27, 78, 261). Molecular chaperones facilitate efficient folding and complex assembly by transiently associating with nascent polypeptides and supressing interactions between the hydrophobic amino acids and helping them fold according to Anfinsen's dogma, prior to dissociation from its now corrected native form (61, 145).

Protein folding involves hydrophobic collapse, in which several side chains attempt to shield each other from surrounding water, and thus form the core of the protein (199, 210). Burial of electrostatic interactions in the hydrophobic core, such as hydrogen or disulfide bonds, initiate folding as well and allow it to maintain the lowest possible energy state (160, 199, 210). The final configuration of the protein excludes any water from its core (199, 210). Therefore, misfolded or unfolded proteins are characterized by a protein's exposure of its hydrophobic core to the exterior environment, which is not only proteotoxic, but also the inappropriate interactions between the "sticky" hydrophobic amino acids can cause aggregation (6, 145). The imbalance between the unfolded proteins and the folding capacity machinery created thus contributes to "stress" induction (189).

Compartmentalized eukaryotic cells have several independent pathways in place to ensure protein-folding integrity (262). All three compartments, the cytosol, ER, and the mitochondria, encounter nascent unfolded polypeptides, each having their own repertoire of specific chaperones to promote proteostasis (78, 199). Unfolded protein-induced stress can be sensed in a compartment-specific manner, thus propagating signaling to the nucleus for transcription of compartment-specific chaperone genes (199).

2.2. ER Stress Response

In eukaryotic cells, the ER is second to the cytosol in being a major site for protein-folding (200), as it is responsible for orchestrating the synthesis and structural maturation of at least a third of all proteins within a cell (82, 200). An accumulation of unfolded or misfolded proteins in the ER lumen can be induced by stressors such as heat (54, 263), exercise (139, 159, 250), or viral infections or "conformational diseases" that perturb proteome integrity by altering its tertiary structure (160) via calcium imbalance or high protein demands in instances such as Alzheimer's, Parkinson's, and Huntington's diseases [as reviewed in (160, 172)].

The endoplasmic reticulum UPR (UPR^{ER}) is regulated by three ER transmembrane proteins: activating transcription factor (ATF) 6, inositol requiring kinase 1 (IRE1), and protein kinase R (PKR)-like ER kinase (PERK) (**Fig. 1A**). In unstressed conditions, immunoglobin binding protein (BiP) is bound to the luminal domains of these master regulators, keeping them inactive (199). BiP has a dual role in cells: 1) sensing unfolded proteins by binding to them; 2) activating the transmembrane proteins that trigger the UPR^{ER} (31). During ER stress, the accumulated unfolded or misfolded proteins bind to BiP, as it preferentially adheres to the exposed hydrophobic regions of the unfolded proteins (60, 236), thus releasing its allosteric inhibition upon the transmembrane proteins and triggering their signaling pathways (31). The binding of BiP to the unfolded protein does not fold the proteins, rather it maintains the protein in a state competent for subsequent folding pathways and oligomerization (60). Although additional mechanisms that initiate the activity of the UPR branches has been reported (59), the exact mechanisms as to how cells can detect the accumulation of misfolded proteins in the ER lumen remain enigmatic (31, 236).

ATF6 is a type II transmembrane domain protein which consists of a basic leucine zipper

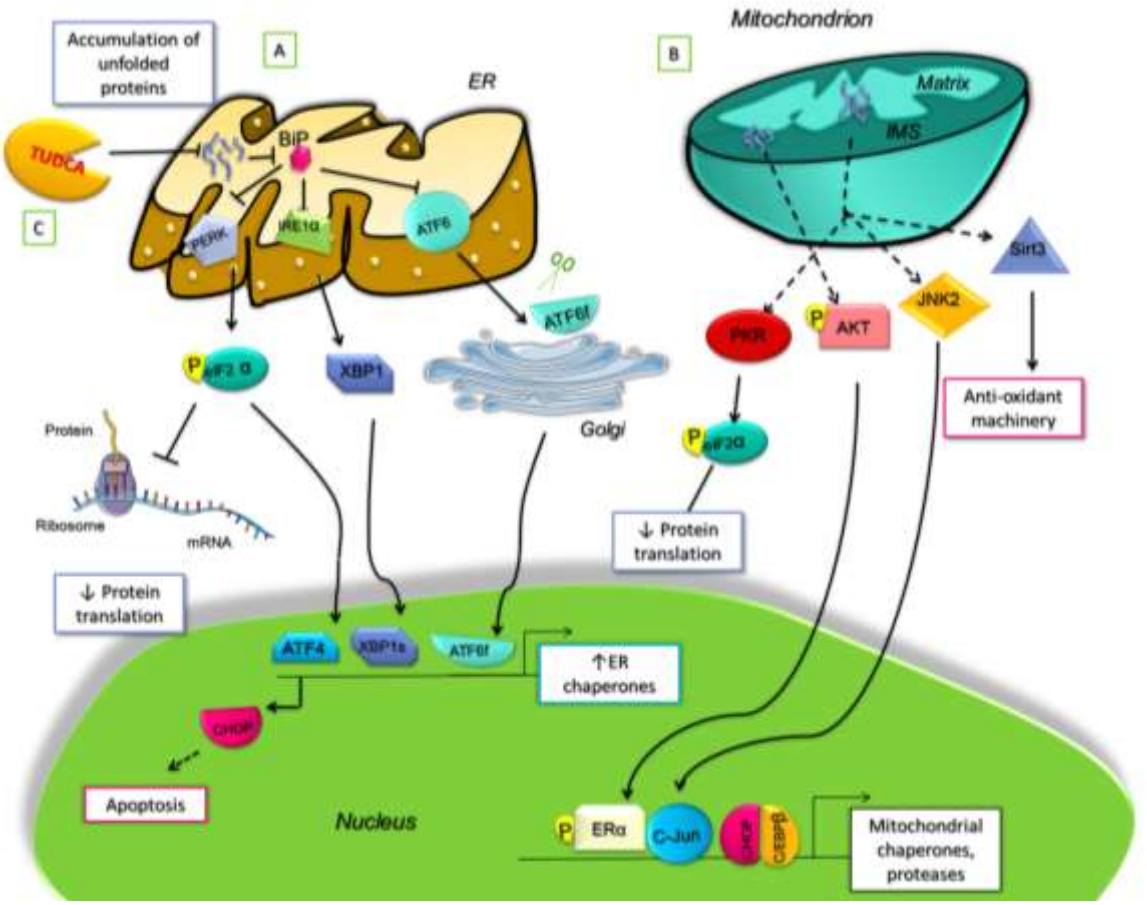

Figure 1. ***(A)*** In the endoplasmic reticulum (ER) under basal conditions, BiP, a binding protein, is bound to the three transmembrane proteins of the ER: ATF6, PERK, IRE1α, keeping them inactive. Upon ER stress, BiP has a higher affinity for the unfolded proteins and binds to them instead, releasing its allosteric inhibition on the UPR^{ER} sensors. The three transmembrane proteins are consequently activated, each initiating the UPR^{ER}. The ATF6 fragment (ATF6f) increases the transcription of ER chaperones. The PERK branch phosphorylates eIF2α which then attenuates global translation. Phosphorylated eIF2α can activate transcription factor ATF4 to increase CHOP, which can induce cell apoptosis. The IRE1α branch splices XBP1 (XBP1s) to increase the transcription of additional ER chaperones to assist in protein folding. ***(B)*** In the mitochondria (UPR^{MT}), an accumulation of unfolded proteins in the mitochondrial matrix can induce reactive oxygen species (ROS) formation which triggers the activation of subsequent pathways. PKR decreases protein translation via the phosphorylation of eIF2α. The transcription factor, CHOP, is transcribed by C-Jun binding to the AP-1 promoter upon JNK2 activation. CHOP then forms a heterodimer with C/EBPβ to trigger UPR^{MT} responsive genes which are translated to proteases and heat shock proteins used to attain proteostasis. Unfolded protein-induced ROS recruits Sirt3 to trigger the anti-oxidant response. In the intermembrane space, ROS can activate AKT signaling to the nucleus and transcribe for OMI protease via phosphorylation of ERα, in order to downgrade any misfolded proteins. ***(C)*** Tauroursodeoxycholic acid (TUDCA) acts a potent chaperone mimetic in the ER to assist in protein folding and hence attenuating the terminal UPR^{ER} response.

(bZIP) transcription factor within its cytosolic domain (257). Upon BiP release, ATF6, with the assistance of the PERK branch of the UPR^{ER} (223), is translocated to the Golgi apparatus where serine proteases, namely site-1 and -2 proteases (S1P and S2P), cleave ATF6 releasing its activated bZIP factor (80). It is then translocated into the nucleus as an active transcription factor, binding to the ATF/cAMP response element (CRE) and ER stress response elements I and II (ERSE-I and -II). Subsequently, UPR genes involved in protein folding, processing, and degradation (259), including ER chaperones, such as BiP, transcription factor X-box binding protein 1 (XBP1), and components of the ER-associated degradation (ERAD) pathway are all upregulated (1, 189, 251, 258).

The IRE1 pathway is the most evolutionary conserved branch of the UPR^{ER} and is expressed in all cell types, alluding to its significance to overall cell function (225). IRE1 is a type I ER transmembrane kinase protein with endoribonuclease (RNase) and serine/threonine kinase activities. There are two isoforms of IRE1, IRE1α and IRE1β (225). In response to luminal activation, IRE1α dimerizes and autophosphorylates, inducing a conformational change that triggers its RNase domain. Its RNase activity is involved in degradation of ER-targeted messenger RNAs (mRNA) and ribosomal RNAs to decrease protein load on the folding machinery, also known as regulated IRE1-dependent decay (RIDD) (35). The RNase catalyzes the splicing of a 26-nucleotide intron within the XBP1 mRNA to a form a stable and highly active transcription factor, known as XBP1s (225). Once in the nucleus, XBP1s transcribes for genes involved in protein folding such as the foldase protein disulfide isomerase (PDI) (260), as well as components involved in ERAD (117). Under chronic stress, IRE1α can bind to TNF-receptor-associated factor 2 (TRAF2) and activate apoptosis-signaling kinase 1 (ASK1). Subsequently, ASK1 activates c-Jun N-terminal protein kinase (JNK), which in turn triggers

apoptosis of the cell (157). Thus, IRE1 is involved not only in the amelioration of accumulated unfolded proteins in the ER, but also induces apoptosis in conditions where proteostasis cannot be restored (124, 236, 249).

Similar to structure and function of IRE1, PERK is also a type II transmembrane kinase protein that undergoes oligomerization and subsequent autophosphorylation. It then directly phosphorylates serine-51 on the α subunit of eukaryotic initiation factor 2 (eIF2α) (74). Phosphorylated eIF2α paradoxically becomes deactivated which prevents the formation of ribosomal initiation complexes, leading to attenuated global mRNA translation (73, 74). Inhibition of eIF2α allows for the selective expression of certain mRNAs, such as activating transcription factor 4 (ATF4). ATF4 is a transcription factor encoding for genes involved in protein folding, antioxidant machinery, autophagy, and apoptosis (75, 255). Additionally, ATF4 upregulates the pro-apoptotic transcription factor, CCAAT-enhancer binding protein (C/EBP) homologous protein (CHOP), promoting cell death (72). Furthermore, PERK phosphorylates and activates transcription factor NF-E2 related factor 2 (Nrf2) responsible for upregulating the antioxidant machinery (39).

The three UPR^{ER} can be independently activated in a temporal manner (236, 260). ATF6 and IRE1 activation occurs immediately upon ER stress and over time is attenuated, whilst PERK activation follows that of ATF6 and IRE1 and persists during chronic ER stress (124, 193, 260). Yet, XBP1 of the IRE1 branch cannot be produced unless ATF6 is activated (260). In liver cells, PERK was found to be required for ATF6 translocation to the Golgi for its subsequent proteolysis and activation (223). Together, these infer the interrelatedness of the UPR^{ER} pathways.

The UPR^{ER} branches can function as a binary switch between life and death of a cell (166). During chronically mild ER stress, all three UPR^{ER} sensors are activated. The adaptive response, or the pro-survival inducers of the UPR, are favoured due to the intrinsic instabilities of the mRNAs and proteins involved in apoptosis in comparison to those that facilitate protein folding and adaptation (193). As a result, apoptotic proteins are transiently induced during mild stress as cells adapt. Prolonged ER stress attenuates the ATF6 branch as well as the IRE1 pathway whilst amplifying PERK signaling. Hence, severe or chronic stress-induced PERK activation and its downstream targets favours the maladaptive response of the UPR^{ER} where apoptosis, or cell death, is preferred over survival as the UPR fails to restore proteostasis (166, 260). The mechanisms as to how the UPR act as a binary switch between an adaptive or apoptotic response remains enigmatic (166, 236).

2.2.1. ATF6 branch of the UPR^{ER}

There are two isoforms of ATF6: ATF6α and ATF6β, in which the former has been more extensively studied in relation to ER stress (80). Predominant UPR^{ER} genes are transcribed by ATF6α (ATF6) (1, 224), which will be the primary focus of this paper. The ATF6 branch not only regulates a subset of genes, but also augments the protective mechanisms induced by the PERK and IRE1 pathways in order to better withstand chronic stress and suppress apoptosis. Lack of ATF6 compromises cells ability to adapt or recover from ER stress in mouse embryonic fibroblasts (MEFs) and in the liver (251). Without activation of ATF6, XBP1 downstream of IRE1 cannot be induced (119). Conversely, ATF6 was found to be dispensable for basal expression of ER protein chaperones as well as for mouse embryonic development (251). While there is considerable overlap in function between the UPR^{ER} branches, each limb induces at least some sort of unique response at times of stress (32, 186). The UPR^{ER} sensors all contribute to

protein folding, maturation, and protein degradation during ER stress. Overlap between their functions ensures that cells have the most optimal ability to adapt to stress rather than capitulate to it (251).

In the context of skeletal muscle, ATF6 activation is of particular interest. The transcriptional coactivator PGC-1α, which regulates several exercise adaptations in skeletal muscle function, is found to mediate the UPR in myotubes and skeletal muscle via coactivation with cleaved ATF6. Wu and coworkers presented that ectopic induction of PGC-1α upregulated UPR^{ER} related genes and was completely abolished in the absence of ATF6 (250). This was not the case with IRE1 deletion, where UPR levels were similar to control. However, this response does have cell or tissue specificity as infecting MEFs or rat embryonic cardiomyocytes with an adenovirus expressing PGC-1α had no impact upon UPR^{ER} marker genes (250). Therefore, it is suggested that certain skeletal muscle-specific factors may be present in the functioning of the PGC-1α/ATF6α protein complex. It may be that the PGC-1α/ATF6α crosstalk in skeletal muscle is present as an additional regulator in skeletal muscle, due to immense stress fluctuations of greater magnitude and frequency in comparison to the cardiac muscle (250). Since PGC-1α is known as the master regulator of mitochondrial biogenesis (53, 126, 227, 252, 266), it would be of interest to investigate whether the regulation of mitochondrial synthesis is dependent upon its regulation of UPR expression.

In addition, ATF6 activity has been specifically implicated in apoptosis associated with muscle development (as will be discussed in further detail in section 2.5) (147, 153). IRE1 and PERK were found to be absent both during differentiation and in dying muscle cells, whereas ATF6 was found to be active (147, 153). In muscle cells, ATF6 can act as a binary switch between self-defence to self-destruction during ER stress. Relatively low levels of ER stress

induces ATF6 to trigger the adaptive response of the UPR^{ER}, whereas at higher levels, apoptosis or the terminal UPR^{ER} is induced (147). During differentiation, ATF6 mediates apoptosis via downregulation of anti-apoptotic protein myeloid cell leukemia sequence 1 (Mcl-1) and augmentation of pro-apoptotic WW binding protein 1 (WBP1) (192). Altogether, these suggest a prominent role for ATF6 in ER stress induced apoptosis during muscle cell differentiation. As was elaborated upon earlier, differentiation is accompanied by an increase in mitochondrial content (36, 57, 132, 149, 204). It would be noteworthy to explore the necessity of the UPR, or more specifically, the activation of ATF6 in regards to differentiation-induced mitochondrial adaptations.

2.2.2. UPR^{ER} and the role of CHOP

CHOP, also known as growth arrest and DNA damage-inducible gene 153 (GADD153), is a highly stress inducible gene (163, 188, 264). Under basal conditions, CHOP is found at low levels, however it is markedly increased in response to ER stress, amino acid starvation, or hypoxia (9, 15, 97). In prolonged or severe ER stress, the maladaptive phase of the UPR^{ER} is triggered when ER stress cannot be resolved. Consequently, CHOP is upregulated via the PERK/eIF2α/ATF4 pathway to induce apoptosis or cell death (52, 72). CHOP is a ubiquitous nuclear protein that heterodimerizes with C/EBP family members to form a highly active transcription factor (264). In promoting cell death, CHOP 1) suppresses anti-apoptotic genes, such as B cell lymphoma 2 (Bcl-2); 2) enhances pro-apoptotic proteins such as Bcl-2 like protein 11 (Bim), p53 upregulate modulator of apoptosis (Puma), and Bcl-2 associated X protein (Bax) to induce mitochondrial permeability transition pore (MPTP) opening; 3) increases protein synthesis and creates an oxidative environment within the ER (136, 138, 179, 188). Downstream of CHOP, growth arrest and DNA damage-inducible protein 34 (GADD34) reverses the

phosphorylation of eIF2α deactivating the translation repression induced by PERK, thus allowing for accumulation of the toxic unfolded proteins in the ER (21, 26, 136). ER oxidase 1α (ERO1α) is another downstream target of CHOP which triggers the ER calcium release channel inositol triphosphate receptor-1 (IP3R1) which increases cytosolic Ca^{2+} and activates CAMKII, leading to eventual apoptosis (121, 165).

CHOP can be induced by the other UPR^{ER} branches (113, 196), namely ATF6 (259) and IRE1/TRAF2/JNK (238) pathways. Despite these other regulators of CHOP, inhibiting PERK activation in murine cells completely ablated or delayed CHOP induction, depicting that CHOP regulation is mainly PERK-dependent (72, 254). CHOP knockouts protect cells from ER stress related death and toxic ROS formation (136, 264). Moreover, in CHOP-deficient MEF cells, there was less overall UPR^{ER} signaling, as upstream regulators such as IRE1 activity and its spliced target XBP1s levels were found to be lower, due to less protein synthesis (136). In addition, CHOP-independent mechanisms that can also induce apoptosis upon ER stress exist, reflecting the multiplicity of pathways in regulating programmed cell death (83, 143).

Interestingly, CHOP can function as a rheostat between pro-survival and cell death due to its antagonized functions. CHOP is not only implicated in cell death programs, but has been found to regulate pro-survival autophagy processes (9, 10, 191). Autophagy enables the recycling of amino acids and nutrients to maintain protein synthesis and ATP generation necessary for cell survival. Autophagy usually precedes apoptosis during many cellular stresses [as reviewed in (135)]. Depending upon the duration and intensity of the stress, CHOP's role in cell fate differs. At the early onset of stress-induced amino acid starvation, CHOP primarily contributes to the later steps of autophagy (9, 10). Both ATF4 and CHOP are required for transcribing a series of autophagy gene transcription factors involved in the formation and

function of the autophagosome necessary for degradation of the targeted dysfunctional organelle (10). Under conditions of chronic stress where the adaptive response is not sufficient enough for survival, CHOP transcribes apoptotic genes while limiting transcription of autophagy-related proteins to induce cell death (9). However, depending on the cell line studied and the type of stress inducer used, varying results can be found (98).

CHOP-induced apoptosis involves both intrinsic and extrinsic pathways. The extrinsic pathway is regulated by death receptors of the TNF family, playing a critical role in death signal transmission from the cell surface to the intracellular signaling pathways (50, 129). Intrinsic pathways are mediated by the mitochondria producing intracellular signals that act directly on targets within the cell. As a result, OMM permeablization can occur, releasing pro-apoptotic factors such as cytochrome c from the IMS (50, 111, 196, 214). Altogether, this reflects the integration of the two organelles, the ER and mitochondria, in regulating the terminal branch of the UPR^{ER}.

2.3. The UPR^{MT}

Although first described in mammals (137, 262), the mitochondrial UPR (UPR^{MT}) has been mainly characterized in *Caenorhabditis elegans* (*C. elegans*). Even less conclusive research has been done in the context of skeletal muscle. Due to the precise mitochondrial and nuclear stoichiometry required for ETC complex assembly, any perturbations in protein import efficiency into the mitochondria can place the organelle under stress and potentially render it as dysfunctional [as reviewed in (92, 134)]. The accumulation of unfolded proteins in mitochondria can trigger second messengers to activate signal transduction pathways involved in transcribing and translating assistive chaperones and proteases to alleviate compartmental stress (8, 105). Stressors that perturb the mito-nuclear encoded protein stoichiometry via import inefficiency and

activate the UPR^{MT} include: mtDNA depletion (137, 256), accumulation of misfolded proteins in the mitochondria (102, 168, 169, 262), mitochondrial chaperone and protease inhibition (42, 102, 256), excess ROS (169, 256), OXPHOS inefficiency (127, 178), as well as high glucose consumption (125, 221). Conversely, stimulation of mitochondrial biogenesis with oxidized nicotinamide adenine dinucleotide (NAD+) supplementation or mammalian/mechanistic target of rapamycin (mTOR) inhibition by rapamycin have also been found to activate the UPR^{MT} in *C. elegans* (148). Mitochondrial dysfunction can induce three main signaling molecules involved in triggering UPR^{MT}-related retrograde signaling: 1) increase in cytosolic Ca^{2+} due to mitochondrial membrane depolarization (16, 17); 2) excess ROS as a by-product of the ETC (42, 211); 3) AMP to ATP ratio associated with energy deprivation (8, 24, 108).

2.4. The UPR^{MT} in *C. elegans*.

In *C. elegans*, accumulated unfolded proteins within the mitochondria are degraded by ATP-dependent Clp protease proteolytic subunit (ClpP) into small peptides which are then actively transported across the IMM by matrix peptide exporter, HAF-1 (77, 79). The peptides then passively diffuse through the OMM into the cytosol, triggering the nuclear translocation of activating transcription factor associated with stress-1 (ATFS-1) (155). ATFS-1 orchestrates the expression of genes encoding mitochondrial chaperones, proteases, mitochondrial protein import, ROS detoxification, and glycolysis (155). ATFS-1 has been recently shown to limit the accumulation of OXPHOS proteins, via coordinating the number of OXPHOS transcripts with the mitochondrial protein-folding capacity (154). Silencing experiments of ClpP and HAF-1 revealed the essentialness of the proteins in ATFS-1 nuclear translocation necessary for UPR^{MT} induction (77, 79). Basally, ATFS-1 is imported into the mitochondria to be degraded by the Lon protease. However, upon mitochondrial proteotoxic stress, mitochondrial protein import

efficiency is decreased, inducing ATFS-1 accumulation in the cytosol and subsequent translocation to the nucleus for transcription of UPR^{MT} components (71, 155). Thus, ATFS-1 promotes OXPHOS recovery by matching mitochondrial biogenesis to its proteostasis capacity (154).

2.5. The Mammalian UPR^{MT}

Similar to *C. elegans*, the mammalian UPR^{MT} is a two-step process involving first the expression of transcription factors, and secondly, the activation of gene expression encoding for mitochondrial chaperonins and proteases (8). In mammals, two independent UPR^{MT} pathways have been described in both the matrix and the mitochondrial IMS (168, 262). Unfolded protein aggregates in the matrix are cleaved by ClpP proteases in which they exit the mitochondria through unknown mechanisms triggering subsequent signaling pathways leading to the activation of JNK and PKR (8, 90, 184). Akin to the UPR^{ER}, global protein translation is inhibited upon phosphorylation of eIF2α by PKR activation (184). Consequently, mitochondrial inner membrane translocase subunit TIM17A levels are decreased, attenuating the import of new proteins into the mitochondria thus easing the protein load on the folding machinery (181). JNK and PKR can both phosphorylate c-Jun which then binds to the activator protein 1 (AP-1) elements in the nucleus (184, 239). C-Jun activation transcribes CHOP and C/EBPβ proteins which then form a heterodimer together (90) (**Fig. 1B**). The dimers bind to the CHOP elements in the promoter of the UPR^{MT} genes that encode for mitochondrial quality control proteins, such as mitochondrial co-chaperonins heat shock proteins 60 (mtHSP60) and 10 (CPN10) that fold the imported protein into its native form, as well as protease ClpP which is involved in misfolded protein degradation (2, 3, 262).

The genes transcribed by CHOP do not contain ERSE in its promoter which would encode for the classical UPR^{ER} proteins. This alludes to the existence of additional factors that may be required for the specificity of UPR^{MT} gene expression (90). Flanked by either side of the CHOP promoter are two other conserved elements in the UPR^{MT} response genes, mitochondrial unfolded protein response elements 1 and 2 (MURE1 and MURE2) (2). The transcription factors for these elements have not been identified yet but have been shown to be necessary for the induction of UPR^{MT} responsive genes. Recently, ATF5 has been found to mediate the UPR^{MT} similar to its worm homologue, ATFS-1 (55). During mitochondrial stress, ATF5 regulates mitochondrial chaperone and protease transcription, such as Lon protease and mitochondrial heat shock protein 70 (mtHSP70) (55).

In addition to the CHOP regulation of the UPR^{MT}, sirtuin-3 (Sirt3) is found to induce antioxidant and mitophagy pathways in response to mitochondrial ROS and unfolded protein accumulation (169). Conversely, CHOP is not essential for autophagic degradation of dysfunctional mitochondria, namely mitophagy, or for the induction of anti-oxidant machinery (169). Inhibition of Sirt3 during proteotoxic stress impairs mitochondrial networks and cell viability, as it serves to limit aggregation in the mitochondria (146, 169). It assists in the sorting of sub-lethal stressed organelles from irreversibly damaged ones via association with forkhead box O3 (FOXO3). However, the mechanisms as to how this is coordinated is unknown (169).

Unfolded protein aggregation in the IMS activates a secondary CHOP-independent UPR^{MT} pathway (168, 169). ROS, produced as by-products of the accumulated proteins, mediate phosphorylation of serine/threonine protein kinase Akt, thus triggering transcription factor estrogen receptor α (ERα) (168). In an attempt to enhance the protein handling machinery of the mitochondria, ERα upregulates the expression of NRF1 transcription to transcribe NUGEMPs

involved in mitochondrial biogenesis, as well as the IMS protease HTRA2/OMI to promote degradation of misfolded proteins in the IMS (168, 180).

Interestingly, although reduced COX activity, a measure of mitochondrial function, has been recently been found to induce mitochondrial biogenesis in both the heart and skeletal muscle of mice, UPR^{MT} upregulation was only present in skeletal muscle tissue and not in the heart (178). This alludes to the induction of compensatory mechanisms in a tissue-specific manner in response to mitochondrial ETC inefficiency. However, whether the activation of the UPR^{MT} in response to COX deficiency is beneficial to skeletal muscle function is unclear (178). The tissue specificity of the UPR^{MT} and its response to various stressors merit further investigation in order to establish its role in cellular stress resistance. Furthermore, albeit several components of the UPR^{MT} pathways in *C. elegans* has been conserved in higher order organisms, no clear mammalian orthologue of the UPR^{MT} mitochondrial peptide exporter, HAF-1 has been identified (8, 105). Additionally, downstream signaling and transcriptional regulation of the mammalian UPR^{MT} has yet to be elucidated.

2.5.1. The role of CHOP in the Mammalian UPR^{MT}

As stated above, CHOP coordinates the transcriptional gene expression of mitochondrial chaperones and proteases (262). Genes encoding cytosolic proteins with CHOP elements in their promoters were not induced upon unfolded protein aggregation in the mitochondria (2). Furthermore, mutating the two regulatory MURE sites located on either side of CHOP decreased UPR^{MT} responsive genes (2). Altogether, this suggests that specific induction of UPR^{MT} responsive genes share a requirement for a CHOP element in their promoters, however, it is not sufficient for the regulation of the UPR^{MT}. It infers the transcriptional regulation by additional unidentified factors.

CHOP is induced by multiple forms of cellular stress, yet, it is unclear as to how CHOP activities integrate to regulate a mitochondrial specific response (8, 170). For instance, the role of CHOP in the UPR^{MT} is in contrast to its mainly autophagic and apoptotic roles in the UPR^{ER} (9, 138). The molecular mechanisms cells use to sense the unfolded proteins within the mitochondrial matrix and transmit its signals across its membranes has yet to be characterized. Upon proteasome inhibition, CHOP has been found to regulate the expression of UPR^{MT} transcription regulator ATF5 (222), however further research is required to better define the mechanisms involved in the UPR^{MT}.

2.6. Mitochondrial—ER Crosstalk

Both mitochondrial and endoplasmic reticula are intimately related in both physical and molecular terms. ER and mitochondrial coupling regulates metabolism, calcium signaling, and apoptosis (30). Precedent findings have established a link between the two in forming inter-connected networks [reviewed in (229)]. The physical contact sites, known as mitochondria-associated endoplasmic reticulum membranes (MAMs) facilitate the transfer of metabolites, such as lipids and calcium, between the ER and the mitochondria, serving as a platform for inter-organelle communication (182). As a result of this intricate relationship, mitochondrial function is sensitive to ER stress inducers. ER stress can alter the transfer of metabolites to mitochondria as well as trigger the UPR, both of which impact mitochondrial functioning. Depending on the intensity and length of the stress, signaling from the ER can induce pro-apoptotic or pro-survival pathways of the mitochondria (182).

The mitochondrial and ER juxtaposition depends structurally upon the ER transmembrane protein PERK. ER-mitochondrial coupling relies on the PERK cytosolic domain, independent of its kinase canonical activity (232). Cells in which the ablation of PERK signaling

occurs show defects in the regulation of ETC activity reflected in the increase in basal and maximal mitochondrial respiration, increased mitochondrial fragmentation, defected morphology, and hypersensitivity to ER stress (93, 150). PERK is enriched in MAMs (232) and is found to be physically associated with the mitochondrial tethering protein, Mitofusin 2 (Mfn2) (182). Unconventional to its role as a mitochondrial fusion protein, Mfn2 is also found to modulate the UPR^{ER} as it senses ER stress and thus, coordinates the ER stress response. As a basal repressor of PERK, Mfn2-deficient cells showed exaggerated activation of UPR pathways (150, 151). Altogether, Mfn2 is suggested to be an upstream negative regulator of PERK pointing to a physical interaction between the two in serving a major role in mitochondrial-ER coupling (150, 151).

Additionally, PERK activation upon ER stress induces downstream expression of mitochondrial PQC factors. It influences mitochondrial proteostasis through translational attenuation via downregulation of TIM17A (181). Furthermore, there is a PERK-dependent increase in mitochondrial proteins Lon, mtHSP70, VDAC, and IP_3R Ca^{2+} release channel (74, 89, 229). As a result, Lon protease which is a critical regulator of mitochondrial proteostasis (231), functions to downregulate oxidatively damaged mitochondria, assemble COX-IV of the ETC, and regulate mtDNA replication (89, 231). Taken together, PERK signaling and structure serve as conduits between the ER and mitochondrial crosstalk during ER stress.

Constitutive ER localized IP_3R Ca^{2+} release from the ER to the mitochondria is essential for mitochondrial bioenergetics and respiration as its transfer is fundamentally required for mitochondrial reduced nicotinamide adenine dinucleotide (NADH) production in B lymphocytes. This response is necessary for oxidative phosphorylation (30). During the early adaptive phase of ER stress, mitochondrial and ER networks are more physically associated than at basal levels,

allowing the Ca^{2+} leakage associated with ER stress to be uptaken by the mitochondria and enhance metabolism. The increase in localized Ca^{2+} uptake by the mitochondria provides the required energy substrates, thus augmenting ATP production, oxygen consumption, and overall bioenergetics adaptation (23). Later phases of ER stress facilitate further tightening of the ER–mitochondria interface along with increased mitochondrial Ca^{2+} influx and consequent apoptosis (23, 30).

In all, it has been well illustrated that the ER and mitochondria engage in intricate crosstalk. Therefore, dysfunction in one organelle can have implications for the other. Elucidating how ER stress impacts the function and biogenesis of the mitochondria is of importance as it paves a way for better understanding of chronic disorders (229, 236).

2.7. The UPR and Differentiation

Differentiation entails an increase in protein synthesis which the protein folding machinery of the cell must handle (68, 112). As part of the PQC system, UPR induction is necessary for optimal differentiation (153, 207, 241). The role of the UPR in cell differentiation was first demonstrated in plasma cells' dependency on the IRE1/XBP1 pathway (186). Knocking down other UPR^{ER} sensors, namely PERK, eIF2α-P (phosphorylated eIF2α) or ATF6, had no impact upon B cell lymphocyte to plasma cell differentiation (186). Conversely, PERK's intrinsic lipid kinase activity promotes adipocyte differentiation via induction of lipogenic pathways (18). This further depicts the different functions that UPR pathways can have in various cell types.

During myogenic differentiation, myoblast fusion is associated with a portion of the cell population undergoing apoptosis (41, 153, 207). During myogenesis, most cells likely experience stress in which the vulnerable ones undergo elimination via apoptosis, allowing for the optimal

fusion of myoblasts. In murine skeletal muscle cells, the ATF6 branch of the UPR^{ER} and ER stress specific caspase-12 has been found to mediate the naturally occurring apoptosis during myogenesis (147, 153). Although differentiation induces the UPR^{ER} evident by the induction of BiP chaperones, active ATF6 plays the decisive role in the induction of apoptosis in murine skeletal muscle cells, whereas activation of IRE1 and PERK pathway were absent in differentiating cells and thus, not required (153). It may be that the ER stress induced during myoblast differentiation is not intense enough to activate the other UPR^{ER} sensors IRE1 and PERK.

Regardless, a certain amount of stress is necessary for optimal differentiation (153, 237). In studies which abrogated ER stress, a defect in myoblast fusion was observed (207, 241). However, this was reversed with the induction of stress via a chemical inducer, thapsigargin (241). Moreover, ER stress was also found to enhance myofiber formation due to triggered apoptosis, thereby eliminating vulnerable cells (152). Hence, the UPR can be selectively activated to control cell growth and proper tissue differentiation, which can have implications for muscle atrophy and myogenesis (22, 153, 237).

As discussed earlier, myogenesis is accompanied by mitochondrial biogenesis which is essential for muscle development (36, 57, 132, 149, 204). However, this can place cells under proteotoxic stress and may require PQC pathways, namely the UPR^{MT}, which has been postulated to be an intrinsic part of myogenesis in synchronizing genomes (3). During differentiation, ClpX, the ATP-dependent chaperone which forms complexes with ClpP subunit to form the major mitochondrial matrix ClpXP protease, is upregulated playing an uncharacterized, yet important role in the mitochondria during myogenesis (3). Although ClpP levels remained unchanged during skeletal muscle development (3), the reduction of ClpP is

found to alter mitochondrial morphology (not biogenesis), increase ROS, and decrease membrane potential, leading to impaired myoblast fusion, translation inhibition, and cellular proliferation, thus implicating a regulatory role in the mammalian UPR^{MT} (42). In contrast, loss of ClpP in mice cardiac muscle was dispensable in UPR^{MT} induction, pointing to tissue-specific responses (202). In line with this, ClpP is expressed at higher levels in skeletal muscle than in other tissues (25). En masse, further research is required to shed light upon the modulation of the UPR, in particular mitochondrial UPR, during differentiation-induced mitochondrial adaptations.

2.8. The UPR, Skeletal Muscle, and Exercise

Basally, skeletal muscle has low levels of UPR activation (99). Whilst ER stress can become pathological under chronic or apoptotic UPR signaling, a certain level of ER stress is necessary for the integrity of skeletal muscle. Bohnert and coworkers' study (19) recently revealed that diminished ER stress and UPR signaling with chemical chaperone 4-phenylbutrate (PBA) reduced skeletal muscle strength and was further aggravated in cancer cachexia mice models, which are characterized by progressive weight loss due to skeletal muscle wasting. The study provided initial evidence of ER stress and UPR pathways being integral to the maintenance of skeletal muscle mass, fiber type composition, and strength (19).

Conversely, high levels of stress in which the $UPR^{MT/ER}$ protein handling is compromised and homeostasis is perturbed, pathological conditions can develop which is extensively reviewed elsewhere (104, 105, 172, 183). ER stress is implicated in myopathies such as myotonic dystrophy type 1 (94), sporadic inclusion body myositis (230), and limb girdle muscular dystrophy 1c (114). The amelioration of ER stress via chemical chaperone mimetics has been found to have beneficial effects in certain conditions (49, 141, 228).

Similarly, exercise can also exert ER-stress reducing benefits which have been associated with ameliorating the debilitating conditions of obstructive sleep apnea (20), insulin resistance (131), and muscle apoptosis (109). An acute bout of aerobic or resistance exercise activates the UPR, and the response is amplified in naïve subjects versus trained individuals (107, 109, 159, 250). Furthermore, chronic contractile activity (CCA) of the muscle elicits an attenuated response of the UPR^{ER}, although the UPR^{MT} remains elevated throughout (139, 164).

In addition to duration, exercise intensity is implicated in the magnitude of UPR activation (109). Rats trained at high exercise intensity for 5 weeks had more attenuated ER stress response and apoptotic signaling responses in skeletal muscle than those trained at a lower intensity (109). According to Rayavarapu et al., exercise-induced skeletal muscle ER stress is considered adaptive, yet it becomes pathological when uncontrolled stress leads to crosstalk with inflammatory pathways (185). In a mice study incorporating an overtraining protocol, high levels of skeletal muscle ER stress were induced which remained elevated and failed to recover even after their 2-week recovery period, suggesting a pathological development in the muscles exercised (171). Thus, moderate intensity exercise training adapts the UPR and can be used to prevent several inflammatory processes in which the ER stress induced with this type of exercise acts as a protective mechanism against current and future exercise stresses (107, 139, 250).

The molecular mechanisms of UPR-mediated exercise adaptations is currently poorly understood. PGC-1α is highly versatile in function as it is involved in several exercise-induced adaptations (110, 205, 226, 250). In a study involving exercising rats, an acute bout of exercise induced an elevation in PGC-1α mRNA (11), yet no increase in mitochondrial content or function was measurable until approximately 72 h later (110). The signals preceding mitochondrial biogenesis during this 3-day window is of particular interest. During this time

frame, protein folding being the fifth most regulated pathway by PGC-1α, as aforementioned, functions to mediate the UPR via co-activation of UPR sensor, ATF6α (250). ATF6α knockout mice displayed compromised recovery from acute exercise and significant intolerance to repeated exercise bouts. Additionally, PGC-1α deficient mice have previously been shown to be exercise intolerant (69, 70, 123, 227). This can be attributed to PGC-1α regulation of mitochondrial biogenesis and gene expression of neuromuscular junctions, as both are involved in endurance capacity. However, Wu and coworkers' study (250) implicated that the exercise intolerance observed may be in part due to PGC-1α control of physiological ER stress. The blockage of detrimental ER stress, via deletion of CHOP expression in the PGC-1α knockout animals partially rescued exercise intolerance and improved total running distance by 50% (250). It is noteworthy that in this study, the adaptation of ER stress by regulating genes involved in protein processing occurred prior to the training-induced increase in mitochondrial cytochrome c, a surrogate marker of mitochondrial content. This suggests that initial improvements to ER proteostasis may be necessary to precede mitochondrial protein synthesis (206). Interestingly, a recent study which used a chemical chaperone mimetic to attenuate CHOP expression found no impact on exercise-induced mitochondrial adaptations (139). With regards to the UPR^{MT}, a link has been made to mitochondrial biogenesis (34, 148), however its relation to exercise-induced adaptations merits further work as few studies hve been done. As the UPR branches are involved in crosstalk with many other regulatory pathways, teasing out what functions each branch serves carries exciting therapeutic potential.

2.9. Tauroursodeoxycholic Acid (TUDCA)

As ER stress, aberrant UPR activation, and protein misfolding underlie many diseases and health conditions discussed earlier, drug administration of tauroursodeoxycholic acid

(TUDCA) is an active field of study (196, 228). TUDCA is a natural occurring bile acid produced in trace amounts by the liver (228). It is the taurine conjugate of ursodeoxycholic acid, the most hydrophilic compound of its kind (14). It has currently been approved by the FDA for treatment of cirrhosis of the liver (203) and suggested for therapeutic use in Duchenne muscular dystrophy (143). A review of the literature reveals the pleiotropic effects of TUDCA in a variety of cell lines in interfering with the mitochondrial-mediated cell death, ROS production, ER stress reduction, and caspase activation (67, 167, 187, 253). Similar to BiP, TUDCA is found to be calcium-sensitive as well, altering intracellular Ca^{2+} levels via modulation of ER ATPases (58, 235) and inhibiting caspase-12 activation associated with apoptotic ER stress (210, 228, 253). TUDCA prohibits mitochondrial-mediated cell death by inhibiting BAX translocation to the mitochondrial membrane (187). Additionally, it binds to the hydrophobic regions of unfolded proteins preventing aggregation and thus allowing for enhanced degradation (4, 58, 167) (**Fig. 1C**). As a result, TUDCA functions as a potent general ER stress inhibitor, resulting in the reduction of CHOP levels and consequent cell death (167). It should be noted that the type of cell line observed and the stress induced can result in varying mediatory effects of TUDCA. In skeletal muscle of rats, TUDCA was found to have no impact on UPR^{ER} markers except for exercise-induced CHOP (139). However, TUDCA inhibited PERK phosphorylation and ATF4 induction upon palmitate-induced stress in skeletal muscle *in vitro* (67) as well as in liver and adipose tissue of mice models of Type 2 diabetes (167). Altogether, although the mechanisms of TUDCA in repressing ER stress remains to be further elucidated, TUDCA is considered a potent agent in the general amelioration of ER stress.

3.0. Research Objectives

Thus, based on the review of literature, the main objectives of my thesis, using C_2C_{12} murine skeletal muscle cells, were to:

1) Characterize UPR^{MT} and UPR^{ER} modulation during differentiation-induced mitochondrial biogenesis, and its relation to mitochondrial biogenesis markers;
2) Investigate the role of ER stress in differentiation- and CCA-induced mitochondrial biogenesis using a chemical chaperone mimetic drug, TUDCA, by measuring surrogate markers of mitochondrial biogenesis, UPR^{MT} and UPR^{ER};
3) Identify the necessity of certain UPR^{MT} and UPR^{ER} components, specifically CHOP induction, in CCA-induced mitochondrial adaptations via silencing RNA (siRNA).

Hypotheses

1) We hypothesize that UPR signaling prior to differentiation may serve as a precursor to mitochondrial adaptations and thus, its inhibition will hinder differentiation-induced mitochondrial biogenesis;
2) We hypothesize that attenuation of the UPR with TUDCA will impact mitochondrial adaptations during CCA;
3) We hypothesize that inhibition of CHOP expression will alter CCA-induced mitochondrial biogenesis.

References

1. **Adachi Y**, **Yamamoto K**, **Okada T**, **Yoshida H**, **Harada A**, **Mori K**. ATF6 is a transcription factor specializing in the regulation of quality control proteins in the endoplasmic reticulum. *Cell Struct Funct* 33: 75–89, 2008.

2. **Aldridge JE**, **Horibe T**, **Hoogenraad NJ**. Discovery of genes activated by the mitochondrial unfolded protein response (mtUPR) and cognate promoter elements. *PLoS One* 2: e874, 2007.

3. **Al-Furoukh N**, **Ianni A**, **Nolte H**, **Hölper S**, **Krüger M**, **Wanrooij S**, **Braun T**. ClpX stimulates the mitochondrial unfolded protein response (UPR(mt)) in mammalian cells. *Biochim Biophys Acta* 1853: 2580–2591, 2015.

4. **de Almeida SF**, **Picarote G**, **Fleming J V**, **Carmo-Fonseca M**, **Azevedo JE**, **de Sousa M**. Chemical chaperones reduce endoplasmic reticulum stress and prevent mutant HFE aggregate formation. *J Biol Chem* 282: 27905–12, 2007.

5. **Andersson SG**, **Zomorodipour A**, **Andersson JO**, **Sicheritz-Pontén T**, **Alsmark UC**, **Podowski RM**, **Näslund AK**, **Eriksson AS**, **Winkler HH**, **Kurland CG**. The genome sequence of Rickettsia prowazekii and the origin of mitochondria. *Nature* 396: 133–40, 1998.

6. **Anfinsen CB**, **Haber E**, **Sela M**, **White FH**. The kinetics of formation of native ribonuclease during oxidation of the reduced polypeptide chain. *Proc Natl Acad Sci U S A* 47: 1309–14, 1961.

7. **Antico Arciuch VG**, **Elguero ME**, **Poderoso JJ**, **Carreras MC**. Mitochondrial regulation of cell cycle and proliferation. *Antioxid Redox Signal* 16: 1150–80, 2012.

8. **Arnould T**, **Michel S**, **Renard P**. Mitochondria retrograde signaling and the UPR(mt): where are we in mammals? *Int J Mol Sci* 16: 18224–51, 2015.

9. **B'chir W**, **Chaveroux C**, **Carraro V**, **Averous J**, **Maurin A-C**, **Jousse C**, **Muranishi Y**, **Parry L**, **Fafournoux P**, **Bruhat A**. Dual role for CHOP in the crosstalk between autophagy and apoptosis to determine cell fate in response to amino acid deprivation. *Cell Signal* 26: 1385–1391, 2014.

10. **B'Chir W**, **Maurin AC**, **Carraro V**, **Averous J**, **Jousse C**, **Muranishi Y**, **Parry L**, **Stepien G**, **Fafournoux P**, **Bruhat A**. The eIF2α/ATF4 pathway is essential for stress-induced autophagy gene expression. *Nucleic Acids Res* 41: 7683–7699, 2013.

11. **Baar K**, **Wende AR**, **Jones TE**, **Marison M**, **Nolte LA**, **Chen M**, **Kelly DP**, **Holloszy JO**. Adaptations of skeletal muscle to exercise: rapid increase in the transcriptional coactivator PGC-1. *FASEB J* 16: 1879–86, 2002.

12. **Balch WE**, **Morimoto RI**, **Dillin A**, **Kelly JW**. Adapting proteostasis for disease intervention. *Science* 319: 916–9, 2008.

13. **Becker T**, **Pfannschmidt S**, **Guiard B**, **Stojanovski D**, **Milenkovic D**, **Kutik S**, **Pfanner N**, **Meisinger C**, **Wiedemann N**. Biogenesis of the mitochondrial TOM complex: Mim1 promotes insertion and assembly of signal-anchored receptors. *J Biol Chem* 283: 120–7, 2008.

14. **Berger E**, **Haller D**. Structure-function analysis of the tertiary bile acid TUDCA for the resolution of endoplasmic reticulum stress in intestinal epithelial cells. *Biochem Biophys Res Commun* 409: 610–5, 2011.

15. **Bi M**, **Naczki C**, **Koritzinsky M**, **Fels D**, **Blais J**, **Hu N**, **Harding H**, **Novoa I**, **Varia M**, **Raleigh J**, **Scheuner D**, **Kaufman RJ**, **Bell J**, **Ron D**, **Wouters BG**, **Koumenis C**. ER stress-regulated translation increases tolerance to extreme hypoxia and promotes tumor growth. *EMBO J* 24: 3470–81, 2005.

16. **Biswas G**, **Adebanjo OA**, **Freedman BD**, **Anandatheerthavarada HK**, **Vijayasarathy C**, **Zaidi M**, **Kotlikoff M**, **Avadhani NG**. Retrograde Ca2+ signaling in C2C12 skeletal myocytes in response to mitochondrial genetic and metabolic stress: a novel mode of inter-organelle crosstalk. *EMBO J* 18: 522–33, 1999.

17. **Biswas G**, **Anandatheerthavarada HK**, **Zaidi M**, **Avadhani NG**. Mitochondria to nucleus stress signaling: a distinctive mechanism of NFkappaB/Rel activation through calcineurin-mediated inactivation of IkappaBbeta. *J Cell Biol* 161: 507–19, 2003.

18. **Bobrovnikova-Marjon E**, **Hatzivassiliou G**, **Grigoriadou C**, **Romero M**, **Cavener DR**, **Thompson CB**, **Diehl JA**. PERK-dependent regulation of lipogenesis during mouse mammary gland development and adipocyte differentiation. *Proc Natl Acad Sci U S A* 105: 16314–9, 2008.

19. **Bohnert KR**, **Gallot YS**, **Sato S**, **Xiong G**, **Hindi SM**, **Kumar A**. Inhibition of ER stress and unfolding protein response pathways causes skeletal muscle wasting during cancer cachexia. *FASEB J* 30: 3053–68, 2016.

20. **Bourdier G**, **Flore P**, **Sanchez H**, **Pepin J-L**, **Belaidi E**, **Arnaud C**. High-intensity training reduces intermittent hypoxia-induced ER stress and myocardial infarct size. *Am J Physiol Heart Circ Physiol* 310: H279-89, 2016.

21. **Boyce M**, **Bryant KF**, **Jousse C**, **Long K**, **Harding HP**, **Scheuner D**, **Kaufman RJ**, **Ma D**, **Coen DM**, **Ron D**, **Yuan J**. A selective inhibitor of eIF2alpha dephosphorylation protects cells from ER stress. *Science* 307: 935–9, 2005.

22. **Bradshaw RA**, **Dennis EA**, editors. Regulation of organelle and cell compartment signaling. London: Elsevier Academic Press, 2011, p. 374, 413.

23. **Bravo R**, **Vicencio JM**, **Parra V**, **Troncoso R**, **Munoz JP**, **Bui M**, **Quiroga C**, **Rodriguez AE**, **Verdejo HE**, **Ferreira J**, **Iglewski M**, **Chiong M**, **Simmen T**, **Zorzano A**, **Hill JA**, **Rothermel BA**, **Szabadkai G**, **Lavandero S**. Increased ER-mitochondrial coupling promotes mitochondrial respiration and bioenergetics during early phases of ER stress. *J Cell Sci* 124: 2143–52, 2011.

24. **Brehm A**, **Krssak M**, **Schmid AI**, **Nowotny P**, **Waldhausl W**, **Roden M**. Increased lipid availability impairs insulin-stimulated ATP synthesis in human skeletal muscle. *Diabetes* 55: 136–140, 2005.

25. **Bross P**, **Andresen BS**, **Knudsen I**, **Kruse TA**, **Gregersen N**. Human ClpP protease: cDNA sequence, tissue-specific expression and chromosomal assignment of the gene. *FEBS Lett* 377: 249–252, 1995.

26. **Brush MH**, **Weiser DC**, **Shenolikar S**. Growth arrest and DNA damage-inducible protein GADD34 targets protein phosphatase 1 alpha to the endoplasmic reticulum and promotes dephosphorylation of the alpha subunit of eukaryotic translation initiation factor 2. *Mol Cell Biol* 23: 1292–303, 2003.

27. **Bukau B**, **Weissman J**, **Horwich A**. Molecular chaperones and protein quality control. *Cell* 125: 443–51, 2006.

28. **Burch N**, **Arnold A-S**, **Item F**, **Summermatter S**, **Brochmann Santana Santos G**, **Christe M**, **Boutellier U**, **Toigo M**, **Handschin C**. Electric pulse stimulation of cultured murine muscle cells reproduces gene expression changes of trained mouse muscle. *PLoS One* 5: e10970, 2010.

29. **Calvo SE**, **Clauser KR**, **Mootha VK**. MitoCarta2.0: an updated inventory of mammalian mitochondrial proteins. *Nucleic Acids Res* : gkv1003, 2015.

30. **Cárdenas C**, **Miller RA**, **Smith I**, **Bui T**, **Molgó J**, **Müller M**, **Vais H**, **Cheung K-H**, **Yang J**, **Parker I**, **Thompson CB**, **Birnbaum MJ**, **Hallows KR**, **Foskett JK**. Essential regulation of cell bioenergetics by constitutive InsP3 receptor Ca2+ transfer to mitochondria. *Cell* 142: 270–83, 2010.

31. **Carrara M**, **Prischi F**, **Nowak PR**, **Kopp MC**, **Ali MM**. Noncanonical binding of BiP ATPase domain to Ire1 and Perk is dissociated by unfolded protein CH1 to initiate ER stress signaling. *Elife* 4: e03522, 2015.

32. **Carrasco DR**, **Sukhdeo K**, **Protopopova M**, **Sinha R**, **Enos M**, **Carrasco DE**, **Zheng M**, **Mani M**, **Henderson J**, **Pinkus GS**, **Munshi N**, **Horner J**, **Ivanova E V**, **Protopopov A**, **Anderson KC**, **Tonon G**, **DePinho RA**. The differentiation and stress response factor XBP-1 drives multiple myeloma pathogenesis. *Cancer Cell* 11: 349–60, 2007.

33. **Carroll S**, **Nicotera P**, **Pette D**. Calcium transients in single fibers of low-frequency stimulated fast-twitch muscle of rat. *Am J Physiol* 277: C1122–C1129, 1999.

34. **Cerutti R**, **Pirinen E**, **Lamperti C**, **Marchet S**, **Sauve AA**, **Li W**, **Leoni V**, **Schon EA**, **Dantzer F**, **Auwerx J**, **Viscomi C**, **Zeviani M**. NAD+-dependent activation of Sirt1 corrects the phenotype in a mouse model of mitochondrial disease. *Cell Metab* 19: 1042–1049, 2014.

35. **Coelho DS**, **Domingos PM**. Physiological roles of regulated Ire1 dependent decay. *Front Genet* 5: 76, 2014.

36. **Collu-Marchese M**, **Shuen M**, **Pauly M**, **Saleem A**, **Hood DA**. The regulation of mitochondrial transcription factor A (Tfam) expression during skeletal muscle cell differentiation. *Biosci Rep* 35: e00221, 2015.

37. **Comelia CL**, **Stebbins GT**, **Brown-Toms N**, **Goetz CG**. Physical therapy and Parkinson's disease: A controlled clinical trial. *Neurology* 44: 376–376, 1994.

38. **Connor MK**, **Irrcher I**, **Hood DA**. Contractile activity-induced transcriptional activation of cytochrome C involves Sp1 and is proportional to mitochondrial ATP synthesis in C2C12 muscle cells. *J Biol Chem* 276: 15898–904, 2001.

39. **Cullinan SB**, **Zhang D**, **Hannink M**, **Arvisais E**, **Kaufman RJ**, **Diehl JA**. Nrf2 is a direct

PERK substrate and effector of PERK-dependent cell survival. *Mol Cell Biol* 23: 7198–7209, 2003.

40. **Davies KJA**, **Packer L**, **Brooks GA**. Biochemical adaptation of mitochondria, muscle, and whole-animal respiration to endurance training. *Arch Biochem Biophys* 209: 539–554, 1981.

41. **Dee K**, **Freer M**, **Mei Y**, **Weyman CM**. Apoptosis coincident with the differentiation of skeletal myoblasts is delayed by caspase 3 inhibition and abrogated by MEK-independent constitutive Ras signaling. *Cell Death Differ* 9: 209–18, 2002.

42. **Deepa SS**, **Bhaskaran S**, **Ranjit R**, **Qaisar R**, **Nair BC**, **Liu Y**, **Walsh ME**, **Fok WC**, **Van Remmen H**. Down-regulation of the mitochondrial matrix peptidase ClpP in muscle cells causes mitochondrial dysfunction and decreases cell proliferation. *Free Radic Biol Med* 91: 281–92, 2016.

43. **Detmer SA**, **Chan DC**. Functions and dysfunctions of mitochondrial dynamics. *Nat Rev Mol Cell Biol* 8: 870–9, 2007.

44. **Dolezal P**, **Likic V**, **Tachezy J**, **Lithgow T**. Evolution of the molecular machines for protein import into mitochondria. *Science* 313: 314–8, 2006.

45. **Dominy JE**, **Puigserver P**. Mitochondrial biogenesis through activation of nuclear signaling proteins. *Cold Spring Harb Perspect Biol* 5, 2013.

46. **Donnelly K**, **Khodabukus A**, **Philp A**, **Deldicque L**, **Dennis RG**, **Baar K**. A novel bioreactor for stimulating skeletal muscle in vitro. *Tissue Eng Part C Methods* 16: 711–8, 2010.

47. **Duguez S**, **Féasson L**, **Denis C**, **Freyssenet D**. Mitochondrial biogenesis during skeletal muscle regeneration. *Am J Physiol Endocrinol Metab* 282: E802-9, 2002.

48. **Egan B**, **Zierath JR**. Exercise metabolism and the molecular regulation of skeletal muscle adaptation. *Cell Metab* 17: 162–84, 2013.

49. **Elia AE**, **Lalli S**, **Monsurrò MR**, **Sagnelli A**, **Taiello AC**, **Reggiori B**, **La Bella V**, **Tedeschi G**, **Albanese A**. Tauroursodeoxycholic acid in the treatment of patients with amyotrophic lateral sclerosis. *Eur J Neurol* 23: 45–52, 2016.

50. **Elmore S**. Apoptosis: a review of programmed cell death. *Toxicol Pathol* 35: 495–516, 2007.

51. **Evans MJ**, **Scarpulla RC**. NRF-1: a trans-activator of nuclear-encoded respiratory genes in animal cells. *Genes Dev* 4: 1023–1034, 1990.

52. **Fawcett TW**, **Martindale JL**, **Guyton KZ**, **Hai T**, **Holbrook NJ**. Complexes containing activating transcription factor (ATF)/cAMP-responsive-element-binding protein (CREB) interact with the CCAAT/enhancer-binding protein (C/EBP)–ATF composite site to regulate Gadd153 expression during the stress response. *Biochem J* 339: 135–141, 1999.

53. **Fernandez-Marcos P**, **Auwerx J**. Regulation of PGC-1a , a nodal regulator of mitochondrial biogenesis. *Am J Clin …* 93: 884–890, 2011.

54. **Finka A**, **Mattoo RUH**, **Goloubinoff P**. Meta-analysis of heat- and chemically upregulated

chaperone genes in plant and human cells. *Cell Stress Chaperones* 16: 15–31, 2011.

55. **Fiorese CJ**, **Schulz AM**, **Lin Y-F**, **Rosin N**, **Pellegrino MW**, **Haynes CM**. The transcription factor ATF5 mediates a mammalian mitochondrial UPR. *Curr Biol* 26:2037-43, 2016.

56. **Fitts RH**, **Booth FW**, **Winder WW**, **Holloszy JO**. Skeletal muscle respiratory capacity, endurance, and glycogen utilization. *Am J Physiol* 228: 1029–33, 1975.

57. **Fortini P**, **Ferretti C**, **Iorio E**, **Cagnin M**, **Garribba L**, **Pietraforte D**, **Falchi M**, **Pascucci B**, **Baccarini S**, **Morani F**, **Phadngam S**, **De Luca G**, **Isidoro C**, **Dogliotti E**. The fine tuning of metabolism, autophagy and differentiation during in vitro myogenesis. *Cell Death Dis* 7: e2168, 2016.

58. **Gani AR**, **Uppala JK**, **Ramaiah KVA**. Tauroursodeoxycholic acid prevents stress induced aggregation of proteins in vitro and promotes PERK activation in HepG2 cells. *Arch Biochem Biophys* 568: 8–15, 2015.

59. **Gardner BM**, **Walter P**. Unfolded proteins are Ire1-activating ligands that directly induce the unfolded protein response. *Science* 333: 1891–4, 2011.

60. **Gething MJ**. Role and regulation of the ER chaperone BiP. *Semin Cell Dev Biol* 10: 465–472, 1999.

61. **Gething MJ**, **Sambrook J**. Protein folding in the cell. *Nature* 355: 33–45, 1992.

62. **Gibala MJ**, **McGee SL**, **Garnham AP**, **Howlett KF**, **Snow RJ**, **Hargreaves M**. Brief intense interval exercise activates AMPK and p38 MAPK signaling and increases the expression of PGC-1alpha in human skeletal muscle. *J Appl Physiol* 106: 929–34, 2009.

63. **Giorgi C**, **Agnoletto C**, **Bononi A**, **Bonora M**, **De Marchi E**, **Marchi S**, **Missiroli S**, **Patergnani S**, **Poletti F**, **Rimessi A**, **Suski JM**, **Wieckowski MR**, **Pinton P**. Mitochondrial calcium homeostasis as potential target for mitochondrial medicine. *Mitochondrion* 12: 77–85, 2012.

64. **Gollnick PD**, **King DW**. Effect of exercise and training on mitochondria of rat skeletal muscle. *Am J Physiol* 216: 1502–9, 1969.

65. **Gordon JW**, **Rungi a a**, **Inagaki H**, **Hood D a**. Effects of contractile activity on mitochondrial transcription factor A expression in skeletal muscle. *J Appl Physiol* 90: 389–396, 2001.

66. **Graef M**, **Nunnari J**. Mitochondria regulate autophagy by conserved signalling pathways. *EMBO J* 30: 2101–14, 2011.

67. **Hage Hassan R**, **Hainault I**, **Vilquin J-T**, **Samama C**, **Lasnier F**, **Ferré P**, **Foufelle F**, **Hajduch E**. Endoplasmic reticulum stress does not mediate palmitate-induced insulin resistance in mouse and human muscle cells. *Diabetologia* 55: 204–14, 2012.

68. **Hamai N**, **Nakamura M**, **Asano A**. Inhibition of Mitochondrial Protein Synthesis Impaired C2C12 Myoblast Differentiation. *Cell Struct Funct* 22: 421–431, 1997.

69. **Handschin C**, **Chin S**, **Li P**, **Liu F**, **Maratos-Flier E**, **Lebrasseur NK**, **Yan Z**, **Spiegelman**

BM. Skeletal muscle fiber-type switching, exercise intolerance, and myopathy in PGC-1alpha muscle-specific knock-out animals. *J Biol Chem* 282: 30014–21, 2007.

70. **Handschin C**, **Kobayashi YM**, **Chin S**, **Seale P**, **Campbell KP**, **Spiegelman BM**. PGC-1alpha regulates the neuromuscular junction program and ameliorates Duchenne muscular dystrophy. *Genes Dev* 21: 770–83, 2007.

71. **Harbauer AB**, **Zahedi RP**, **Sickmann A**, **Pfanner N**, **Meisinger C**. The protein import machinery of mitochondria-a regulatory hub in metabolism, stress, and disease. *Cell Metab* 19: 357–72, 2014.

72. **Harding HP**, **Novoa I**, **Zhang Y**, **Zeng H**, **Wek R**, **Schapira M**, **Ron D**. Regulated translation initiation controls stress-induced gene expression in mammalian cells. *Mol Cell* 6: 1099–1108, 2000.

73. **Harding HP**, **Zhang Y**, **Bertolotti A**, **Zeng H**, **Ron D**. Perk is essential for translational regulation and cell survival during the unfolded protein response. *Mol Cell* 5: 897–904, 2000.

74. **Harding HP**, **Zhang Y**, **Ron D**. Protein translation and folding are coupled by an endoplasmic-reticulum-resident kinase. *Nature* 397: 271–4, 1999.

75. **Harding HP**, **Zhang Y**, **Zeng H**, **Novoa I**, **Lu PD**, **Calfon M**, **Sadri N**, **Yun C**, **Popko B**, **Paules R**, **Stojdl DF**, **Bell JC**, **Hettmann T**, **Leiden JM**, **Ron D**. An integrated stress response regulates amino acid metabolism and resistance to oxidative stress. *Mol Cell* 11: 619–633, 2003.

76. **Harrington JL**, **Murphy E**. The mitochondrial calcium uniporter: mice can live and die without it. *J Mol Cell Cardiol* 78: 46–53, 2015.

77. **Haynes CM**, **Petrova K**, **Benedetti C**, **Yang Y**, **Ron D**. ClpP mediates activation of a mitochondrial unfolded protein response in C. elegans. *Dev Cell* 13: 467–480, 2007.

78. **Haynes CM**, **Ron D**. The mitochondrial UPR - protecting organelle protein homeostasis. *J Cell Sci* 123: 3849–55, 2010.

79. **Haynes CM**, **Yang Y**, **Blais SP**, **Neubert TA**, **Ron D**. The matrix peptide exporter HAF-1 signals a mitochondrial UPR by activating the transcription factor ZC376.7 in C. elegans. *Mol Cell* 37: 529–540, 2010.

80. **Haze K**, **Yoshida H**, **Yanagi H**, **Yura T**, **Mori K**. Mammalian transcription factor ATF6 is synthesized as a transmembrane protein and activated by proteolysis in response to endoplasmic reticulum stress. *Mol Biol Cell* 10: 3787–3799, 1999.

81. **Herzberg NH**, **Zwart R**, **Wolterman RA**, **Ruiter JPN**, **Wanders RJA**, **Bolhuis PA**, **van den Bogert C**. Differentiation and proliferation of respiration-deficient human myoblasts. *Biochim Biophys Acta - Mol Basis Dis* 1181: 63–67, 1993.

82. **Hetz C**, **Chevet E**, **Oakes SA**. Proteostasis control by the unfolded protein response. *Nat Cell Biol* 17: 829–38, 2015.

83. **Hitomi J**, **Katayama T**, **Eguchi Y**, **Kudo T**, **Taniguchi M**, **Koyama Y**, **Manabe T**, **Yamagishi S**, **Bando Y**, **Imaizumi K**, **Tsujimoto Y**, **Tohyama M**. Involvement of caspase-4

in endoplasmic reticulum stress-induced apoptosis and Abeta-induced cell death. *J Cell Biol* 165: 347–56, 2004.

84. **Holloszy JO**. Biochemical Adaptations in Muscle. Effects of exercise on mitochondrial oxygen uptakead respiratory enzyme activity in skeletal muscle. *J Biol Chem* 242: 2278–2282, 1967.

85. **Hood DA**. Plasticity in Skeletal, Cardiac, and Smooth Muscle: Invited Review: Contractile activity-induced mitochondrial biogenesis in skeletal muscle. *J Appl Physiol* 90: 1137–1157, 2001.

86. **Hood DA**, **Uguccioni G**, **Vainshtein A**, **D'souza D**. Mechanisms of exercise-induced mitochondrial biogenesis in skeletal muscle: implications for health and disease. *Compr Physiol* 1: 1119–34, 2011.

87. **Hood DA**, **Zak R**, **Pette D**. Chronic stimulation of rat skeletal muscle induces coordinate increases in mitochondrial and nuclear mRNAs of cytochrome-c-oxidase subunits. *Eur J Biochem* 179: 275–80, 1989.

88. **Hoppeler H**, **Luthi P**, **Claassen H**, **Weibel ER**, **Howald H**. The ultrastructure of the normal human skeletal muscle. *Pflugers Arch Eur J Physiol* 344: 217–232, 1973.

89. **Hori O**, **Ichinoda F**, **Tamatani T**, **Yamaguchi A**, **Sato N**, **Ozawa K**, **Kitao Y**, **Miyazaki M**, **Harding HP**, **Ron D**, **Tohyama M**, **M Stern D**, **Ogawa S**. Transmission of cell stress from endoplasmic reticulum to mitochondria: enhanced expression of Lon protease. *J Cell Biol* 157: 1151–60, 2002.

90. **Horibe T**, **Hoogenraad NJ**. The chop gene contains an element for the positive regulation of the mitochondrial unfolded protein response. *PLoS One* 2: e835, 2007.

91. **Horvath SE**, **Rampelt H**, **Oeljeklaus S**, **Warscheid B**, **van der Laan M**, **Pfanner N**. Role of membrane contact sites in protein import into mitochondria. *Protein Sci* 24: 277–297, 2015.

92. **Houtkooper RH**, **Mouchiroud L**, **Ryu D**, **Moullan N**, **Katsyuba E**, **Knott G**, **Williams RW**, **Auwerx J**. Mitonuclear protein imbalance as a conserved longevity mechanism. *Nature* 497: 451–7, 2013.

93. **Huang G**, **Yao J**, **Zeng W**, **Mizuno Y**, **Kamm KE**, **Stull JT**, **Harding HP**, **Ron D**, **Muallem S**. ER stress disrupts Ca2+-signaling complexes and Ca2+ regulation in secretory and muscle cells from PERK-knockout mice. *J Cell Sci* 119: 153–61, 2006.

94. **Ikezoe K**, **Nakamori M**, **Furuya H**, **Arahata H**, **Kanemoto S**, **Kimura T**, **Imaizumi K**, **Takahashi MP**, **Sakoda S**, **Fujii N**, **Kira J**. Endoplasmic reticulum stress in myotonic dystrophy type 1 muscle. *Acta Neuropathol* 114: 527–535, 2007.

95. **Irrcher I**, **Adhihetty PJ**, **Joseph A-M**, **Ljubicic V**, **Hood DA**. Regulation of mitochondrial biogenesis in muscle by endurance exercise. *Sports Med* 33: 783–93, 2003.

96. **Irrcher I**, **Adhihetty PJ**, **Sheehan T**, **Joseph A-M**, **Hood D a**. PPARgamma coactivator-1alpha expression during thyroid hormone- and contractile activity-induced mitochondrial adaptations. *Am J Physiol Cell Physiol* 284: C1669–C1677, 2003.

97. **Iurlaro R**, **Muñoz Pinedo C**. Cell death induced by endoplasmic reticulum stress. *FEBS J.* (November 20, 2015). doi: 10.1111/febs.13598.

98. **Iwasaki N**, **Sugiyama Y**, **Miyazaki S**, **Nakagawa H**, **Nishimura K**, **Matsuo S**. An ATF4-signal-modulating machine other than GADD34 acts in ATF4-to-CHOP signaling to block CHOP expression in ER-stress-related autophagy. *J Cell Biochem* 116: 1300–9, 2015.

99. **Iwawaki T**, **Akai R**, **Kohno K**, **Miura M**. A transgenic mouse model for monitoring endoplasmic reticulum stress. *Nat Med* 10: 98–102, 2004.

100. **Jacobs RA**, **Lundby C**. Mitochondria express enhanced quality as well as quantity in association with aerobic fitness across recreationally active individuals up to elite athletes. *J Appl Physiol* 114: 344–50, 2013.

101. **Jeppesen TD**, **Schwartz M**, **Olsen DB**, **Wibrand F**, **Krag T**, **Dunø M**, **Hauerslev S**, **Vissing J**. Aerobic training is safe and improves exercise capacity in patients with mitochondrial myopathy. *Brain* 129: 3402–12, 2006.

102. **Jin SM**, **Youle RJ**. The accumulation of misfolded proteins in the mitochondrial matrix is sensed by PINK1 to induce PARK2/Parkin-mediated mitophagy of polarized mitochondria. *Autophagy* 9: 1750–7, 2013.

103. **Jornayvaz FR**, **Shulman GI**. Regulation of mitochondrial biogenesis. *Essays Biochem* 47: 69–84, 2010.

104. **Joshi AU**, **Kornfeld OS**, **Mochly-Rosen D**. The entangled ER-mitochondrial axis as a potential therapeutic strategy in neurodegeneration: A tangled duo unchained. *Cell Calcium* (May 7, 2016). doi: 10.1016/j.ceca.2016.04.010.

105. **Jovaisaite V**, **Mouchiroud L**, **Auwerx J**. The mitochondrial unfolded protein response, a conserved stress response pathway with implications in health and disease. *J Exp Biol* 217: 137–43, 2014.

106. **Kawakami T**, **Gomez IG**, **Ren S**, **Hudkins K**, **Roach A**, **Alpers CE**, **Shankland SJ**, **D'Agati VD**, **Duffield JS**. Deficient autophagy results in mitochondrial dysfunction and FSGS. *J Am Soc Nephrol* 26: 1040–52, 2015.

107. **Kim HJ**, **Jamart C**, **Deldicque L**, **An G**, **Lee YH**, **Kim CK**, **Raymackers J**, **Francaux M**. Endoplasmic reticulum stress markers and ubiquitin–proteasome pathway activity in response to a 200-km run. *Med Sci Sports Exerc* 43: 18–25, 2011.

108. **Kim J-A**, **Wei Y**, **Sowers JR**. Role of mitochondrial dysfunction in insulin resistance. *Circ Res* 102: 401–14, 2008.

109. **Kim K**, **Kim Y-H**, **Lee S-H**, **Jeon M-J**, **Park S-Y**, **Doh K-O**. Effect of exercise intensity on unfolded protein response in skeletal muscle of rat. *Korean J Physiol Pharmacol* 18: 211–6, 2014.

110. **Kim SH**, **Koh JH**, **Higashida K**, **Jung SR**, **Holloszy JO**, **Han D-H**. PGC-1α mediates a rapid, exercise-induced downregulation of glycogenolysis in rat skeletal muscle. *J Physiol* 593: 635–43, 2015.

111. **Kluck RM**. The release of cytochrome c from mitochondria: A primary site for Bcl-2 regulation of apoptosis. *Science (80-)* 275: 1132–1136, 1997.

112. **Korohoda W**, **Pietrzkowski Z**, **Reiss K**. Chloramphenicol, an inhibitor of mitochondrial protein synthesis, inhibits myoblast fusion and myotube differentiation. *Folia Histochem Cytobiol* 31: 9–13, 1993.

113. **Kroemer G**, **Galluzzi L**, **Brenner C**. Mitochondrial membrane permeabilization in cell death. *Physiol Rev* 87: 99–163, 2007.

114. **Kuga A**, **Ohsawa Y**, **Okada T**, **Kanda F**, **Kanagawa M**, **Toda T**, **Sunada Y**. Endoplasmic reticulum stress response in P104L mutant caveolin-3 transgenic mice. *Hum Mol Genet* 20: 2975–83, 2011.

115. **Kutik S**, **Guiard B**, **Meyer HE**, **Wiedemann N**, **Pfanner N**. Cooperation of translocase complexes in mitochondrial protein import. *J Cell Biol* 179: 585–91, 2007.

116. **Leary SC**, **Battersby BJ**, **Hansford RG**, **Moyes CD**. Interactions between bioenergetics and mitochondrial biogenesis. *Biochim Biophys Acta - Bioenerg* 1365: 522–530, 1998.

117. **Lee A-H**, **Iwakoshi NN**, **Glimcher LH**. XBP-1 regulates a subset of endoplasmic reticulum resident chaperone genes in the unfolded protein response. *Mol Cell Biol* 23: 7448–7459, 2003.

118. **Lee H-C**, **Wei Y-H**. Mitochondrial biogenesis and mitochondrial DNA maintenance of mammalian cells under oxidative stress. *Int J Biochem Cell Biol* 37: 822–34, 2005.

119. **Lee K**, **Tirasophon W**, **Shen X**, **Michalak M**, **Prywes R**, **Okada T**, **Yoshida H**, **Mori K**, **Kaufman RJ**. IRE1-mediated unconventional mRNA splicing and S2P-mediated ATF6 cleavage merge to regulate XBP1 in signaling the unfolded protein response. *Genes Dev* 16: 452–66, 2002.

120. **Lee KS**, **Ladinsky H**, **Choi SJ**, **Kasuya Y**. Studies on the in vitro interaction of electrical stimulation and Ca++ movement in sarcoplasmic reticulum. *J Gen Physiol* 49: 689–715, 1966.

121. **Li G**, **Mongillo M**, **Chin KT**, **Harding H**, **Ron D**, **Marks AR**, **Tabas I**. Role of ERO1-α-mediated stimulation of inositol 1,4,5-triphosphate receptor activity in endoplasmic reticulum stress-induced apoptosis. *J Cell Biol* 186: 783–792, 2009.

122. **Lim J-A**, **Li L**, **Kakhlon O**, **Myerowitz R**, **Raben N**. Defects in calcium homeostasis and mitochondria can be reversed in Pompe disease. *Autophagy* 11: 385–402, 2015.

123. **Lin J**, **Handschin C**, **Spiegelman BM**. Metabolic control through the PGC-1 family of transcription coactivators. *Cell Metab* 1: 361–70, 2005.

124. **Lin JH**, **Li H**, **Yasumura D**, **Cohen HR**, **Zhang C**, **Panning B**, **Shokat KM**, **Lavail MM**, **Walter P**. IRE1 signaling affects cell fate during the unfolded protein response. *Science* 318: 944–9, 2007.

125. **Lin Y-F**, **Haynes CM**. Metabolism and the UPR(mt). *Mol Cell* 61: 677–82, 2016.

126. **Little JP**, **Safdar A**, **Bishop D**, **Tarnopolsky MA**, **Gibala MJ**. An acute bout of high-

intensity interval training increases the nuclear abundance of PGC-1α and activates mitochondrial biogenesis in human skeletal muscle. *Am J Physiol Regul Integr Comp Physiol* 300: R1303-10, 2011.

127. **Liu Y**, **Samuel BS**, **Breen PC**, **Ruvkun G**. Caenorhabditis elegans pathways that surveil and defend mitochondria. *Nature* 508: 406–10, 2014.

128. **Ljubicic V**, **Adhihetty PJ**, **Hood DA**. Application of animal models: chronic electrical stimulation-induced contractile activity. *Can J Appl Physiol* 30: 625–643, 2005.

129. **Locksley RM**, **Killeen N**, **Lenardo MJ**. The TNF and TNF receptor superfamilies. *Cell* 104: 487–501, 2001.

130. **Logan DC**. The mitochondrial compartment. *J Exp Bot* 57: 1225–43, 2006.

131. **da Luz G**, **Frederico MJS**, **da Silva S**, **Vitto MF**, **Cesconetto PA**, **de Pinho RA**, **Pauli JR**, **Silva ASR**, **Cintra DE**, **Ropelle ER**, **De Souza CT**. Endurance exercise training ameliorates insulin resistance and reticulum stress in adipose and hepatic tissue in obese rats. *Eur J Appl Physiol* 111: 2015–2023, 2011.

132. **Lyons CN**, **Leary SC**, **Moyes CD**. Bioenergetic remodeling during cellular differentiation: changes in cytochrome c oxidase regulation do not affect the metabolic phenotype. *Biochem Cell Biol* 82: 391–9, 2004.

133. **MacDougall JD**, **Sale DG**, **Moroz JR**, **Elder GC**, **Sutton JR**, **Howald H**. Mitochondrial volume density in human skeletal muscle following heavy resistance training. *Med Sci Sports* 11: 164–6, 1979.

134. **MacKenzie JA**, **Payne RM**. Mitochondrial protein import and human health and disease. *Biochim Biophys Acta* 1772: 509–23, 2007.

135. **Maiuri MC**, **Zalckvar E**, **Kimchi A**, **Kroemer G**. Self-eating and self-killing: crosstalk between autophagy and apoptosis. *Nat Rev Mol Cell Biol* 8: 741–52, 2007.

136. **Marciniak SJ**, **Yun CY**, **Oyadomari S**, **Novoa I**, **Zhang Y**, **Jungreis R**, **Nagata K**, **Harding HP**, **Ron D**. CHOP induces death by promoting protein synthesis and oxidation in the stressed endoplasmic reticulum. *Genes Dev* 18: 3066–77, 2004.

137. **Martinus RD**, **Garth GP**, **Webster TL**, **Cartwright P**, **Naylor DJ**, **Høj PB**, **Hoogenraad NJ**. Selective induction of mitochondrial chaperones in response to loss of the mitochondrial genome. *Eur J Biochem* 240: 98–103, 1996.

138. **McCullough KD**, **Martindale JL**, **Klotz LO**, **Aw TY**, **Holbrook NJ**. Gadd153 sensitizes cells to endoplasmic reticulum stress by down-regulating Bcl2 and perturbing the cellular redox state. *Mol Cell Biol* 21: 1249–59, 2001.

139. **Memme JM**, **Oliveira AN**, **Hood DA**. The chronology of UPR activation in skeletal muscle adaptations to chronic contractile activity. *Am. J. Physiol. Cell Physiol.* (April 27, 2016). doi: 10.1152/ajpcell.00009.2016.

140. **Menshikova E V.**, **Ritov VB**, **Fairfull L**, **Ferrell RE**, **Kelley DE**, **Goodpaster BH**. Effects of exercise on mitochondrial content and function in aging human skeletal muscle. *Journals*

Gerontol Ser A Biol Sci Med Sci 61: 534–540, 2006.

141. **Mimori S**, **Okuma Y**, **Kaneko M**, **Kawada K**, **Hosoi T**, **Ozawa K**, **Nomura Y**, **Hamana H**. Protective effects of 4-phenylbutyrate derivatives on the neuronal cell death and endoplasmic reticulum stress. *Biol Pharm Bull* 35: 84–90, 2012.

142. **Mohamad N**, **Gutiérrez A**, **Núñez M**, **Cocca C**, **Martín G**, **Cricco G**, **Medina V**, **Rivera E**, **Bergoc R**. Mitochondrial apoptotic pathways. *Biocell* 29: 149–161, 2005.

143. **Moorwood C**, **Barton ER**. Caspase-12 ablation preserves muscle function in the mdx mouse. *Hum Mol Genet* 23: 5325–41, 2014.

144. **Mori K**. Signalling pathways in the unfolded protein response: development from yeast to mammals. *J Biochem* 146: 743–50, 2009.

145. **Mori K**. The unfolded protein response: the dawn of a new field. *Proc Jpn Acad Ser B Phys Biol Sci* 91: 469–80, 2015.

146. **Morigi M**, **Perico L**, **Rota C**, **Longaretti L**, **Conti S**, **Rottoli D**, **Novelli R**, **Remuzzi G**, **Benigni A**. Sirtuin 3-dependent mitochondrial dynamic improvements protect against acute kidney injury. *J Clin Invest* 125: 715–26, 2015.

147. **Morishima N**, **Nakanishi K**, **Nakano A**. Activating transcription factor-6 (ATF6) mediates apoptosis with reduction of myeloid cell leukemia sequence 1 (Mcl-1) protein via induction of WW domain binding protein 1. *J Biol Chem* 286: 35227–35, 2011.

148. **Mouchiroud L**, **Houtkooper RH**, **Moullan N**, **Katsyuba E**, **Ryu D**, **Canto C**, **Mottis A**, **Jo YS**, **Viswanathan M**, **Schoonjans K**, **Guarente L**, **Auwerx J**. The NAD(+)/Sirtuin pathway modulates longevity through activation of mitochondrial UPR and FOXO signaling. *Cell* 154: 430–441, 2013.

149. **Moyes CD**, **Mathieu-Costello OA**, **Tsuchiya N**, **Filburn C**, **Hansford RG**. Mitochondrial biogenesis during cellular differentiation. *Am J Physiol Cell Physiol* 272: C1345-1351, 1997.

150. **Muñoz JP**, **Ivanova S**, **Sánchez-Wandelmer J**, **Martínez-Cristóbal P**, **Noguera E**, **Sancho A**, **Díaz-Ramos A**, **Hernández-Alvarez MI**, **Sebastián D**, **Mauvezin C**, **Palacín M**, **Zorzano A**. Mfn2 modulates the UPR and mitochondrial function via repression of PERK. *EMBO J* 32: 2348–61, 2013.

151. **Muñoz JP**, **Zorzano A**. Mfn2 modulates the unfolded protein response. *Cell Cycle* 13: 491–2, 2014.

152. **Nakanishi K**, **Dohmae N**, **Morishima N**. Endoplasmic reticulum stress increases myofiber formation in vitro. *FASEB J* 21: 2994–3003, 2007.

153. **Nakanishi K**, **Sudo T**, **Morishima N**. Endoplasmic reticulum stress signaling transmitted by ATF6 mediates apoptosis during muscle development. *J Cell Biol* 169: 555–60, 2005.

154. **Nargund AM**, **Fiorese CJ**, **Pellegrino MW**, **Deng P**, **Haynes CM**. Mitochondrial and Nuclear Accumulation of the Transcription Factor ATFS-1 Promotes OXPHOS Recovery during the UPR(mt). *Mol Cell* 58: 123–33, 2015.

155. **Nargund AM**, **Pellegrino MW**, **Fiorese CJ**, **Baker BM**, **Haynes CM**. Mitochondrial import efficiency of ATFS-1 regulates mitochondrial UPR activation. *Science* 337: 587–90, 2012.

156. **Neupert W**. A perspective on transport of proteins into mitochondria: a myriad of open questions. *J Mol Biol* 427(Part A: 1135–58, 2015.

157. **Nishitoh H**, **Matsuzawa A**, **Tobiume K**, **Saegusa K**, **Takeda K**, **Inoue K**, **Hori S**, **Kakizuka A**, **Ichijo H**. ASK1 is essential for endoplasmic reticulum stress-induced neuronal cell death triggered by expanded polyglutamine repeats. *Genes Dev* 16: 1345–1355, 2002.

158. **Normington K**, **Kohno K**, **Kozutsumi Y**, **Gething MJ**, **Sambrook J**. S. cerevisiae encodes an essential protein homologous in sequence and function to mammalian BiP. *Cell* 57: 1223–36, 1989.

159. **Ogborn DI**, **McKay BR**, **Crane JD**, **Parise G**, **Tarnopolsky MA**. The unfolded protein response is triggered following a single, unaccustomed resistance-exercise bout. *Am J Physiol Regul Integr Comp Physiol* 307: R664-9, 2014.

160. **Ogen-Shtern N**, **Ben David T**, **Lederkremer GZ**. Protein aggregation and ER stress. *Brain Res* In Press, 2016.

161. **Ojuka EO**. Role of calcium and AMP kinase in the regulation of mitochondrial biogenesis and GLUT4 levels in muscle. *Proc Nutr Soc* 63: 275–8, 2004.

162. **Ojuka EO**, **Jones TE**, **Han D-H**, **Chen M**, **Holloszy JO**. Raising Ca2+ in L6 myotubes mimics effects of exercise on mitochondrial biogenesis in muscle. *FASEB J* 17: 675–81, 2003.

163. **Okada T**, **Yoshida H**, **Akazawa R**, **Negishi M**, **Mori K**. Distinct roles of activating transcription factor 6 (ATF6) and double-stranded RNA-activated protein kinase-like endoplasmic reticulum kinase (PERK) in transcription during the mammalian unfolded protein response. *Biochem J* 366: 585–94, 2002.

164. **Ornatsky OI**, **Connor MK**, **Hood DA**. Expression of stress proteins and mitochondrial chaperonins in chronically stimulated skeletal muscle. *Biochem J* 311 (Pt 1: 119–23, 1995.

165. **Orrenius S**, **Zhivotovsky B**, **Nicotera P**. Regulation of cell death: the calcium–apoptosis link. *Nat Rev Mol Cell Biol* 4: 552–565, 2003.

166. **Oslowski CM**, **Urano F**. The binary switch between life and death of endoplasmic reticulum-stressed beta cells. *Curr Opin Endocrinol Diabetes Obes* 17: 107–12, 2010.

167. **Ozcan U**, **Yilmaz E**, **Ozcan L**, **Furuhashi M**, **Vaillancourt E**, **Smith RO**, **Görgün CZ**, **Hotamisligil GS**. Chemical chaperones reduce ER stress and restore glucose homeostasis in a mouse model of type 2 diabetes. *Science* 313: 1137–40, 2006.

168. **Papa L**, **Germain D**. Estrogen receptor mediates a distinct mitochondrial unfolded protein response. *J Cell Sci* 124: 1396–402, 2011.

169. **Papa L**, **Germain D**. SirT3 regulates the mitochondrial unfolded protein response. *Mol Cell Biol* 34: 699–710, 2014.

170. **Pellegrino MW**, **Nargund AM**, **Haynes CM**. Signaling the mitochondrial unfolded protein

response. *Biochim Biophys Acta - Mol Cell Res* 1833: 410–416, 2013.

171. **Pereira BC**, **da Rocha AL**, **Pinto AP**, **Pauli JR**, **de Souza CT**, **Cintra DE**, **Ropelle ER**, **de Freitas EC**, **Zagatto AM**, **da Silva ASR**. Excessive eccentric exercise-induced overtraining model leads to endoplasmic reticulum stress in mice skeletal muscles. *Life Sci* 145: 144–51, 2016.

172. **Perri ER**, **Thomas CJ**, **Parakh S**, **Spencer DM**, **Atkin JD**. The unfolded protein response and the role of protein disulfide isomerase in neurodegeneration. *Front Cell Dev Biol* 3: 80, 2016.

173. **Pette D**, **Smith ME**, **Staudte HW**, **Vrbova G**. Effects of long-term electrical stimulation on some contractile and metabolic characteristics of fast rabbit muscles. *Pflugers Arch Eur J Physiol* 338: 257–272, 1973.

174. **Pette D**, **Vrbová G**. Adaptation of mammalian skeletal muscle fibers to chronic electrical stimulation. *Rev Physiol Biochem Pharmacol* 120: 115–202, 1992.

175. **Porter C**, **Reidy PT**, **Bhattarai N**, **Sidossis LS**, **Rasmussen BB**. Resistance exercise training alters mitochondrial function in human skeletal muscle. *Med Sci Sports Exerc* 47: 1922–31, 2015.

176. **Pothakos K**, **Kurz MJ**, **Lau Y-S**. Restorative effect of endurance exercise on behavioral deficits in the chronic mouse model of Parkinson's disease with severe neurodegeneration. *BMC Neurosci* 10: 6, 2009.

177. **Prokisch H**, **Scharfe C**, **Camp DG**, **Xiao W**, **David L**, **Andreoli C**, **Monroe ME**, **Moore RJ**, **Gritsenko MA**, **Kozany C**, **Hixson KK**, **Mottaz HM**, **Zischka H**, **Ueffing M**, **Herman ZS**, **Davis RW**, **Meitinger T**, **Oefner PJ**, **Smith RD**, **Steinmetz LM**. Integrative analysis of the mitochondrial proteome in yeast. *PLoS Biol* 2: e160, 2004.

178. **Pulliam DA**, **Deepa SS**, **Liu Y**, **Hill S**, **Lin A-L**, **Bhattacharya A**, **Shi Y**, **Sloane L**, **Viscomi C**, **Zeviani M**, **Van Remmen H**. Complex IV-deficient Surf1(-/-) mice initiate mitochondrial stress responses. *Biochem J* 462: 359–71, 2014.

179. **Puthalakath H**, **O'Reilly LA**, **Gunn P**, **Lee L**, **Kelly PN**, **Huntington ND**, **Hughes PD**, **Michalak EM**, **McKimm-Breschkin J**, **Motoyama N**, **Gotoh T**, **Akira S**, **Bouillet P**, **Strasser A**. ER stress triggers apoptosis by activating BH3-only protein Bim. *Cell* 129: 1337–49, 2007.

180. **Radke S**, **Chander H**, **Schäfer P**, **Meiss G**, **Krüger R**, **Schulz JB**, **Germain D**. Mitochondrial protein quality control by the proteasome involves ubiquitination and the protease Omi. *J Biol Chem* 283: 12681–5, 2008.

181. **Rainbolt TK**, **Atanassova N**, **Genereux JC**, **Wiseman RL**. Stress-regulated translational attenuation adapts mitochondrial protein import through Tim17A degradation. *Cell Metab* 18: 908–19, 2013.

182. **Rainbolt TK**, **Saunders JM**, **Wiseman RL**. Stress-responsive regulation of mitochondria through the ER unfolded protein response. *Trends Endocrinol Metab* 25: 528–37, 2014.

183. **Rambold AS**, **Lippincott-Schwartz J**. Mechanisms of mitochondria and autophagy

crosstalk. *Cell Cycle* 10: 4032–8, 2011.

184. **Rath E**, **Berger E**, **Messlik A**, **Nunes T**, **Liu B**, **Kim SC**, **Hoogenraad N**, **Sans M**, **Sartor RB**, **Haller D**. Induction of dsRNA-activated protein kinase links mitochondrial unfolded protein response to the pathogenesis of intestinal inflammation. *Gut* 61: 1269–78, 2012.

185. **Rayavarapu S**, **Coley W**, **Nagaraju K**. Endoplasmic reticulum stress in skeletal muscle homeostasis and disease. *Curr Rheumatol Rep* 14: 238–243, 2012.

186. **Reimold AM**, **Iwakoshi NN**, **Manis J**, **Vallabhajosyula P**, **Szomolanyi-Tsuda E**, **Gravallese EM**, **Friend D**, **Grusby MJ**, **Alt F**, **Glimcher LH**. Plasma cell differentiation requires the transcription factor XBP-1. *Nature* 412: 300–7, 2001.

187. **Rodrigues CMP**, **Solá S**, **Sharpe JC**, **Moura JJG**, **Steer CJ**. Tauroursodeoxycholic acid prevents Bax-induced membrane perturbation and cytochrome C release in isolated mitochondria. *Biochemistry* 42: 3070–80, 2003.

188. **Ron D**, **Habener JF**. CHOP, a novel developmentally regulated nuclear protein that dimerizes with transcription factors C/EBP and LAP and functions as a dominant-negative inhibitor of gene transcription. *Genes Dev* 6: 439–453, 1992.

189. **Ron D**, **Walter P**. Signal integration in the endoplasmic reticulum unfolded protein response. *Nat Rev Mol Cell Biol* 8: 519–29, 2007.

190. **Rose MD**, **Misra LM**, **Vogel JP**. KAR2, a karyogamy gene, is the yeast homolog of the mammalian BiP/GRP78 gene. *Cell* 57: 1211–1221, 1989.

191. **Rouschop KMA**, **van den Beucken T**, **Dubois L**, **Niessen H**, **Bussink J**, **Savelkouls K**, **Keulers T**, **Mujcic H**, **Landuyt W**, **Voncken JW**, **Lambin P**, **van der Kogel AJ**, **Koritzinsky M**, **Wouters BG**. The unfolded protein response protects human tumor cells during hypoxia through regulation of the autophagy genes MAP1LC3B and ATG5. *J Clin Invest* 120: 127–41, 2010.

192. **Ruiz-Meana M**, **Inserte J**, **Fernandez-Sanz C**, **Hernando V**, **Miro-Casas E**, **Barba I**, **Garcia-Dorado D**. The role of mitochondrial permeability transition in reperfusion-induced cardiomyocyte death depends on the duration of ischemia. *Basic Res Cardiol* 106: 1259–68, 2011.

193. **Rutkowski DT**, **Arnold SM**, **Miller CN**, **Wu J**, **Li J**, **Gunnison KM**, **Mori K**, **Sadighi Akha AA**, **Raden D**, **Kaufman RJ**. Adaptation to ER stress is mediated by differential stabilities of pro-survival and pro-apoptotic mRNAs and proteins. *PLoS Biol* 4: e374, 2006.

194. **Sabourin LA**, **Rudnicki MA**. The molecular regulation of myogenesis. *Clin Genet* 57: 16–25, 2001.

195. **Sakaki K**, **Kaufman RJ**. Interaction between quality control systems for ER protein folding and RNA biogenesis. *Worm* 2: e23005, 2013.

196. **Sano R**, **Reed JC**. ER stress-induced cell death mechanisms. *Biochim Biophys Acta* 1833: 3460–70, 2013.

197. **Scarpulla RC**. Nuclear respiratory factors and the pathways of nuclear-mitochondrial

interaction. *Trends Cardiovasc Med* 6: 39–45, 1996.

198. **Scarpulla RC**. Transcriptional paradigms in mammalian mitochondrial biogenesis and function. *Physiol Rev* 88: 611–38, 2008.

199. **Schröder M**, **Kaufman RJ**. the Mammalian Unfolded Protein Response. *Annu Rev Biochem* 74: 739–789, 2005.

200. **Schröder M**, **Kaufman RJ**. ER stress and the unfolded protein response. *Mutat Res* 569: 29–63, 2005.

201. **Schultz E**, **Jaryszak DL**, **Valliere CR**. Response of satellite cells to focal skeletal muscle injury. *Muscle Nerve* 8: 217–22.

202. **Seiferling D**, **Szczepanowska K**, **Becker C**, **Senft K**, **Hermans S**, **Maiti P**, **König T**, **Kukat A**, **Trifunovic A**. Loss of CLPP alleviates mitochondrial cardiomyopathy without affecting the mammalian UPR mt. *EMBO Rep*. (2016). doi: 10.15252/embr.201642077.

203. **Setchell KD**, **Rodrigues CM**, **Podda M**, **Crosignani A**. Metabolism of orally administered tauroursodeoxycholic acid in patients with primary biliary cirrhosis. *Gut* 38: 439–446, 1996.

204. **Sin J**, **Andres AM**, **Taylor DJR**, **Weston T**, **Hiraumi Y**, **Stotland A**, **Kim BJ**, **Huang C**, **Doran KS**, **Gottlieb RA**. Mitophagy is required for mitochondrial biogenesis and myogenic differentiation of C2C12 myoblasts. *Autophagy* 12: 369–80, 2016.

205. **Smiles WJ**, **Camera DM**. More than mitochondrial biogenesis: alternative roles of PGC-1α in exercise adaptation. *J Physiol* 5939: 2115–2117, 2015.

206. **Smiles WJ**, **Hawley JA**, **Camera DM**. Effects of skeletal muscle energy availability on protein turnover responses to exercise. *J Exp Biol* 219: 214–25, 2016.

207. **Song H**, **Kim H**, **Park T**, **Lee D-H**. Characterization of myogenic differentiation under endoplasmic reticulum stress and taurine treatment. *Adv Exp Med Biol* 643: 253–61, 2009.

208. **Speelman AD**, **van de Warrenburg BP**, **van Nimwegen M**, **Petzinger GM**, **Munneke M**, **Bloem BR**. How might physical activity benefit patients with Parkinson disease? *Nat Rev Neurol* 7: 528–34, 2011.

209. **Sreter F a**, **Lopez JR**, **Alamo L**, **Mabuchi K**, **Gergely J**. Changes in intracellular ionized Ca concentration associated with muscle fiber type transformation. *Am J Physiol* 253: C296-300, 1987.

210. **Stevens FJ**, **Argon Y**. Protein folding in the ER. *Semin Cell Dev Biol* 10: 443–54, 1999.

211. **Storz P**, **Döppler H**, **Toker A**. Protein kinase D mediates mitochondrion-to-nucleus signaling and detoxification from mitochondrial reactive oxygen species. *Mol Cell Biol* 25: 8520–30, 2005.

212. **Suetta C**, **Andersen JL**, **Dalgas U**, **Berget J**, **Koskinen S**, **Aagaard P**, **Magnusson SP**, **Kjaer M**. Resistance training induces qualitative changes in muscle morphology, muscle architecture, and muscle function in elderly postoperative patients. *J Appl Physiol* 105: 180–6, 2008.

213. **Susin SA**, **Lorenzo HK**, **Zamzami N**, **Marzo I**, **Snow BE**, **Brothers GM**, **Mangion J**, **Jacotot E**, **Costantini P**, **Loeffler M**, **Larochette N**, **Goodlett DR**, **Aebersold R**, **Siderovski DP**, **Penninger JM**, **Kroemer G**. Molecular characterization of mitochondrial apoptosis-inducing factor. *Nature* 397: 441–6, 1999.

214. **Tabas I**, **Ron D**. Integrating the mechanisms of apoptosis induced by endoplasmic reticulum stress. *Nat Cell Biol* 13: 184–90, 2011.

215. **Tait SWG**, **Green DR**. Mitochondria and cell death: outer membrane permeabilization and beyond. *Nat Rev Mol Cell Biol* 11: 621–32, 2010.

216. **Tait SWG**, **Green DR**. Mitochondria and cell signalling. *J Cell Sci* 125: 807–15, 2012.

217. **Taivassalo T**, **De Stefano N**, **Argov Z**, **Matthews PM**, **Chen J**, **Genge A**, **Karpati G**, **Arnold DL**. Effects of aerobic training in patients with mitochondrial myopathies. *Neurology* 50: 1055–1060, 1998.

218. **Takahashi M**, **Chesley a**, **Freyssenet D**, **Hood D a**. Contractile activity-induced adaptations in the mitochondrial protein import system. *Am J Physiol* 274: C1380-7, 1998.

219. **Takahashi M**, **Hood DA**. Chronic stimulation-induced changes in mitochondria and performance in rat skeletal muscle. *J Appl Physiol* 74: 934–941, 1993.

220. **Tang JE**, **Hartman JW**, **Phillips SM**. Increased muscle oxidative potential following resistance training induced fibre hypertrophy in young men. *Appl Physiol Nutr Metab = Physiol Appl Nutr métabolisme* 31: 495–501, 2006.

221. **Tauffenberger A**, **Vaccaro A**, **Parker J**. Fragile lifespan expansion by dietary mitohormesis in C. elegans. *Aging (Albany NY)* 8: 50–61, 2016.

222. **Teske BF**, **Fusakio ME**, **Zhou D**, **Shan J**, **McClintick JN**, **Kilberg MS**, **Wek RC**. CHOP induces activating transcription factor 5 (ATF5) to trigger apoptosis in response to perturbations in protein homeostasis. *Mol Biol Cell* 24: 2477–2490, 2013.

223. **Teske BF**, **Wek SA**, **Bunpo P**, **Cundiff JK**, **McClintick JN**, **Anthony TG**, **Wek RC**. The eIF2 kinase PERK and the integrated stress response facilitate activation of ATF6 during endoplasmic reticulum stress. *Mol Biol Cell* 22: 4390–4405, 2011.

224. **Thuerauf DJ**, **Morrison L**, **Glembotski CC**. Opposing roles for ATF6alpha and ATF6beta in endoplasmic reticulum stress response gene induction. *J Biol Chem* 279: 21078–84, 2004.

225. **Tirasophon W**, **Welihinda AA**, **Kaufman RJ**. A stress response pathway from the endoplasmic reticulum to the nucleus requires a novel bifunctional protein kinase/endoribonuclease (Ire1p) in mammalian cells. *Genes Dev* 12: 1812–1824, 1998.

226. **Uguccioni G**, **Hood DA**. The importance of PGC-1α in contractile activity-induced mitochondrial adaptations. *Am J Physiol Endocrinol Metab* 300: E361-71, 2011.

227. **Vainshtein A**, **Tryon LD**, **Pauly M**, **Hood DA**. Role of PGC-1α during acute exercise-induced autophagy and mitophagy in skeletal muscle. *Am J Physiol Cell Physiol* 308: C710-9, 2015.

228. **Vang S**, **Longley K**, **Steer CJ**, **Low WC**. The Unexpected Uses of Urso- and Tauroursodeoxycholic Acid in the Treatment of Non-liver Diseases. *Glob Adv Health Med* 3: 58–69, 2014.

229. **Vannuvel K**, **Renard P**, **Raes M**, **Arnould T**. Functional and morphological impact of ER stress on mitochondria. *J Cell Physiol* 228: 1802–18, 2013.

230. **Vattemi G**, **Engel WK**, **McFerrin J**, **Askanas V**. Endoplasmic reticulum stress and unfolded protein response in inclusion body myositis muscle. *Am J Pathol* 164: 1–7, 2004.

231. **Venkatesh S**, **Lee J**, **Singh K**, **Lee I**, **Suzuki CK**. Multitasking in the mitochondrion by the ATP-dependent Lon protease. *Biochim Biophys Acta* 1823: 56–66, 2012.

232. **Verfaillie T**, **Rubio N**, **Garg AD**, **Bultynck G**, **Rizzuto R**, **Decuypere J-P**, **Piette J**, **Linehan C**, **Gupta S**, **Samali A**, **Agostinis P**. PERK is required at the ER-mitochondrial contact sites to convey apoptosis after ROS-based ER stress. *Cell Death Differ* 19: 1880–91, 2012.

233. **Virbasius J V.**, **Scarpulla RC**. Activation of the human mitochondrial transcription factor A gene by nuclear respiratory factors: a potential regulatory link between nuclear and mitochondrial gene expression in organelle biogenesis. *Proc Natl Acad Sci* 91: 1309–1313, 1994.

234. **Wang C**, **Youle RJ**. The role of mitochondria in apoptosis. *Annu Rev Genet* 43: 95–118, 2009.

235. **Wang L**, **Piguet AC**, **Schmidt K**, **Tordjmann T**, **Dufour JF**. Activation of CREB by tauroursodeoxycholic acid protects cholangiocytes from apoptosis induced by mTOR inhibition. *Hepatology* 41: 1241–51, 2005.

236. **Wang M**, **Kaufman RJ**. Protein misfolding in the endoplasmic reticulum as a conduit to human disease. *Nature* 529: 326–335, 2016.

237. **Wang S**, **Kaufman RJ**. The impact of the unfolded protein response on human disease. *J Cell Biol* 197: 857–67, 2012.

238. **Wang XZ**, **Harding HP**, **Zhang Y**, **Jolicoeur EM**, **Kuroda M**, **Ron D**. Cloning of mammalian Ire1 reveals diversity in the ER stress responses. *EMBO J* 17: 5708–17, 1998.

239. **Weiss C**, **Schneider S**, **Wagner EF**, **Zhang X**, **Seto E**, **Bohmann D**. JNK phosphorylation relieves HDAC3-dependent suppression of the transcriptional activity of c-Jun. *EMBO J* 22: 3686–95, 2003.

240. **Wiedemann N**, **Frazier AE**, **Pfanner N**. The protein import machinery of mitochondria. *J Biol Chem* 279: 14473–6, 2004.

241. **Wiles B**, **Miao M**, **Coyne E**, **Larose L**, **Cybulsky A**, **Wing SS**. USP19 deubiquitinating enzyme inhibits muscle cell differentiation by suppressing unfolded-protein response signaling. *Mol Biol Cell* 26: 913–923, 2015.

242. **Williams R**, **Garcia-Moll M**, **Mellor J**, **Salmons S**, **Harlan W**. Adaptation of skeletal muscle to increased contractile activity. Expression nuclear genes encoding mitochondrial

proteins. *J Biol Chem* 262: 2764–2767, 1987.

243. **Williams RS**. Mitochondrial gene expression in mammalian striated muscle. Evidence that variation in gene dosage is the major regulatory event. *J Biol Chem* 261: 12390–12394, 1986.

244. **Williams RS**, **Salmons S**, **Newsholme EA**, **Kaufman RE**, **Mellor J**. Regulation of nuclear and mitochondrial gene expression by contractile activity in skeletal muscle. *J Biol Chem* 261: 376–380, 1986.

245. **Winder WW**, **Holmes BF**, **Rubink DS**, **Jensen EB**, **Chen M**, **Holloszy JO**. Activation of AMP-activated protein kinase increases mitochondrial enzymes in skeletal muscle. *J Appl Physiol* 88: 2219–2226, 2000.

246. **Wright DC**, **Geiger PC**, **Han D-H**, **Jones TE**, **Holloszy JO**. Calcium induces increases in peroxisome proliferator-activated receptor gamma coactivator-1alpha and mitochondrial biogenesis by a pathway leading to p38 mitogen-activated protein kinase activation. *J Biol Chem* 282: 18793–9, 2007.

247. **Wright DC**, **Han D-H**, **Garcia-Roves PM**, **Geiger PC**, **Jones TE**, **Holloszy JO**. Exercise-induced mitochondrial biogenesis begins before the increase in muscle PGC-1alpha expression. *J Biol Chem* 282: 194–9, 2007.

248. **Wu H**, **Kanatous SB**, **Thurmond FA**, **Gallardo T**, **Isotani E**, **Bassel-Duby R**, **Williams RS**. Regulation of mitochondrial biogenesis in skeletal muscle by CaMK. *Science* 296: 349–52, 2002.

249. **Wu J**, **He GT**, **Zhang WJ**, **Xu J**, **Huang QB**. IRE1α signaling pathways involved in mammalian cell fate determination. *Cell Physiol Biochem* 38: 847–58, 2016.

250. **Wu J**, **Ruas JL**, **Estall JL**, **Rasbach KA**, **Choi JH**, **Ye L**, **Boström P**, **Tyra HM**, **Crawford RW**, **Campbell KP**, **Rutkowski DT**, **Kaufman RJ**, **Spiegelman BM**. The unfolded protein response mediates adaptation to exercise in skeletal muscle through a PGC-1α/ATF6α complex. *Cell Metab* 13: 160–9, 2011.

251. **Wu J**, **Rutkowski DT**, **Dubois M**, **Swathirajan J**, **Saunders T**, **Wang J**, **Song B**, **Yau GD**, **Kaufman RJ**. ATF6alpha optimizes long-term endoplasmic reticulum function to protect cells from chronic stress. *Dev Cell* 13: 351–364, 2007.

252. **Wu Z**, **Puigserver P**, **Andersson U**, **Zhang C**, **Adelmant G**, **Mootha V**, **Troy A**, **Cinti S**, **Lowell B**, **Scarpulla RC**, **Spiegelman BM**. Mechanisms controlling mitochondrial biogenesis and respiration through the thermogenic coactivator PGC-1. *Cell* 98: 115–124, 1999.

253. **Xie Q**, **Khaoustov VI**, **Chung CC**, **Sohn J**, **Krishnan B**, **Lewis DE**, **Yoffe B**. Effect of tauroursodeoxycholic acid on endoplasmic reticulum stress-induced caspase-12 activation. *Hepatology* 36: 592–601, 2002.

254. **Yamaguchi Y**, **Larkin D**, **Lara-Lemus R**, **Ramos-Castañeda J**, **Liu M**, **Arvan P**. Endoplasmic reticulum (ER) chaperone regulation and survival of cells compensating for deficiency in the ER stress response kinase, PERK. *J Biol Chem* 283: 17020–9, 2008.

255. **Ye J**, **Koumenis C**. ATF4, an ER stress and hypoxia-inducible transcription factor and its

potential role in hypoxia tolerance and tumorigenesis. .

256. **Yoneda T**, **Benedetti C**, **Urano F**, **Clark SG**, **Harding HP**, **Ron D**. Compartment-specific perturbation of protein handling activates genes encoding mitochondrial chaperones. *J Cell Sci* 117: 4055–66, 2004.

257. **Yoshida H**. Identification of the cis-acting endoplasmic reticulum stress response element responsible for transcriptional induction of mammalian glucose-regulated proteins. Invovlement of basic leucine zipper transcription factors. *J Biol Chem* 273: 33741–33749, 1998.

258. **Yoshida H**, **Matsui T**, **Yamamoto A**, **Okada T**, **Mori K**. XBP1 mRNA Is Induced by ATF6 and Spliced by IRE1 in Response to ER Stress to Produce a Highly Active Transcription Factor. *Cell* 107: 881–891, 2001.

259. **Yoshida H**, **Okada T**, **Haze K**, **Yanagi H**, **Yura T**, **Negishi M**, **Mori K**. ATF6 activated by proteolysis binds in the presence of NF-Y (CBF) directly to the cis-acting element responsible for the mammalian unfolded protein response. *Mol Cell Biol* 20: 6755–6767, 2000.

260. **Yoshida H**, **Toshie M**, **Hosokawa N**, **Kaufman RJ**, **Nagata K**, **Mori K**. A time-dependent phase shift in the mammalian unfolded protein response. *Dev Cell* 4: 265–271, 2003.

261. **Young JC**, **Agashe VR**, **Siegers K**, **Hartl FU**. Pathways of chaperone-mediated protein folding in the cytosol. *Nat Rev Mol Cell Biol* 5: 781–91, 2004.

262. **Zhao Q**, **Wang J**, **Levichkin I V**, **Stasinopoulos S**, **Ryan MT**, **Hoogenraad NJ**. A mitochondrial specific stress response in mammalian cells. *EMBO J* 21: 4411–9, 2002.

263. **Zhong Y**, **Yang L**, **Guo Y**, **Fang F**, **Wang D**, **Li R**, **Jiang M**, **Kang W**, **Ma J**, **Sun J**, **Xiao W**. High-temperature cultivation of recombinant Pichia pastoris increases endoplasmic reticulum stress and decreases production of human interleukin-10. *Microb Cell Fact* 13: 163, 2014.

264. **Zinszner H**, **Kuroda M**, **Wang X**, **Batchvarova N**, **Lightfoot RT**, **Remotti H**, **Stevens JL**, **Ron D**. CHOP is implicated in programmed cell death in response to impaired function of the endoplasmic reticulum. *Genes Dev* 12: 982–95, 1998.

265. **Zoll J**, **Sanchez H**, **N'Guessan B**, **Ribera F**, **Lampert E**, **Bigard X**, **Serrurier B**, **Fortin D**, **Geny B**, **Veksler V**, **Ventura-Clapier R**, **Mettauer B**. Physical activity changes the regulation of mitochondrial respiration in human skeletal muscle. *J Physiol* 543: 191–200, 2002.

266. **Zong H**, **Ren JM**, **Young LH**, **Pypaert M**, **Mu J**, **Birnbaum MJ**, **Shulman GI**. AMP kinase is required for mitochondrial biogenesis in skeletal muscle in response to chronic energy deprivation. *Proc Natl Acad Sci U S A* 99: 15983–7, 2002.

CHAPTER 2: MANUSCRIPT

THE UNFOLDED PROTEIN RESPONSE IN RELATION TO MITOCHONDRIAL BIOGENESIS IN SKELETAL MUSCLE CELLS

Zahra S. Mesbah Moosavi[1] and David A. Hood[1, 2]

Summary

Mitochondria are comprised of both nuclear- and mitochondrial-encoded proteins requiring precise stoichiometry for their integration into functional complexes. The augmented protein synthesis associated with mitochondrial biogenesis results in the accumulation of unfolded proteins, thus triggering cellular stress. As such, the unfolded protein responses emanating from the endoplasmic reticulum (UPR^{ER}) or the mitochondrion (UPR^{MT}) are triggered to ensure correct protein handling. Whether this response is necessary to facilitate mitochondrial adaptations is unknown. Two models of mitochondrial biogenesis were used: skeletal muscle differentiation and chronic contractile activity (CCA) in C_2C_{12} muscle cells. After 4 days of differentiation, our findings depict selective activation of the UPR^{MT} in which UPR^{MT} chaperones decreased, however Sirt3 was elevated along with UPR^{ER} markers. To delineate the role of ER stress in mitochondrial adaptations, the ER stress inhibitor TUDCA was administered prior to differentiation. Surprisingly, mitochondrial markers COX-I, COX-IV, and PGC-1α protein levels were augmented (by 1.3-1.5-fold) above that of vehicle-treated cells. Similar results were obtained in myotubes undergoing CCA in which mitochondrial biogenesis was enhanced by ~2-3-fold, along with elevated UPR^{MT} markers Sirt3 and CPN10. To verify whether

[1] Muscle Health Research Centre, School of Kinesiology and Health Science, York University, Toronto, Ontario, M3J 1P3, Canada.

[2] This work was supported by funding from the Natural Sciences and Engineering Research Council of Canada (NSERC) to D. A. Hood. D. A. Hood is also the holder of a Canada Research Chair in Cell Physiology.

the findings were attributable to the terminal UPR^{ER} branch directed by the transcription factor CHOP, cells were transfected with CHOP siRNA. Basally, COX-I levels increased (~20%) and COX-IV decreased (~30%), suggesting that CHOP influences mitochondrial composition. This effect was fully restored by CCA. Therefore, our results suggest that mitochondrial biogenesis is independent of the terminal UPR^{ER}. Under basal conditions CHOP is required for the maintenance of mitochondrial composition, but not for differentiation- or CCA-induced mitochondrial biogenesis.

Introduction

Muscle differentiation from the myoblast to the myotube stage requires a large increase in the synthesis of new proteins. This increase in protein synthesis can perturb the proteostasis of a cell via an accumulation of unfolded or misfolded proteins in the endoplasmic reticulum (ER), or in the mitochondrial matrix (27, 43). Unfolded proteins trigger the activation of a quality control system termed the unfolded protein response (UPR). The UPR involves a transcriptional program that feeds back to decrease global protein translation, while increasing the synthesis of selected chaperones and proteases involved in protein folding in order to restore homeostasis (33). In the ER lumen, the UPR (UPR^{ER}) is triggered by aggregated unfolded proteins binding to the BiP chaperone. This results in the release of BiP's inhibition upon UPR transmembrane sensors, and the activation of ATF6α, IRE1α, and PERK. Subsequently, a series of transcription factors are upregulated to attenuate the originating ER stress (31). A similar, yet independent mechanism lies within the mitochondrial matrix and intermembrane space (29). This mitochondrial UPR (UPR^{MT}) also induces organelle-specific chaperones and proteases to restore inter-organelle homeostasis (3). If the unfolded proteins exceed the capacity of the folding machinery and proteostasis cannot be attained, autophagy, or ultimately, apoptosis are triggered (29, 37).

Although the UPR functions to attenuate cellular stress, it appears that a certain amount is required for optimal muscle differentiation (27, 42). Myotube fusion has been shown to be defective when ER stress is inhibited, and reversed with the induction of stress via a chemical inducer, thapsigargin (42). ER stress was also found to enhance myofiber formation due to triggered apoptosis, eliminating vulnerable cells (26). Hence, the UPR can be selectively

activated to control cell growth and proper tissue differentiation, which may have implications for myogenesis and muscle fiber size (6, 27, 42).

The UPR is also activated with exercise-induced mitochondrial biogenesis (19, 23, 44). Skeletal muscle has a relatively low mitochondrial content under basal conditions, but muscle mitochondria are highly adaptive during physiological processes such as myogenesis or exercise, in which the cellular energy demands are increased (8, 11, 14, 15). Both of these conditions trigger signal transduction pathways that activate the master transcriptional regulator PGC-1α, leading to an increased expression of nuclear and mitochondrial genes (32). This mitochondrial biogenesis requires signaling to transcription and translation for the production of additional proteins for import into the organelle. However, the signals preceding mitochondrial biogenesis remain enigmatic. Is the UPR required for adequate mitochondrial biogenesis, as it is for muscle differentiation? It is known that an increase in ER stress and UPR activation is associated with exercise, particularly in untrained subjects during acute contractile activity (19, 23, 44). This may serve as a precursor signaling system for exercise-induced mitochondrial biogenesis. Despite this, CHOP deletion, a stress induced transcription factor involved in both the UPR^{ER} and the UPR^{MT}, has been found to ameliorate phenotypic exercise intolerance (44), inferring a potential role of UPR components in mitochondrial adaptations. Therefore, it is of interest to us to investigate whether mitochondrial biogenesis relies upon intracellular communication with the UPR.

In order to investigate this, recent work has employed the chemical chaperone mimetic drug, Tauroursodeoxycholic acid (TUDCA) to attenuate stress-induced CHOP (23). TUDCA functions to diminish the terminal UPR^{ER} via assisting in protein folding in the ER lumen, and thus reducing overall stress induction and UPR activation (9, 23, 40). Recently, it was observed

that the mitochondrial biogenesis induced in TUDCA-injected rats undergoing chronic contractile activity (CCA) did not significantly differ from those injected with vehicle control (23). Therefore, this would suggest that the exercise-induced mitochondrial adaptations occurred independently of ER stress induced CHOP expression. Thus, the purposes of the present study were to investigate the necessity of the UPR during mitochondrial biogenesis induced during muscle cell differentiation, as well as subsequent chronic contractile activity, with a specific focus on the role of CHOP protein.

Methods

Cell culture. C_2C_{12} murine skeletal muscle cells were proliferated on 6-well cell culture plates in Dulbecco's modified Eagle's medium (DMEM) supplemented with 10% fetal bovine serum and 1% penicillin-streptomycin (P/S) [growth medium (GM)]. The cells were incubated at 37˚C in 5% CO_2. Upon reaching 95-100% confluency, the medium was switched to DMEM supplemented with 5% heat-inactivated horse serum and 1% P/S in order to induce differentiation of the myoblasts into myotubes. Cells were harvested either immediately prior to the GM being switched to differentiation medium (DM; day 0), or 4 days after differentiation in DM. The DM was changed daily. To investigate the role of the UPR in myoblast differentiation, we aimed to attenuate UPR activation prior to cells exiting the cell cycle. Thus, tauroursodeoxycholic acid (TUDCA; Millipore) was used for the partial inhibition of the UPR^{ER} (23). Cells were grown to subconfluence and then pretreated with 500 µg/ml of either water or TUDCA in GM for 24 h. Thereafter, cells were switched to DM in the absence of TUDCA to differentiate for 4 days prior to subsequent collection.

Fusion Index. For quantification of myoblast fusion, cells were washed twice with ice-cold phosphate-buffered saline (PBS, Sigma-Aldrich) and fixed in 100% methanol at -20˚C for 5 minutes before being left to air dry for 10 minutes. Wells were then incubated in 1 mL of Giemsa stain (Electron Microscopy Sciences, Hatfield, PA) diluted 1:20 in 1 mM sodium phosphate buffer (pH 5.6) for 10 minutes at room temperature. Thereafter, the solution was aspirated and rinsed with distilled water. Phase-contrast images were captured using a Canon Powershot G5 camera adapted to a light microscope at a 10× magnification. Nuclei were also manually counted from three randomly chosen regions per experimental group. The fusion index was calculated by determining the fraction of total nuclei found in myotubes. Myotubes were defined as cells with two or more nuclei (43). All treatments were performed in triplicate.

Fluorescence microscopy. C_2C_{12} muscle cells were grown and differentiated on custom made glass bottom 6-well dishes that were pre-coated with gelatin. On day 4 of differentiation, myotubes were treated with 100 nM of MitoTracker Green FM (Life Technologies) and incubated at 37℃ for 45 minutes. Following incubation, the media was aspirated and the cells were washed with PBS and re-incubated in fresh DM. Fluorescence was visualized using the Nikon Eclipse TE2000-U microscope. All images were captured at the same exposure.

Electrical Stimulation. Myotubes were stimulated on the fifth day of differentiation, as done previously (7, 39). In brief, customized six-well plate lids outfitted with two platinum wires per well were submerged into the media of plates. The DM was changed 1 h before stimulation and immediately after. For TUDCA experiments, fully differentiated myotubes were treated with 500 µg/ml of either TUDCA or sterile water in DM on day 5, 1 h prior to chronic contractile activity (CCA), and was replenished following stimulation. Electrically-induced CCA was conducted for 3 h per day (9V, 5Hz) with 21 h recovery periods for a total of 4 days. Cells were harvested on the fifth day, 21 hours after the last stimulation.

Transfection. On day 3 of myotube differentiation, cells were incubated in pre-transfection media (5% HS in DMEM). The following day, myotubes were transfected for 6 h with 30 nM of scrambled (Silencer select negative control; Life technologies; 4390846;) or CHOP siRNA (Life Technologies; s201245 and s64888) using 10 µl of Lipofectamine 2000 in 2 ml of DMEM. The media was then changed back to DMEM supplemented with 5% HS and 1% P/S. On day 5, cells were kept under control conditions or were subjected to CCA, as described previously (7, 39). On day 6, cells were incubated in pre-transfection media for another siRNA treatment of 6h transfection at day 7 prior to subsequent stimulation. Cells were collected 21 h after the fourth day of CCA.

Protein Extraction. Cells were rinsed twice with ice-cold PBS and then trypsinized at 37 ˚C for collection on days 0 and 4 of differentiation. Protein extracts were prepared by suspending the collected cells in lysis buffer supplemented with protease and phosphatase inhibitors. Thereafter, the cells were frozen in liquid N_2 and subsequently thawed in a 37˚C water bath for 5 freeze-thaw cycles. Following centrifugation at 16,000 *g* at 4˚C for 10 minutes, the pellets were discarded and the supernatant fractions were collected and stored at -80 ˚C for subsequent immunoblotting analysis.

Immunoblotting. The protein content of samples were measured using the Bradford method. Equal amounts of protein (25-50 µg) were separated by electrophoresis on 8-15% SDS-polyacrylamide gels. The proteins were then wet transferred (Mini Trans-Blot electrophoretic transfer cell, Bio-Rad, Mississauga, Canada) onto nitrocellulose membranes. After blocking the membranes for 1 h in 5% skim milk, they were then probed overnight at 4˚C with primary antibodies. For full list of proteins probed and antibodies, see Table 1. Blots were washed (3 × 5 min) in 1 × TBST [Tris-buffered saline-Tween-20, 25 mM Tris·HCl (pH 7.5), 1 mM NaCl, and 0.1% Tween-20] solution and incubated for 1 h at room temperature with the appropriate anti-mouse or anti-rabbit secondary antibody, followed by 1 × TBST wash (3 × 5 min). Membranes were visualized with enhanced chemiluminescence using Clarity Western ECL Substrate (Bio-Rad) and exposed to film. Signals were quantified with Image J Software (NIH, Bethesda, MD, USA). Values were normalized to the appropriate loading controls: α-Tubulin, β-Actin, or GAPDH.

Statistical analysis. All data are represented as means ± SEM. Comparisons between days 0 and 4 were made with Student's paired t-tests. Similar statistics were performed for the differentiated TUDCA-treated versus vehicle cells, as well as for control versus CCA myotubes. For

experiments involving CCA in combination with TUDCA-treatment or CHOP siRNA, two-way ANOVA were performed followed by Bonferroni's Post Hoc tests when appropriate. Analyses were made with GraphPad Prism 7.0. Differences were considered significant if $p < 0.05$.

Table 1. List of primary antibodies used for immunoblotting.

Antibody	Manufacturer	Product No.
α-Tubulin	Millipore	CPO6
ATF4	Santa Cruz Biotechnology	SC-200
ATF6	Santa Cruz Biotechnology	SC-22799
β-Actin	Santa Cruz Biotechnology	SC-47778
BiP	Cell Signaling	3183S
CHOP	Cell Signaling Santa Cruz Biotechnology	2895 SC-7351
COX I	Abcam	Ab14705
COX IV	Abcam	Ab14744
CPN10	Enzo Life Sciences	ADI-SPA-110
GAPDH	Abcam	Ab8245
MHC-II (MY-32)	Abcam	Ab51263
mtHSP60	Enzo Life Sciences	ADI-SPA-806
mtHSP70	Enzo Life Sciences	ADI-SPA-825
PGC-1α	Millipore	AB3242
Tfam	In house	n/a
Sirt3	Cell Signaling	5490S

Results

Differentiation model of C_2C_{12} induces mitochondrial biogenesis. C_2C_{12} cells were stained with MitoTracker Green (Life Technologies) on day 0 and 4 of differentiation to identify the mitochondrial network. As depicted in Fig. 1A, myotubes had greater green fluorescence representing a higher mitochondrial content than myoblasts. To confirm this qualitative analysis, C_2C_{12} whole-cell lysates were collected at days 0 and 4 of differentiation and mitochondrial markers were probed as measure of mitochondrial content. COX-I, a mitochondrially-encoded subunit of Complex IV, increased by 5-fold from day 0 to 4 ($P < 0.05$; Fig. 1C). Similarly COX-IV, a nuclear-encoded subunit of Complex IV increased 3-fold by day 4 of differentiation ($P < 0.05$; Fig. 1D). During the same timeframe, a 2-fold increase in mitochondrial transcription factor, Tfam ($P < 0.05$; Fig. 1E) was also observed. These data strongly confirm the increase in mitochondrial biogenesis during myocyte differentiation, similar to previous studies (8, 21).

The UPR is selectively activated during differentiation. UPR protein markers of both the ER and mitochondria were analyzed in whole cell lysates at days 0 and 4 of differentiation by immunoblotting. The intra-mitochondrial chaperones, mtHSP70, mtHSP60, and CPN10 were all decreased significantly by day 4 ($P < 0.05$; Figs. 2B-D). In contrast, the antioxidant protein Sirt3 increased by 3-fold during differentiation (Fig. 2E). In relation to the UPR^{ER} markers, there was no change in CHOP protein between days 0 to 4 of differentiation (Figs. 2F) however, transcription factor ATF4 increased by 3.4–fold at day 4 ($P < 0.05$; Fig. 2G). BiP chaperone was at undetectable immunoblotting levels at day 0 but increased significantly by day 4 indicative of increased ER stress ($P < 0.05$; Fig. 2H). Taken together, the UPR^{ER} is activated while there is a decrease in UPR^{MT} activity, with a very selective UPR^{MT} protein induction in response to differentiation in muscle cells.

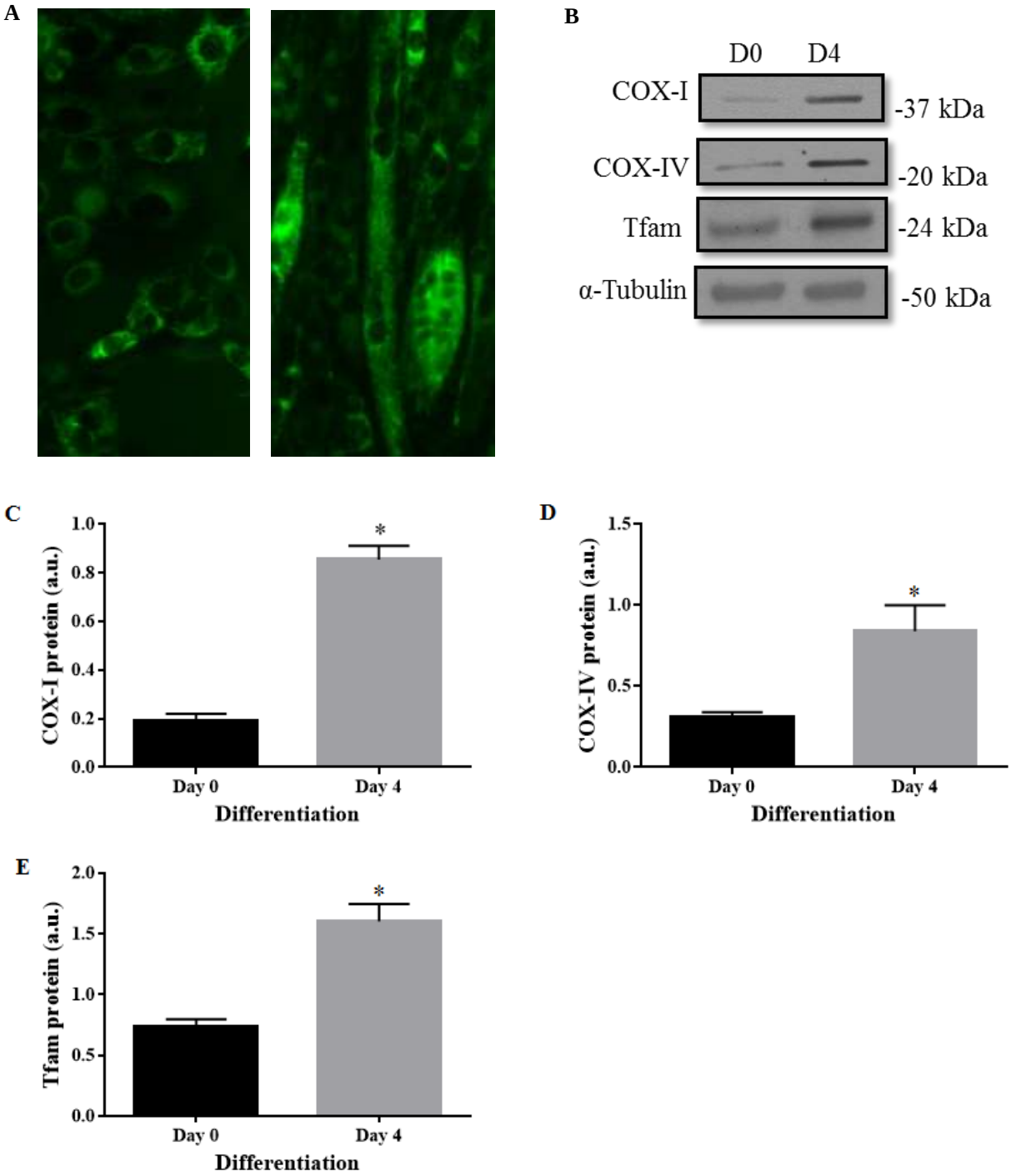

Figure 1. *C_2C_{12} differentiation induces mitochondrial biogenesis. (A)* MitoTracker green fluorescent images captured at 20× magnification of C_2C_{12} myoblasts versus myotubes on day (D) 4 of differentiation. *(B)*Representative western blots and graphical quantifications of: *(C)* COX-I, *(D)* COX-IV, *(E)* and Tfam at days (D) 0 and day 4 of differentiation. Data are represented as mean ± SEM and are measured in arbitrary units (a.u.). (*, $P < 0.05$ vs. day 0; n=3 experiments).

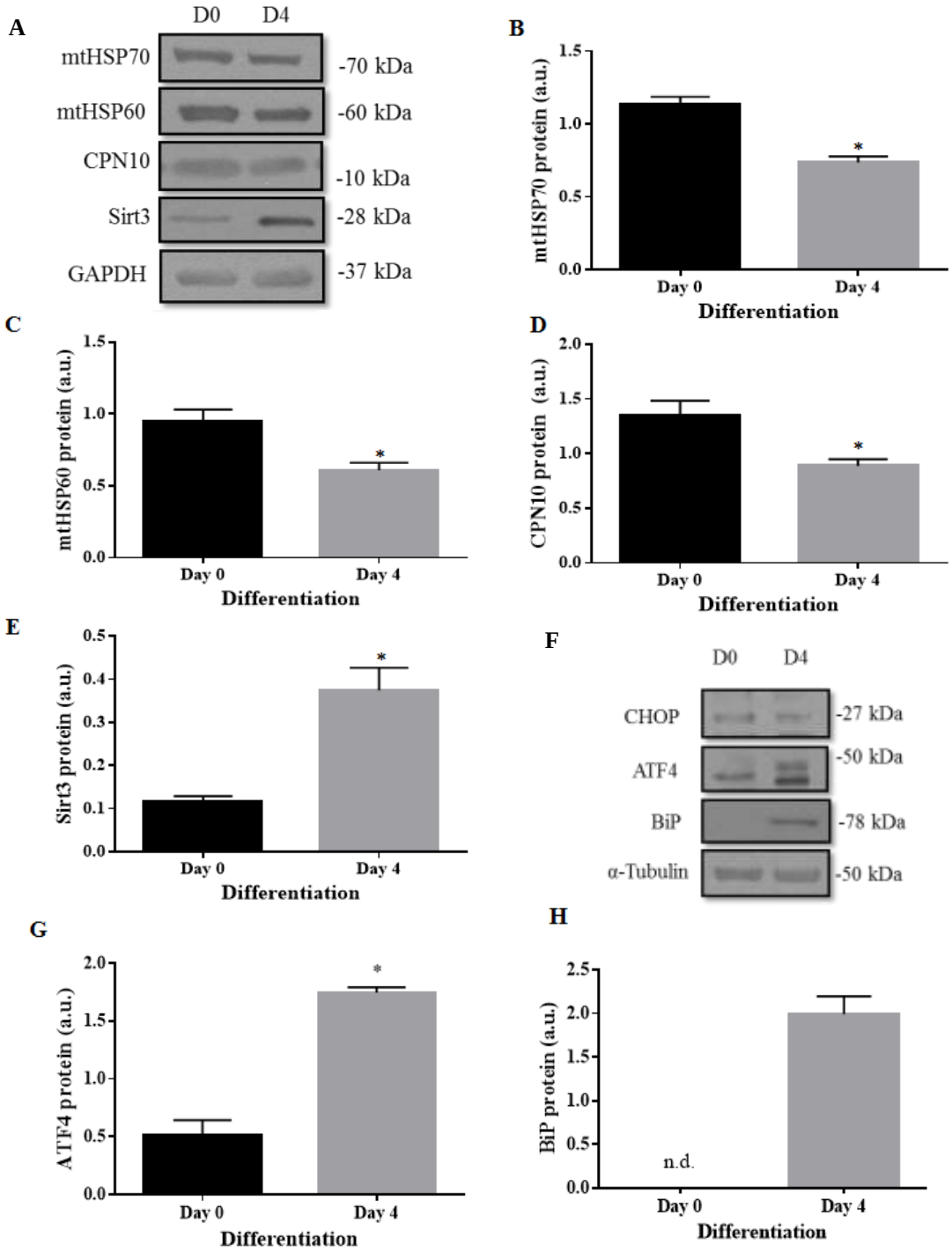

Figure 2. *Skeletal muscle differentiation induces ER stress while the UPR^{MT} is largely inactivated*. *(A)* Representative western blots of *UPR^{MT}* markers. Graphical quantifications of muscle cells during differentiation on days (D) 0 and 4: *(B)* mtHSP70, *(C)* mtHSP70, *(D)* CPN10, and *(E)* Sirt3. *(F)* Representative blots of *UPR^{ER}* markers. *(G)* Graphical quantification of *(G)* ATF4 and *(H)* BiP. Data are represented as mean ± SEM and are measured in arbitrary units (a.u.). (*, $P < 0.05$ vs. day 0; n.d., not detectable; n=3 experiments).

UPR^{ER} inhibition with TUDCA augments mitochondrial content, despite reduced differentiation. Cultured murine myoblasts were pretreated with one dose of TUDCA for 24 h prior to subsequent differentiation for 4 days. Phase-contrast images of stained cells were captured at day 4 of differentiation (Fig. 3A) to assess the fusion index (FI) as a measure of myotube formation. In vehicle-treated cells, differentiation was accompanied by enhanced myotube formation and fusion, as expected. In comparison to vehicle, cells treated with TUDCA had a greater number of nuclei dispersed outside of the myotubes remaining as unfused myoblasts (Fig. 3A). The percent of nuclei in myotubes (fusion index, (FI)) on day 4 of differentiation in TUDCA-treated cells (73%) was less than the vehicle (89%; $P < 0.05$, Fig. 3B). In addition, significantly less MHC-II was present in TUDCA-treated cells than in the vehicle-treated cells, due to fewer myotube formations by day 4 ($P < 0.05$; Fig. 3C). Thus, partial inhibition of the UPR with TUDCA compromises myoblast fusion and the differentiation of muscle cells into myotubes.

To gain a better insight into the significance of the UPR in differentiation-induced mitochondrial biogenesis, mitochondrial biogenesis markers were measured on day 4 of differentiation in vehicle- and TUDCA-treated cells. While Tfam was unaffected by TUDCA treatment, PGC-1α, COX-I, and COX-IV were all ~1.3 to 1.5-times higher than control ($P < 0.05$; Figs. 3D-G). Our results suggest that inhibition of the UPR^{ER} during myogenesis augments mitochondrial content, despite reduced differentiation.

TUDCA pretreatment in myoblasts decreased BiP induction but had no impact upon the UPR^{MT} after 4 days of skeletal muscle differentiation. UPR protein markers were assessed at day 4 of differentiation after 24 h of TUDCA or vehicle treatment in myoblasts. UPR^{MT} markers mtHSP70, mtHSP60, and its co-chaperone CPN10, and Sirt3 were not affected by TUDCA, as protein levels remained elevated at day 4 of differentiation, 4 days after the treatment (Figs. 4A).

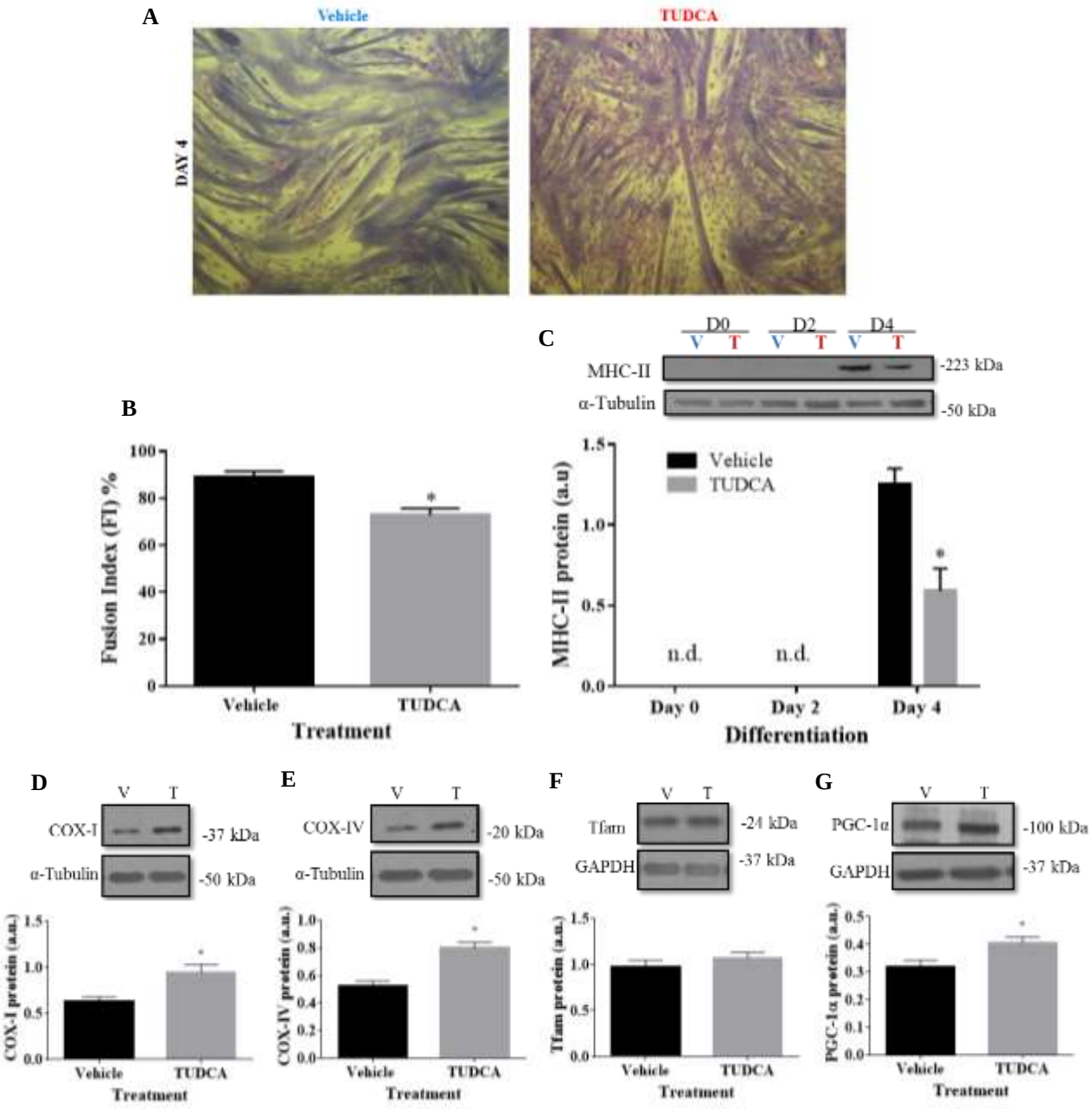

Figure 3. *TUDCA treatment increases mitochondrial biogenesis markers despite inhibiting differentiation.* C_2C_{12} cells were pretreated once for 24 h at subconfluence with TUDCA (T) or water [vehicle (V)] prior to either immediate collection (day 0) or differentiation (for 2 or 4 days). *(A)* Phase-contrast imaging was captured on day (D) 4 of differentiation. Lightly-stained dots represent nuclei. *(B)* Fusion index (FI) was calculated as % of nuclei within myotubes. *(C)* Representative blot and quantification of MHC-II during differentiation D0, D2, and D4 of pretreated cells. Representative western blots and their graphical summaries in TUDCA-treated cells mitochondrial markers: *(D)* COX-I, *(E)* COX-IV, *(F)* Tfam, and *(G)* PGC-1α level measured in arbitrary units (a.u.). Data are represented as mean ± SEM. (*, $P <$ 0.05 vs. vehicle (V); n.d., not detectable; n=3 to 10 experiments).

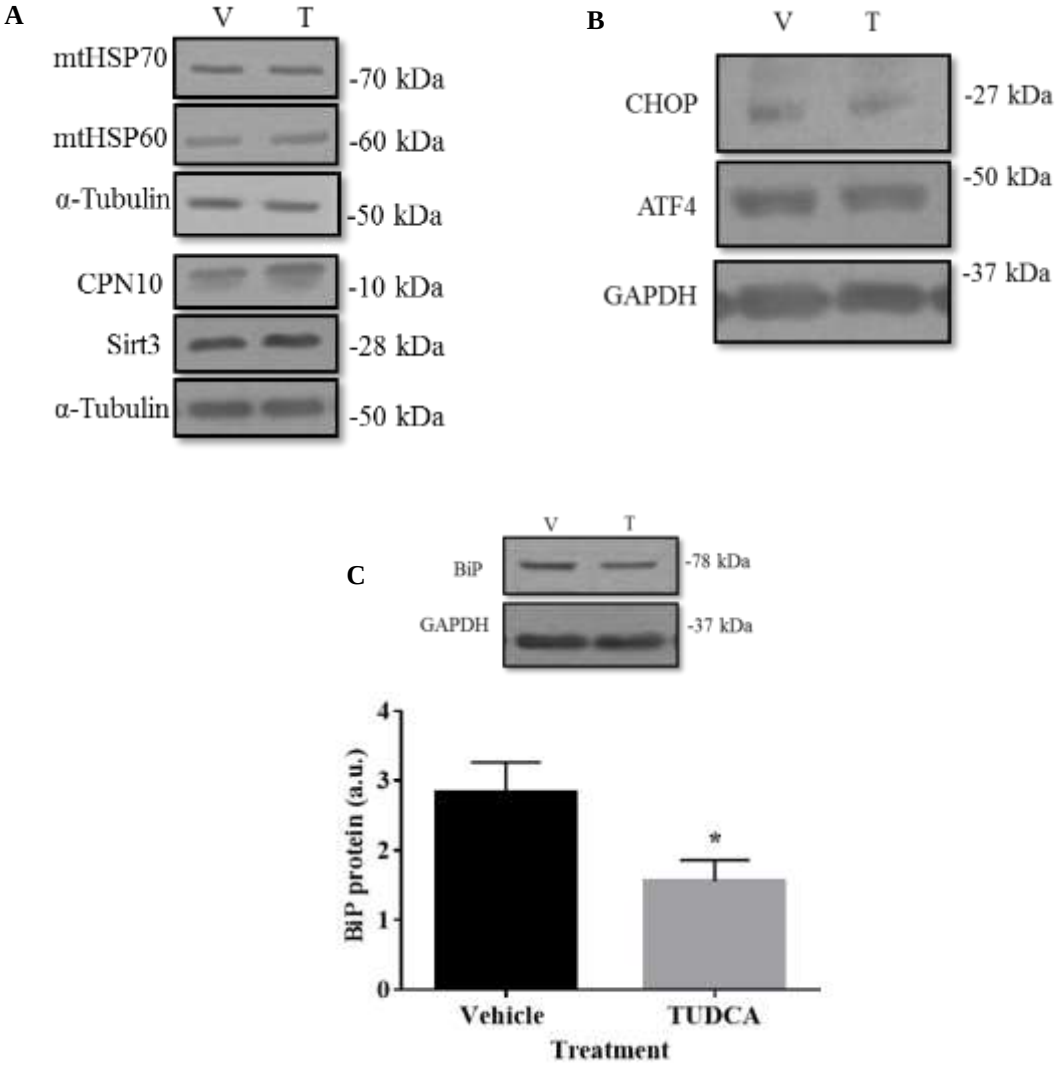

Figure 4. *TUDCA treatment decreased BiP protein but had no impact upon the UPR^{MT} after 4 days of skeletal muscle differentiation.* Cells were pretreated for 24 h in 500 µg/ml of TUDCA (T) or water [vehicle (V)] prior to differentiation for four days. Representative western blots of UPR^{MT} proteins *(A)* mtHSP70, mtHSP60, CPN10, and Sirt3 were all similar in protein expression between vehicle- or TUDCA-treated cells. No effect of TUDCA was observed for UPR^{ER} markers *(B)* CHOP and ATF4. *(C)* Representative blot and graphical quantification of BiP protein. α-Tubulin serves as the loading control. Data are represented as mean ± SEM and are measured in arbitrary units (a.u.). (*, $P < 0.05$ vs. vehicle; n=3 or 4 experiments).

Additionally, there was no difference in UPR^{ER} markers CHOP and ATF4 protein content between treated and vehicle cells on day 4 of differentiation (Figs. 4B). However, levels of the ER chaperone BiP were attenuated by 45% in TUDCA-treated cells ($P < 0.05$; *Fig*. 4C).

TUDCA treatment attenuates the increase in CHOP, while augmenting CCA-induced mitochondrial biogenesis. To confirm whether our CCA-model induces mitochondrial biogenesis, murine skeletal muscle cells were electrically stimulated on day 5 of differentiation for 4 consecutive days. As expected, CCA augmented COX-I and COX-IV by approximately 2.7-fold, and PGC-1α levels by 1.9-fold ($P < 0.05$; Figs. 5A-C). Incubating cells with TUDCA from day 5 of differentiation increased mitochondrial markers in both resting (control) and CCA conditions, with a larger effect of TUDCA on COX-I and PGC-1α levels under CCA stimulated conditions relative to the vehicle-treated myotubes ($P < 0.05$; Figs. 5D and 5F). Interestingly, the nuclear-encoded subunit COX-IV was increased by 2.6-fold with CCA as expected, but this increase was dependent upon the presence or absence of TUDCA ($P < 0.05$; Fig. 5E). These findings suggest that CCA-induced mitochondrial biogenesis can be augmented under conditions of potent TUDCA treatment in skeletal muscle cells.

With respect to UPR markers, TUDCA inhibited CCA-induced CHOP on both day 2 and 4 of stimulation by 64% and 30% respectively relative to control, thus attenuating this branch of the UPR^{ER} during CCA ($P < 0.05$; Fig. 6A). Of note, CHOP levels were unaltered by TUDCA under control conditions. In accordance with previously conducted studies, TUDCA inhibition of CHOP was not significant at basal levels unless an additional stressor was included (23). Furthermore, TUDCA had no impact on upstream general UPR^{ER} signaling evident by unchanged ATF4 and BiP content (Figs. 6C and 6D).

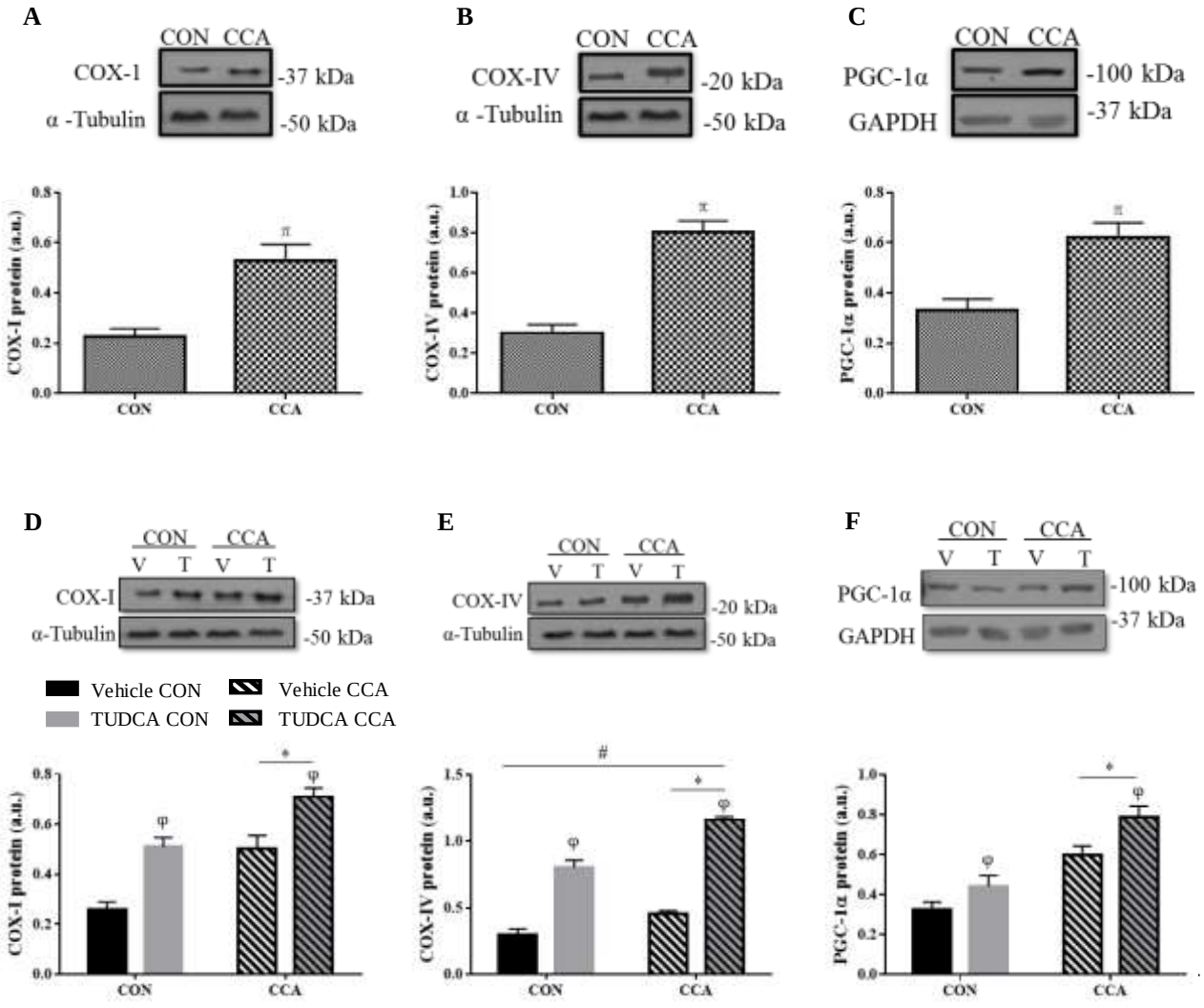

Figure 5. *Chronic contractile activity induces mitochondrial biogenesis and is further augmented with TUDCA treatment.* C_2C_{12} cells were differentiated for 5 days prior to chronic contractile activity (CCA) for 4 successive days. Representative blots and graphical representations of mitochondrial markers *(A)* COX-I, *(B)* COX-IV, and *(C)* PGC-1α. Representative blots and graphical representations of cells treated with either TUDCA (T) or water (vehicle [V]) before and after CCA: *(D)* COX-1, *(E)* COX-IV, and *(F)* PGC-1α. Data are represented as mean ± SEM and are measured in arbitrary units (a.u.). (π, $P < 0.05$ vs. control (CON); *, $P < 0.05$ main effect of CCA; φ, $P < 0.05$ main effect of TUDCA treatment; #, $P < 0.05$ interaction effect of CCA and TUDCA treatment; n=5 to 7 experiments).

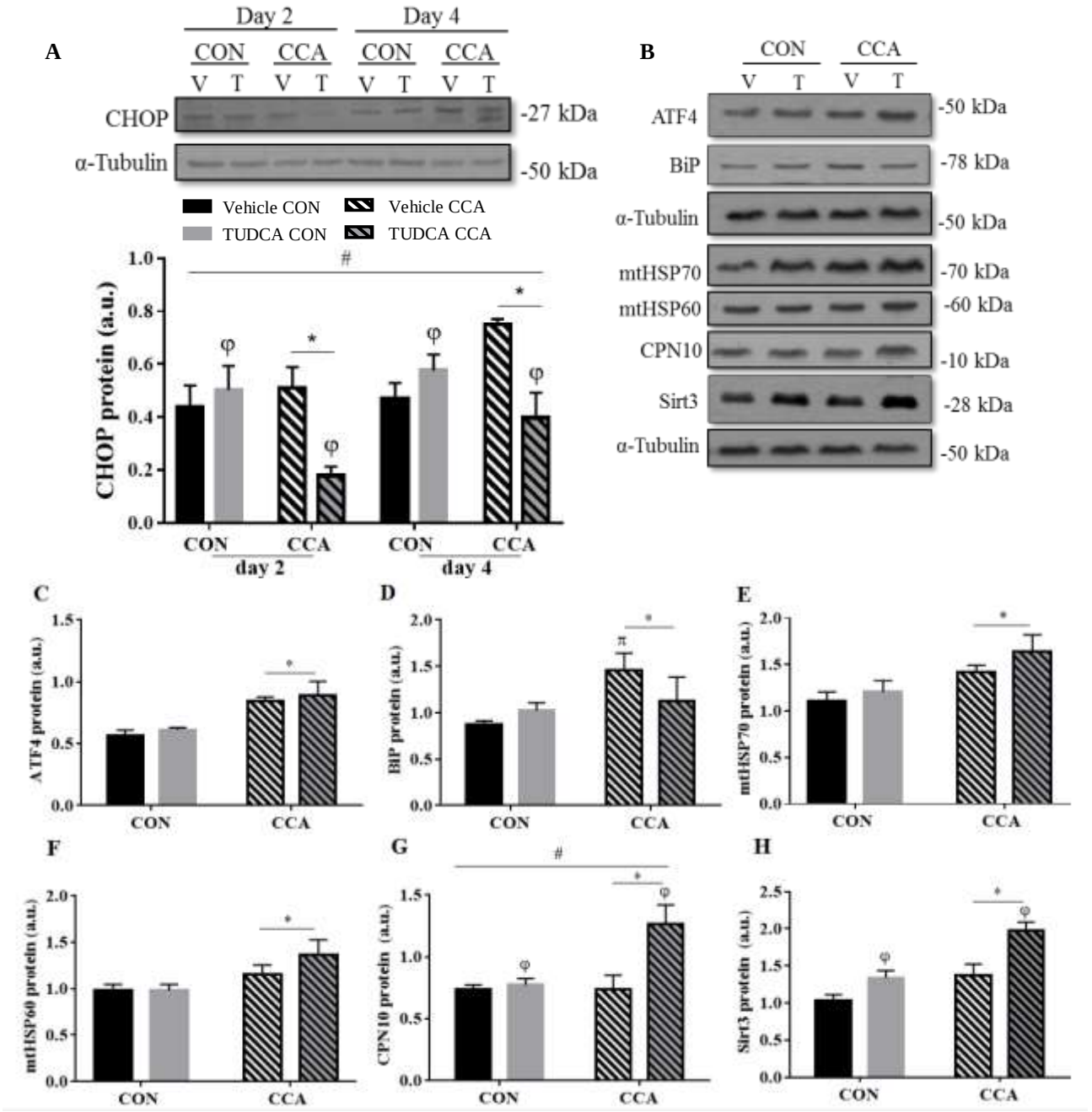

Figure 6. *TUDCA attenuates ER stress-induced CHOP associated with CCA and increases UPR^{MT} antioxidant marker Sirt3 and CPN10 chaperone.* C_2C_{12} cells were differentiated for 5 days one hour before chronic contractile activity (CCA), cells were treated with either TUDCA (T) or water (vehicle [V]) for 4 consecutive days prior to collection. *(A)* UPR^{ER} marker CHOP representative blot and graphical representation. *(B)* Representative blots of other UPR markers and their graphical representations: *(C)* ATF4, *(D)* BIP, *(E)* mtHSP70, *(F)* mtHSP60, *(G)* CPN10, and *(H)* Sirt3. Data are expressed as mean ± SEM and are measured in arbitrary units (a.u.). (π, $P < 0.05$ vs. control; *, $P < 0.05$ main effect of CCA; φ, $P < 0.05$ main effect of TUDCA treatment; #, $P < 0.05$ interaction effect of CCA and TUDCA treatment; n=4 to 6 experiments).

TUDCA enhances the UPR^{MT} antioxidant response and CPN10 induction with CCA. As discussed above, UPR^{ER} markers CHOP, ATF4, and BiP remained unaffected with TUDCA treatment under basal conditions (Fig. 6A, 6C and 6D). Similar results were obtained basally with UPR^{MT} chaperones mtHSP70, mtHSP60, and CPN10 (Fig. 6E-6G). However, the mitochondrial antioxidant marker of the UPR, Sirt3, increased by 30% ($P < 0.05$; Fig. 6G) with TUDCA treatment in comparison to vehicle control.

UPR^{ER} transcription factor ATF4 was elevated by an average of ~48% with CCA-induced stress, regardless of treatment ($P < 0.05$; Fig. 6C). BiP levels were augmented with CCA as well, particularly in vehicle-treated cells (66% vs. 8%; $P <0.05$; Fig. 6D). Likewise, UPR^{MT} markers increased with CCA, as displayed by the elevated levels of mtHSP70, mtHSP60, and Sirt3 ($P < 0.05$; Figs. 6E, 6F, and 6H). Moreover, similar to basal levels, Sirt3, was 44% greater with in TUDCA-treated cells ($P < 0.05$; Fig. 6H), putatively as an antioxidant response accompanying the augmented mitochondrial content. Interestingly, CPN10 was augmented by 1.7-fold with CCA only upon TUDCA treatment ($P < 0.05$; Fig. 6G).

CHOP is required basally for correct stoichiometry of electron transport chain subunits, and is compensated with CCA. Since TUDCA attenuated CCA-induced CHOP expression, but led to an increase in mitochondrial markers during differentiation and as a result of CCA, it was of interest to investigate whether knocking down CHOP via siRNA would reproduce similar results of augmenting mitochondrial biogenesis. One day prior to CCA on day 4 of differentiation, C_2C_{12} cells were transfected with CHOP or scrambled siRNA. To prolong the knockdown during the subsequent 4-day CCA treatment, cells were transfected a second time on day 7. CHOP knockdown was confirmed at the protein level. Basally, CHOP levels in knockdown cells were reduced by 42% relative to control. Under CCA conditions, CHOP protein was induced by 3-fold

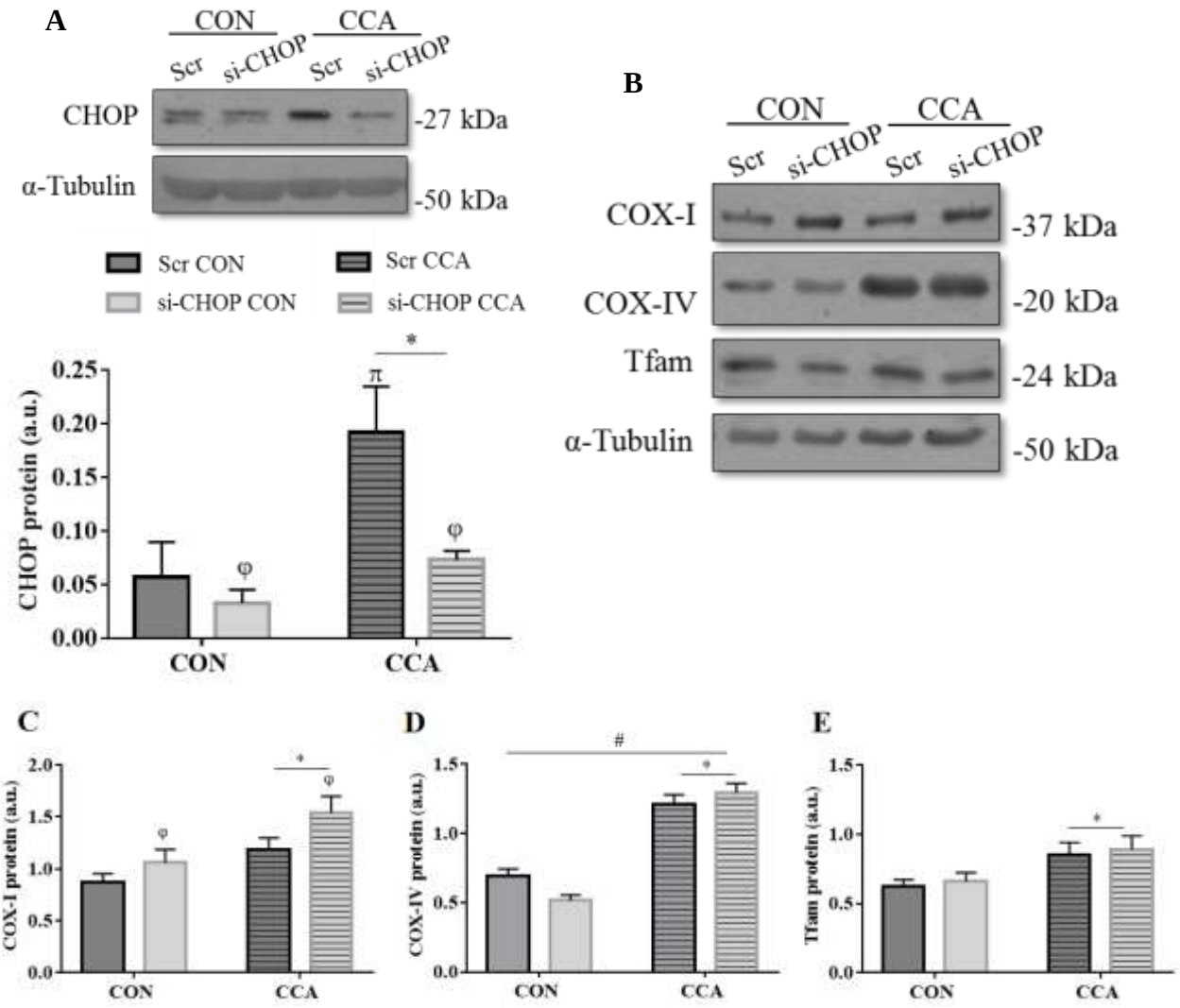

Figure 7. *CHOP influences mitochondrial content basally and is not required for CCA-induced mitochondrial biogenesis*. Cells were transfected with either 30 nM of scrambled (Scr) or CHOP siRNA (si-CHOP) on days 4 and 7 of differentiation. Myotubes underwent 4 days of successive chronic contractile activity (CCA) starting on day 5. *(A)* CHOP representative blot and graphical representation. *(B)* Representative blots and graphical representations of mitochondrial markers *(C)* COX-I, *(D)* COX-IV, and *(E)* Tfam. Data are expressed as mean ± SEM and are measured in arbitrary units (a.u.). (*, $P < 0.05$ main effect of CCA; φ, $P < 0.05$ main effect of CHOP siRNA; n=7 to 11 experiments).

in scrambled-treated cells, but there was no significant effect of CCA in knockdown cells ($P < 0.05$; Fig.7A).

In the presence of CHOP knockdown under basal conditions, mitochondrially-encoded COX-I increased by 1.2-fold, while nuclear-encoded proteins, COX-IV, decreased by 1.4-fold, and Tfam remained unaffected ($P < 0.05$; Fig. 7B-7E). In response to CCA, the increase in COX-I was further augmented by ~1.5-fold as expected, whereas remarkably, the COX-IV decrease observed basally in knockdown cells was compensated by 2.5-fold to levels comparable with scrambled-treated cells (Fig. 7C and 7D). Additionally, Tfam was elevated by 1.3-fold with CCA ($P < 0.05$; Fig. 7E). Altogether, the findings suggest that CHOP influences mitochondrial composition under basal conditions where mitochondrial biogenesis may be potentially impaired by orphaned electron transport chain (ETC) subunits, but this can be rescued with CCA. Moreover, the exercise-induced mitochondrial biogenesis does not rely on CHOP induction of either the ER or mitochondrial UPR.

Of note, general UPR signaling of both the mitochondria and ER remained unaffected by CHOP silencing, as represented by insignificant differences at basal levels (Fig. 8A-8F). UPR^{ER} proteins BiP and ATF4 ($P < 0.05$; Fig.8B and 8C), as well as UPR^{MT} markers mtHSP70, mtHSP60, and Sirt3, were all elevated with CCA indicative of persistent stress induction and UPR activation associated with muscle contractile activity ($P < 0.05$; Fig. 8D-8F). Contrary to TUDCA-treated cells undergoing CCA, CPN10 levels did not increase, but remained unaltered (Fig. 8A).

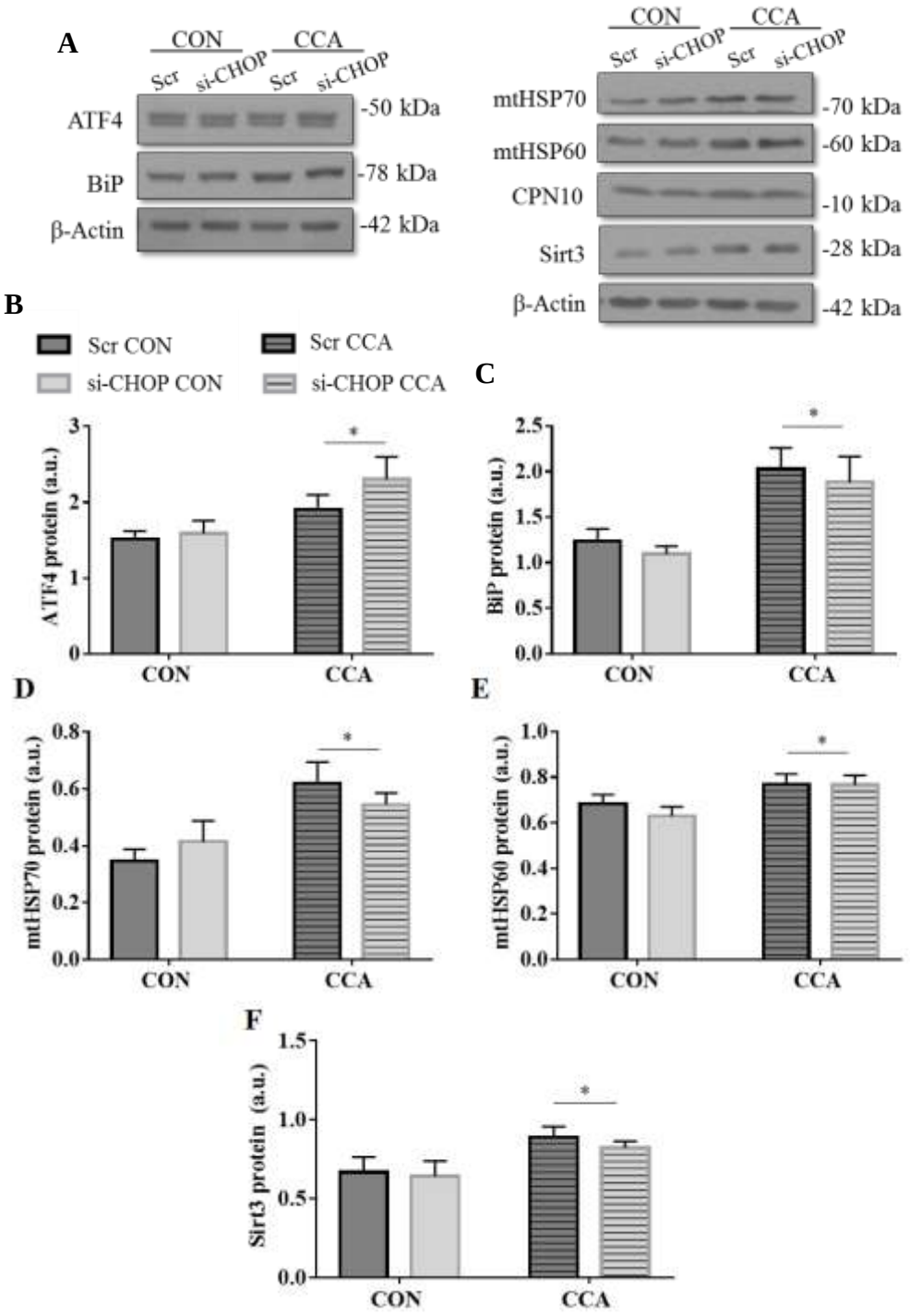

Figure 8. *CHOP knockdown in skeletal muscle cells had no impact on general UPR signaling*. C_2C_{12} cells were transfected with either 30 nM of scrambled (Scr) or CHOP siRNA (si-CHOP) on days 4 and 7 of differentiation. Chronic contractile activity (CCA) began on day 5. *(A)* Representative blots of $UPR^{MT/ER}$ markers. Graphical representations of UPR^{ER} markers *(B)* ATF4, *(C)* BiP, and UPR^{MT} markers *(D)* mtHSP70, *(E)* mtHSP60, and (F) Sirt3. Data are expressed as mean ± SEM and are measured in arbitrary units (a.u.). (*, $P < 0.05$ main effect of CCA; φ, $P < 0.05$ main effect of CHOP siRNA; n=4 to 7 experiments).

Discussion

Mitochondria provide energy in the form of ATP to maintain cellular metabolic homeostasis (38). However, mitochondria also have alternative roles in regulating other pathways such as autophagy (12, 18, 30), apoptosis (20, 25, 36, 41), and calcium homeostasis (10, 13, 22), all of which are vital to skeletal muscle health. During both muscle development and exercise, PGC-1α, the master regulator of mitochondrial biogenesis, is activated resulting in an increase in mitochondrial content (2, 8, 21, 23, 39). Mitochondrial biogenesis involves the synthesis of many nuclear- and mitochondrially-encoded proteins, and the increase in protein synthesis which occurs can potentially perturb cellular homeostasis by exceeding the protein folding capacity of the cell. Thus, to prevent this accumulation of unfolded proteins, the unfolded protein response (UPR) occurs in both the endoplasmic reticulum (UPR^{ER}) and the mitochondrion (UPR^{MT}). This involves the activation of a series of transcription factors to promote the transcription of genes encoding chaperones designed to assist in protein folding. Additionally, in an attempt to regain proteostasis, global protein translation is reduced. In this study, we hypothesized that this breadth of UPR signaling activation will impact mitochondrial adaptations induced either during skeletal muscle differentiation, or as a result of chronic contractile activity (CCA).

Similar to earlier work from our laboratory, C_2C_{12} muscle cell differentiation led to the upregulation of mitochondrial markers as a result of the induced biogenesis (8). Along with this mitochondrial biogenesis triggered during muscle development, our data depict the selective activation of UPR components, which corroborates previous findings (26, 27). In order to investigate the role of ER stress in particular, the terminal UPR^{ER} branch was partially inhibited using TUDCA. TUDCA functions as a chaperone mimetic to ameliorate ER stress by assisting in

protein folding (9, 40). As a result, pro-apoptotic factors CHOP and caspase-12 induction are reduced with TUDCA treatment in response to cellular stress (23, 40, 45). The partial inhibition of UPR^{ER} signaling prior to the onset of differentiation was verified in our model by the decrease in myotube differentiation. Reduced differentiation is characteristic of ER stress attenuation, due to less myoblast fusion and diminished stress-induced myoblast apoptosis (26, 27, 43). Additionally, the ER stress marker BiP protein was decreased at day 4 of differentiation. This is consistent with another study in which the attenuated protein expression of BiP in human liver cells was observed in response to UPR inhibition (45).

Surprisingly, despite the reduced myotube differentiation, augmented mitochondrial biogenesis was observed, indicated by increased mitochondrial markers in the presence of TUDCA. These changes in specific mitochondrial markers occurred with the accompaniment of large increases in ATF4, no changes in CHOP and a decrease in BiP protein level. This suggests that the attenuation of ER stress with TUDCA facilitated the synthesis of mitochondria, and that ATF4 may be important in directing this process. This occurred in the absence of increases in UPR^{MT} proteins mtHSP70, mtHSP60 and CPN10, suggesting that this induction is not central for differentiation-induced mitochondrial biogenesis.

We have previously shown that our cell culture model of CCA results in marked increases in mitochondrial biogenesis, as indicated by changes in MitoTracker green staining, increases in cellular respiration, as well as large changes in mitochondrial markers (24, 39). The current study confirmed these data, and further suggests that the increases in mitochondrial content are accompanied by only modest changes in UPR^{MT} markers, but large increases in BiP, as well as transcription factors ATF4 and CHOP. The inhibition of ER stress with TUDCA led to a further increase in the expression of mitochondrial markers, including PGC-1α, which was

additive with the CCA effect. This occurred despite the fact that the levels of an important transcription factor of the UPR, CHOP, were reduced or unchanged in the presence of TUDCA, while the increases in ATF4 and BiP were unaffected. This suggests that increases in mitochondrial content produced by CCA occur independently of CHOP, but that ATF4 and BiP may be important for the adaptation observed. Importantly also, components of the UPR^{MT} (mtHSP70, mtHsp60 and CPN10) tended to be further elevated during CCA in the presence of TUDCA, suggesting an improvement in intra-organelle protein trafficking and folding capacity as a result of combined treatment of contractile activity and ER stress attenuation.

Our results indicate that the dampening of ER stress with TUDCA improves both differentiation- and CCA-induced mitochondrial biogenesis, while selectively enhancing the UPR^{MT} response during CCA. We were surprised by this result because our previous *in vivo* findings indicated that mitochondrial adaptations during CCA were largely independent of the presence of TUDCA and partial UPR^{ER} inhibition (23). Indeed, the UPR^{ER} inhibition with TUDCA *in vivo* did not amplify CCA-induced mitochondrial markers, such as PGC-1α protein and COX-IV (23) as we found in the current study. This may be the result of a differential magnitude of the TUDCA effect *in vitro* versus *in vivo*, and this requires further investigation.

Wu et al. (44) have previously shown that the absence of CHOP had the potential to lead to an improvement in exercise tolerance. Since favourable changes in endurance are most often attributed to alterations in mitochondrial content, we wanted to verify whether the specific knockdown of CHOP would enhance mitochondrial content in the presence of CCA. Thus, we employed siRNA techniques, as we have done previously (17, 39), to partially reduce CHOP levels. siRNA treatment of myotubes effectively decreased CHOP levels by 43% under basal conditions, and prevented the typical large increase in CHOP which is normally induced by

CCA. Importantly, the increases in other important components of the UPR^{ER} pathway, including BiP and ATF4, were unaffected by CHOP knockdown, and were increased by CCA as expected. The reduction of CHOP under basal conditions led to parallel decreases in nuclear-encoded COX-IV levels, no change in Tfam protein, and reciprocal levels of COX-I subunits, suggesting that CHOP would normally impact the transcription of COX-IV and mtDNA in an opposite fashion. The effect of CCA served to rescue the decline in COX-IV brought about by the absence of CHOP, and had an additive effect on the level of the mtDNA-encoded subunit, COX-I. The expression of the UPR^{MT} components mtHSP70, mtHSP60 and CPN10 was unaffected by CHOP knockdown under basal conditions, or as a result of CCA, as a normal increase was observed. This occurred despite the fact the UPR^{MT} genes are activated through a CHOP-dependent pathway (1, 46). In the nucleus, CHOP forms a heterodimer with C/EBPβ (CCAAT enhancer-binding protein) creating an active transcription factor to upregulate mitochondrial quality control genes (1, 16, 46). However, an overexpression study of CHOP in monkey kidney cells revealed that this protein is not sufficient for the induction of the UPR^{MT} proteins in the presence of stress, and thus, other transcription factors are likely involved (1), certainly in muscle. Alternatively, it may be that the degree of CHOP knockdown was insufficient to exert its effects upon its UPR^{MT} downstream targets. What is evident from our study is that any mitochondrial protein expression imbalance created by the absence of CHOP can be fully rescued by CCA, indicating that CCA triggers alternative signaling pathways to maintain mitochondrial content and composition.

In both TUDCA-treated cells as well as in the presence of CHOP siRNA, CHOP-induction was reduced under cellular stress. However, in contrast to the results obtained in TUDCA-treated cells, siRNA-induced CHOP knockdown did not further augment mitochondrial

biogenesis, under either basal or CCA conditions. As CHOP knockdown did not reproduce similar results to TUDCA-treated cells in enhancing mitochondrial content, the observed increase in mitochondrial content with the drug treatment could be attributed to its pleiotropic effects in activating other mitochondrial biogenesis pathways. An alternative explanation may be that TUDCA has an overall attenuating effect upon cellular stress via facilitation of protein folding in the ER lumen (4, 9, 28, 40). Wilson et al. have suggested that this may result in a reduced ATP consumption by the UPR^{ER} pathway, potentially increasing the energy availability for mitochondrial biogenesis (34). Consequently, a potential increase in protein import into the mitochondria may further activate the UPR^{MT} to ameliorate the mitochondrial stress associated with increased biosynthesis, as observed with our results.

Altogether, it is clear that the UPR is involved to some extent, in exercise-induced remodelling. In Wu's et al.'s (44) study, the adaptation of ER stress markers to repeated bouts of treadmill running occurred prior to increases in mitochondrial cytochrome c, a surrogate marker of mitochondrial content, suggesting that initial improvements to ER proteostasis precede that of the synthesis of mitochondrial proteins (35). Additionally, ATF6 has been implicated during the recovery phase following exercise through a physical interaction with PGC-1α to trigger UPR signaling (44). Thus, a PGC-1α-mediated response suggests that the triggered UPR may be interlinked with other training adaptive responses that are similarly regulated by PGC-1α (35). Moreover, it is likely that different components of the UPR engage in crosstalk with other signaling pathways that are integral to skeletal muscle health (5). Thus, to better delineate what function the UPR serves in mitochondrial adaptations, UPR components other than CHOP, such as ATF6 or ATF5, should be eliminated to tease out whether distinct mechanisms are utilized by

different arms of the UPR, as they may differentially be engaged in crosstalk with other pathways.

In summary, our findings suggest that mitochondrial biogenesis activated during muscle development from the myoblast to the myotube stage is CHOP-independent, and may rely upon other components of the UPR^{ER} to facilitate mitochondrial synthesis. Under basal, steady state conditions, CHOP can influence mitochondrial composition by altering the correct stoichiometry of nuclear- and mitochondrially-encoded proteins of the electron transport chain. This can be salvaged by contractile activity in which other compensatory and redundant pathways of mitochondrial biogenesis may be triggered. Indeed, CCA-induced mitochondrial adaptations occur irrespective of CHOP-induction, and may be augmented via amelioration of ER stress to increase mitochondrial content further. Our study sheds light upon the necessity of UPR signaling for mitochondrial biogenesis during muscle phenotypic adaptations.

References

1. **Aldridge JE**, **Horibe T**, **Hoogenraad NJ**. Discovery of genes activated by the mitochondrial unfolded protein response (mtUPR) and cognate promoter elements. *PLoS One* 2: e874, 2007.

2. **Baar K**, **Wende AR**, **Jones TE**, **Marison M**, **Nolte LA**, **Chen M**, **Kelly DP**, **Holloszy JO**. Adaptations of skeletal muscle to exercise: rapid increase in the transcriptional coactivator PGC-1. *FASEB J* 16: 1879–86, 2002.

3. **Baker BM**, **Haynes CM**. Mitochondrial protein quality control during biogenesis and aging. *Trends Biochem Sci* 36: 254–261, 2011.

4. **Berger E**, **Haller D**. Structure-function analysis of the tertiary bile acid TUDCA for the resolution of endoplasmic reticulum stress in intestinal epithelial cells. *Biochem Biophys Res Commun* 409: 610–5, 2011.

5. **Bohnert KR**, **Gallot YS**, **Sato S**, **Xiong G**, **Hindi SM**, **Kumar A**. Inhibition of ER stress and unfolding protein response pathways causes skeletal muscle wasting during cancer cachexia. *FASEB J* 30: 3053–68, 2016.

6. **Bradshaw RA**, **Dennis EA**, editors. Regulation of organelle and cell compartment signaling. London: Elsevier Academic Press, 2011, p. 374, 413.

7. **Carter HN**, **Hood DA**. Contractile activity-induced mitochondrial biogenesis and mTORC1. *Am J Physiol Cell Physiol* 303: C540-7, 2012.

8. **Collu-Marchese M**, **Shuen M**, **Pauly M**, **Saleem A**, **Hood DA**. The regulation of mitochondrial transcription factor A (Tfam) expression during skeletal muscle cell differentiation. *Biosci Rep* 35: e00221, 2015.

9. **Gani AR**, **Uppala JK**, **Ramaiah KVA**. Tauroursodeoxycholic acid prevents stress induced aggregation of proteins in vitro and promotes PERK activation in HepG2 cells. *Arch Biochem Biophys* 568: 8–15, 2015.

10. **Giorgi C**, **Agnoletto C**, **Bononi A**, **Bonora M**, **De Marchi E**, **Marchi S**, **Missiroli S**, **Patergnani S**, **Poletti F**, **Rimessi A**, **Suski JM**, **Wieckowski MR**, **Pinton P**. Mitochondrial calcium homeostasis as potential target for mitochondrial medicine. *Mitochondrion* 12: 77–85, 2012.

11. **Gollnick PD**, **King DW**. Effect of exercise and training on mitochondria of rat skeletal muscle. *Am J Physiol* 216: 1502–9, 1969.

12. **Graef M**, **Nunnari J**. Mitochondria regulate autophagy by conserved signalling pathways. *EMBO J* 30: 2101–14, 2011.

13. **Harrington JL**, **Murphy E**. The mitochondrial calcium uniporter: mice can live and die without it. *J Mol Cell Cardiol* 78: 46–53, 2015.

14. **Holloszy JO**. Biochemical Adaptations in Muscle. Effects of exercise on mitochondrial

oxygen uptakead respiratory enzyme activity in skeletal muscle. *J Biol Chem* 242: 2278–2282, 1967.

15. **Hoppeler H**, **Luthi P**, **Claassen H**, **Weibel ER**, **Howald H**. The ultrastructure of the normal human skeletal muscle. *Pflugers Arch Eur J Physiol* 344: 217–232, 1973.

16. **Horibe T**, **Hoogenraad NJ**. The chop gene contains an element for the positive regulation of the mitochondrial unfolded protein response. *PLoS One* 2: e835, 2007.

17. **Iqbal S**, **Ostojic O**, **Singh K**, **Joseph A-M**, **Hood DA**. Expression of mitochondrial fission and fusion regulatory proteins in skeletal muscle during chronic use and disuse. *Muscle Nerve* 48: 963–70, 2013.

18. **Kawakami T**, **Gomez IG**, **Ren S**, **Hudkins K**, **Roach A**, **Alpers CE**, **Shankland SJ**, **D'Agati VD**, **Duffield JS**. Deficient autophagy results in mitochondrial dysfunction and FSGS. *J Am Soc Nephrol* 26: 1040–52, 2015.

19. **Kim HJ**, **Jamart C**, **Deldicque L**, **An G**, **Lee YH**, **Kim CK**, **Raymackers J**, **Francaux M**. Endoplasmic reticulum stress markers and ubiquitin–proteasome pathway activity in response to a 200-km run. *Med Sci Sports Exerc* 43: 18–25, 2011.

20. **Kluck RM**. The release of cytochrome c from mitochondria: A primary site for Bcl-2 regulation of apoptosis. *Science (80-)* 275: 1132–1136, 1997.

21. **Kraft CS**, **LeMoine CMR**, **Lyons CN**, **Michaud D**, **Mueller CR**, **Moyes CD**. Control of mitochondrial biogenesis during myogenesis. *Am J Physiol Cell Physiol* 290: C1119-27, 2006.

22. **Lim J-A**, **Li L**, **Kakhlon O**, **Myerowitz R**, **Raben N**. Defects in calcium homeostasis and mitochondria can be reversed in Pompe disease. *Autophagy* 11: 385–402, 2015.

23. **Memme JM**, **Oliveira AN**, **Hood DA**. The chronology of UPR activation in skeletal muscle adaptations to chronic contractile activity. *Am. J. Physiol. Cell Physiol.* (April 27, 2016). doi: 10.1152/ajpcell.00009.2016.

24. **Menzies KJ**, **Singh K**, **Saleem A**, **Hood DA**. Sirtuin 1-mediated effects of exercise and resveratrol on mitochondrial biogenesis. *J Biol Chem* 288: 6968–6979, 2013.

25. **Mohamad N**, **Gutiérrez A**, **Núñez M**, **Cocca C**, **Martín G**, **Cricco G**, **Medina V**, **Rivera E**, **Bergoc R**. Mitochondrial apoptotic pathways. *Biocell* 29: 149–161, 2005.

26. **Nakanishi K**, **Dohmae N**, **Morishima N**. Endoplasmic reticulum stress increases myofiber formation in vitro. *FASEB J* 21: 2994–3003, 2007.

27. **Nakanishi K**, **Sudo T**, **Morishima N**. Endoplasmic reticulum stress signaling transmitted by ATF6 mediates apoptosis during muscle development. *J Cell Biol* 169: 555–60, 2005.

28. **Ozcan U**, **Yilmaz E**, **Ozcan L**, **Furuhashi M**, **Vaillancourt E**, **Smith RO**, **Görgün CZ**, **Hotamisligil GS**. Chemical chaperones reduce ER stress and restore glucose homeostasis in a mouse model of type 2 diabetes. *Science* 313: 1137–40, 2006.

29. **Pellegrino MW**, **Nargund AM**, **Haynes CM**. Signaling the mitochondrial unfolded protein response. *Biochim Biophys Acta - Mol Cell Res* 1833: 410–416, 2013.

30. **Rambold AS**, **Lippincott-Schwartz J**. Mechanisms of mitochondria and autophagy crosstalk. *Cell Cycle* 10: 4032–8, 2011.

31. **Ron D**, **Walter P**. Signal integration in the endoplasmic reticulum unfolded protein response. *Nat Rev Mol Cell Biol* 8: 519–29, 2007.

32. **Scarpulla RC**. Metabolic control of mitochondrial biogenesis through the PGC-1 family regulatory network. *Biochim Biophys Acta* 1813: 1269–78, 2011.

33. **Schröder M**, **Kaufman RJ**. the Mammalian Unfolded Protein Response. *Annu Rev Biochem* 74: 739–789, 2005.

34. **Smiles WJ**, **Camera DM**. More than mitochondrial biogenesis: alternative roles of PGC-1α in exercise adaptation. *J Physiol* 5939: 2115–2117, 2015.

35. **Smiles WJ**, **Hawley JA**, **Camera DM**. Effects of skeletal muscle energy availability on protein turnover responses to exercise. *J Exp Biol* 219: 214–25, 2016.

36. **Susin SA**, **Lorenzo HK**, **Zamzami N**, **Marzo I**, **Snow BE**, **Brothers GM**, **Mangion J**, **Jacotot E**, **Costantini P**, **Loeffler M**, **Larochette N**, **Goodlett DR**, **Aebersold R**, **Siderovski DP**, **Penninger JM**, **Kroemer G**. Molecular characterization of mitochondrial apoptosis-inducing factor. *Nature* 397: 441–6, 1999.

37. **Tabas I**, **Ron D**. Integrating the mechanisms of apoptosis induced by endoplasmic reticulum stress. *Nat Cell Biol* 13: 184–90, 2011.

38. **Tait SWG**, **Green DR**. Mitochondria and cell signalling. *J Cell Sci* 125: 807–15, 2012.

39. **Uguccioni G**, **Hood DA**. The importance of PGC-1α in contractile activity-induced mitochondrial adaptations. *Am J Physiol Endocrinol Metab* 300: E361-71, 2011.

40. **Vang S**, **Longley K**, **Steer CJ**, **Low WC**. The Unexpected Uses of Urso- and Tauroursodeoxycholic Acid in the Treatment of Non-liver Diseases. *Glob Adv Health Med* 3: 58–69, 2014.

41. **Wang C**, **Youle RJ**. The role of mitochondria in apoptosis. *Annu Rev Genet* 43: 95–118, 2009.

42. **Wang S**, **Kaufman RJ**. The impact of the unfolded protein response on human disease. *J Cell Biol* 197: 857–67, 2012.

43. **Wiles B**, **Miao M**, **Coyne E**, **Larose L**, **Cybulsky A**, **Wing SS**. USP19 deubiquitinating enzyme inhibits muscle cell differentiation by suppressing unfolded-protein response signaling. *Mol Biol Cell* 26: 913–923, 2015.

44. **Wu J**, **Ruas JL**, **Estall JL**, **Rasbach KA**, **Choi JH**, **Ye L**, **Boström P**, **Tyra HM**, **Crawford RW**, **Campbell KP**, **Rutkowski DT**, **Kaufman RJ**, **Spiegelman BM**. The unfolded protein response mediates adaptation to exercise in skeletal muscle through a

PGC-1α/ATF6α complex. *Cell Metab* 13: 160–9, 2011.

45. **Xie Q**, **Khaoustov VI**, **Chung CC**, **Sohn J**, **Krishnan B**, **Lewis DE**, **Yoffe B**. Effect of tauroursodeoxycholic acid on endoplasmic reticulum stress-induced caspase-12 activation. *Hepatology* 36: 592–601, 2002.

46. **Zhao Q**, **Wang J**, **Levichkin I V**, **Stasinopoulos S**, **Ryan MT**, **Hoogenraad NJ**. A mitochondrial specific stress response in mammalian cells. *EMBO J* 21: 4411–9, 2002.

Future Work

1) The drug (TUDCA) utilized in this study was a partial inhibitor of the UPR^{ER}, mainly prohibiting CHOP induction. Our data indicate that the mitochondrial biogenesis induced during myogenesis and CCA is independent of ER stress-induced CHOP signaling. However, under basal conditions, CHOP is required for mitochondrial biogenesis. Moreover, attenuating ER stress may further augment mitochondrial content. For a more complete inhibition of the UPR^{ER}, an alternative chemical chaperone mimetic 4-phenylbutyrate (PBA) (4), could be used instead to inhibit all 3 UPR^{ER} branches and thereby investigate the impact of global ER stress and UPR reduction during mitochondrial adaptations.
2) Branches of the UPR may differentially engage in crosstalk with other intracellular pathways in order to regulate various processes. Thus, knocking down other UPR components to better delineate what functions they specifically serve carries therapeutic potential in modulating the UPR in disease states (5).
3) ATF6 has been implicated in mitochondrial adaptations as it physically interacts with PGC-1α to regulate UPR activation triggered during exercise (6) and is active during myogenesis (2, 3). This suggests that the augmented mitochondrial biogenesis observed in our study may be attributable to ATF6 activation. However, we were unable to detect any difference in ATF6 protein levels in TUDCA-treated or untreated cells. This may be due to ATF6 being transiently activated. We attempted to knock down ATF6 via siRNA but were unsuccessful in eliminating the presence of its multiple spliced variants. Future work can aim to knock down ATF6 using multiple siRNAs to target its multiple forms in order to delineate what functional role it may potentially serve during mitochondrial biogenesis.

4) In order to further complement our study, assessing respiration as a measure of mitochondrial function would shed light upon the therapeutic potential of TUDCA for skeletal muscle health. Thus, it is of interest to measure the functionality of the mitochondria induced with TUDCA administration. Moreover, since CHOP knockdown cells had decreased COX-IV protein basally but was rescued with CCA, assessing mitochondrial function via respiration would enhance our data in determining the necessity of CHOP in CCA-induced mitochondrial adaptations.
5) The strength of our study lies in specifically knocking down CHOP to eliminate the pleiotropic effects of TUDCA. Future work can utilize a short-hairpin siRNA to prolong and increase the CHOP knockdown to investigate the potential impact it may have upon the recently discovered UPR^{MT} mammalian homologue ATF5 and its downstream UPR^{MT} components (1). As a result, the necessity of the UPR^{MT} to precede mitochondrial adaptations during CCA can be investigated as well. This is a novel field of research that merits further work.
6) Lastly, it would be prudent to explore our results in a mammalian *in vivo* model. Our results have suggested CHOP to be dispensable during CCA-induced adaptations. However, CHOP deletion has been found to ameliorate exercise intolerance characteristic of PGC-1α knockout animals (6). Therefore, assessing mitochondrial adaptations in a CHOP knockout animal model is of interest.

References

1. **Fiorese CJ**, **Schulz AM**, **Lin Y-F**, **Rosin N**, **Pellegrino MW**, **Haynes CM**. The Transcription Factor ATF5 Mediates a Mammalian Mitochondrial UPR. *Curr Biol* 26:2037-43, 2016.

2. **Morishima N**, **Nakanishi K**, **Nakano A**. Activating transcription factor-6 (ATF6) mediates apoptosis with reduction of myeloid cell leukemia sequence 1 (Mcl-1) protein via induction of WW domain binding protein 1. *J Biol Chem* 286: 35227–35, 2011.

3. **Nakanishi K**, **Sudo T**, **Morishima N**. Endoplasmic reticulum stress signaling transmitted by ATF6 mediates apoptosis during muscle development. *J Cell Biol* 169: 555–60, 2005.

4. **Ozcan U**, **Yilmaz E**, **Ozcan L**, **Furuhashi M**, **Vaillancourt E**, **Smith RO**, **Görgün CZ**, **Hotamisligil GS**. Chemical chaperones reduce ER stress and restore glucose homeostasis in a mouse model of type 2 diabetes. *Science* 313: 1137–40, 2006.

5. **Wang M**, **Kaufman RJ**. Protein misfolding in the endoplasmic reticulum as a conduit to human disease. *Nature* 529: 326–335, 2016.

6. **Wu J**, **Ruas JL**, **Estall JL**, **Rasbach KA**, **Choi JH**, **Ye L**, **Boström P**, **Tyra HM**, **Crawford RW**, **Campbell KP**, **Rutkowski DT**, **Kaufman RJ**, **Spiegelman BM**. The unfolded protein response mediates adaptation to exercise in skeletal muscle through a PGC-1α/ATF6α complex. *Cell Metab* 13: 160–9, 2011.

APPENDIX A - DATA AND STATISTICAL ANALYSES

Table 1. Mitochondrial biogenesis markers after 4 days of muscle differentiation.

	COX-I		COX-IV		Tfam	
N	**Day 0**	**Day 4**	**Day 0**	**Day 4**	**Day 0**	**Day 4**
1	0.252	0.813	0.352	1.015	0.614	1.869
2	0.158	0.784	0.239	0.522	0.762	1.557
3	0.157	0.966	0.325	0.982	0.826	1.379
X	0.189	0.854	0.305	0.840	0.734	1.602
SEM	0.031	0.057	0.034	0.159	0.063	0.143

Paired t-tests			
	COX-I	**COX-IV**	**Tfam**
P value	0.0061	0.0013	0.0260
P value summary	**	**	*
Significantly different? (P<0.05)	Yes	Yes	Yes

Table 2. $UPR^{MT/ER}$ markers after 4 days of muscle differentiation.

	mtHSP70		mtHSP60		CPN10		Sirt3	
N	**Day 0**	**Day 4**	**Day 0**	**Day 4**	**Day 0**	**Day 4**	**Day 0**	**Day 4**
1	1.109	0.750	0.830	0.630	1.463	0.916	0.140	0.479
2	1.237	0.658	1.113	0.524	1.077	0.772	0.110	0.317
3	1.041	0.800	0.887	0.602	2.250	1.462	0.097	0.327
X	1.129	0.736	0.943	0.608	1.597	1.050	0.116	0.374
SEM	0.057	0.042	0.086	0.051	0.345	0.210	0.013	0.052

Paired t-tests				
	mtHSP70	**mtHSP60**	**CPN10**	**Sirt3**
P value	0.0290	0.0469	0.0137	0.0120
P value summary	*	*	*	*
Significantly different? (P<0.05)	Yes	Yes	Yes	Yes

	ATF4		Bip	
N	**Day 0**	**Day 4**	**Day 0**	**Day 4**
1	7.1E-06	0.357	n.d.	1.668
2	8.4E-06	0.198	n.d.	1.936
3	1.2E-05	0.160	n.d.	2.376
X	9.1E-06	0.238	n/a	1.993
SEM	0.000	0.060	n/a	0.206

Paired t-tests	
	ATF4
P value	0.0096
P value summary	**
Significantly different? (P<0.05)	Yes

Table 3A. Fusion Index after 4 days of differentiation since TUDCA pre-treatment.

	Fusion Index	
N	**Vehicle**	**TUDCA**
1	84.55	66.91
2	88.85	75.51
3	93.30	75.87
X	88.90	72.76
SEM	2.52	2.93

Paired t-tests (two-tailed)	
	Fusion Index
P value	0.0074
P value summary	**
Significantly different? (P<0.05)	Yes

Table 3B. MHC-II protein after 4 days of differentiation since TUDCA pre-treatment.

	MHC-II Protein					
	Vehicle			TUDCA		
N	**Day 0**	**Day 2**	**Day 4**	**Day 0**	**Day 2**	**Day 4**
1	n.d.	n.d.	1.39	n.d.	n.d.	0.85
2	n.d.	n.d.	1.30	n.d.	n.d.	0.56
3	n.d.	n.d.	1.06	n.d.	n.d.	0.36
X	n.d.	n.d.	1.25	n.d.	n.d.	0.59
SEM	n.d.	n.d.	0.10	n.d.	n.d.	0.14

Paired t-tests (two-tailed)	
	MHC-II (Day 4)
P value	0.0082
P value summary	**
Significantly different? (P<0.05)	Yes

Table 3C. UPR^{ER} marker, BiP protein level on day 4 of differentiation since TUDCA pre-treatment.

	BiP	
N	**Vehicle**	**TUDCA**
1	2.869	1.436
2	3.951	2.283
3	2.640	1.684
4	1.889	0.827
X	2.837	1.558
SEM	0.426	0.301

Paired t-tests (two-tailed)	
	BiP
P value	0.0044
P value summary	**
Significantly different? (P<0.05)	Yes

Table 3D. Mitochondrial biogenesis markers on day 4 of differentiation since TUDCA pre-treatment.

	COX-I		COX-IV		Tfam		PGC-1α	
N	**Vehicle**	**TUDCA**	**Vehicle**	**TUDCA**	**Vehicle**	**TUDCA**	**Vehicle**	**TUDCA**
1	0.769	1.084	0.406	0.778	1.066	1.184	0.239	0.354
2	0.488	1.257	0.426	0.700	0.798	1.088	0.204	0.313
3	0.857	1.433	0.466	0.986	0.742	1.108	0.268	0.405
4	0.781	1.133	0.580	0.713	0.657	1.005	0.419	0.500
5	0.573	0.860	0.453	0.959	1.000	1.272	0.358	0.503
6	0.428	0.999	0.646	0.767	1.278	1.204	0.343	0.366
7	0.573	0.719	0.597	0.701	1.059	1.177	0.377	0.415
8	0.525	0.654	0.626	0.788	1.263	0.959	0.381	0.375
9	0.630	0.660			0.915	0.636	0.281	0.432
10	0.740	0.653						
X	0.637	0.945	0.525	0.799	0.975	1.070	0.319	0.407
SEM	0.045	0.088	0.034	0.040	0.073	0.063	0.024	0.021

Paired t-tests (two-tailed)				
	COX-I	**COX-IV**	**Tfam**	**PGC-1α**
P value	0.0054	0.0029	0.3022	0.0018
P value summary	**	**	ns	**
Significantly different? (P<0.05)	Yes	Yes	No	Yes

Table 4. Mitochondrial biogenesis markers after 4 days of CCA.

	COX-I		COX-IV		PGC-1α	
N	**CON**	**CCA**	**CON**	**CCA**	**CON**	**CCA**
1	0.175	0.362	0.192	0.825	0.306	0.445
2	0.323	0.735	0.312	0.968	0.324	0.634
3	0.223	0.545	0.223	0.625	0.207	0.560
4	0.136	0.429	0.383	0.844	0.476	0.738
5	0.266	0.574	0.396	0.747	0.349	0.743
X	0.225	0.529	0.301	0.802	0.332	0.624
SEM	0.027	0.052	0.034	0.046	0.035	0.046

Paired t-tests			
	COX-I	**COX-IV**	**PGC-1α**
P value	0.0005	0.0006	0.0013
P value summary	***	***	**
Significantly different? (P<0.05)	Yes	Yes	Yes

Table 5A. COX-I protein expression after 4 days of CCA with TUDCA or vehicle treatment.

	COX-I			
	Vehicle		TUDCA	
N	CON	CCA	CON	CCA
1	0.175	0.362	0.378	0.715
2	0.323	0.735	0.596	0.674
3	0.223	0.545	0.499	0.619
4	0.136	0.429	0.410	0.700
5	0.266	0.574	0.509	0.893
6	0.333	0.313	0.673	0.623
7	0.349	0.548	0.497	0.746
X	0.258	0.501	0.509	0.710
SEM	0.031	0.054	0.038	0.035

2-Way ANOVA			
Source of Variation	P value	P value summary	Significant?
Interaction	0.6122	ns	No
Row Factor	<0.0001	****	Yes
Column Factor	<0.0001	****	Yes

Bonferroni Post Hoc Test – MULTIPLE COMPARISONS				
Comparison	Difference	t	P value	Summary
CON:Vehicle vs. CON:TUDCA	-0.2511	4.358	P < 0.05	**
CON:Vehicle vs. CCA:Vehicle	-0.2429	4.215	P < 0.05	**
CON:Vehicle vs. CCA:TUDCA	-0.4521	7.846	P < 0.05	****
CON:TUDCA vs. CCA:Vehicle	0.008223	0.1427	P > 0.05	ns
CON:TUDCA vs. CCA:TUDCA	-0.201	3.489	P < 0.05	*
CCA:Vehicle vs. CCA:TUDCA	-0.2092	3.631	P < 0.05	**

Table 5B. COX-IV protein expression after 4 days of CCA with TUDCA or vehicle treatment.

	COX-IV			
	Vehicle		TUDCA	
N	**CON**	**CCA**	**CON**	**CCA**
1	0.192	0.397	0.825	1.136
2	0.312	0.525	0.968	1.100
3	0.223	0.397	0.625	1.154
4	0.383	0.489	0.844	1.232
5	0.396	0.452	0.747	1.182
X	0.301	0.452	0.802	1.161
SEM	0.041	0.025	0.057	0.022

2-Way ANOVA			
Source of Variation	P value	P value summary	Significant?
Interaction	0.0165	*	Yes
CCA	<0.0001	****	Yes
TUDCA	<0.0001	****	Yes

Bonferroni Post Hoc Test – MULTIPLE COMPARISONS				
Comparison	Difference	t	P value	Summary
CON:Vehicle vs. CON:TUDCA	-0.5007	9.103	P < 0.05	****
CON:Vehicle vs. CCA:Vehicle	-0.1508	2.741	P > 0.05	ns
CON:Vehicle vs. CCA:TUDCA	-0.8597	15.63	P < 0.05	****
CON:TUDCA vs. CCA:Vehicle	0.35	6.362	P < 0.05	****
CON:TUDCA vs. CCA:TUDCA	-0.359	6.527	P < 0.05	****
CCA:Vehicle vs. CCA:TUDCA	-0.709	12.89	P < 0.05	****

Table 5C. PGC-1α protein expression after 4 days of CCA with TUDCA or vehicle treatment.

	PGC-1α			
	Vehicle		TUDCA	
N	CON	CCA	CON	CCA
1	0.306	0.445	0.167	0.915
2	0.324	0.634	0.403	0.637
3	0.207	0.550	0.606	0.787
4	0.476	0.738	0.478	0.599
5	0.349	0.743	0.565	0.989
6	0.405	0.464	0.433	0.693
7	0.206	0.615	0.442	0.886
X	0.325	0.598	0.442	0.787
SEM	0.037	0.045	0.054	0.056

2-Way ANOVA			
Source of Variation	P value	P value summary	Significant?
Interaction	0.4744	ns	No
CCA	<0.0001	****	Yes
TUDCA	0.0045	**	Yes

Bonferroni Post Hoc Test – MULTIPLE COMPARISONS				
Comparison	Difference	t	P value	Summary
CON:Vehicle vs. CON:TUDCA	-0.1174	1.704	P > 0.05	ns
CON:Vehicle vs. CCA:Vehicle	-0.2739	3.975	P < 0.05	**
CON:Vehicle vs. CCA:TUDCA	-0.4621	6.707	P < 0.05	****
CON:TUDCA vs. CCA:Vehicle	-0.1564	2.271	P > 0.05	ns
CON:TUDCA vs. CCA:TUDCA	-0.3447	5.003	P < 0.05	***
CCA:Vehicle vs. CCA:TUDCA	-0.1882	2.732	P > 0.05	ns

Table 6A. UPR^{MT} marker mtHSP70 protein after 4 days of CCA with TUDCA or vehicle treatment.

	mtHSP70			
	Vehicle		TUDCA	
N	CON	CCA	CON	CCA
1	1.399	1.405	1.455	2.088
2	0.965	1.418	0.865	1.191
3	1.026	1.603	1.225	1.547
4	1.036	1.247	1.274	1.712
X	1.106	1.418	1.205	1.634
SEM	0.099	0.073	0.123	0.186

2-Way ANOVA			
Source of Variation	P value	P value summary	Significant?
Interaction	0.6524	ns	No
CCA	0.0131	*	Yes
TUDCA	0.2411	ns	No

Bonferroni Post Hoc Test – MULTIPLE COMPARISONS				
Comparison	Difference	t	P value	Summary
CON:Vehicle vs. CON:TUDCA	-0.09829	0.5454	P > 0.05	ns
CON:Vehicle vs. CCA:Vehicle	-0.312	1.731	P > 0.05	ns
CON:Vehicle vs. CCA:TUDCA	-0.528	2.93	P > 0.05	ns
CON:TUDCA vs. CCA:Vehicle	-0.2137	1.186	P > 0.05	ns
CON:TUDCA vs. CCA:TUDCA	-0.4297	2.385	P > 0.05	ns
CCA:Vehicle vs. CCA:TUDCA	-0.216	1.199	P > 0.05	ns

Table 6B. UPR^{MT} marker mtHSP60 protein after 4 days of CCA with TUDCA or vehicle treatment.

	mtHSP60			
	Vehicle		TUDCA	
N	**CON**	**CCA**	**CON**	**CCA**
1	1.148	1.192	1.093	1.711
2	0.840	0.897	0.781	0.932
3	0.985	1.381	0.998	1.344
4	0.966	1.157	1.044	1.474
X	0.985	1.157	0.979	1.365
SEM	0.063	0.100	0.069	0.163

2-Way ANOVA			
Source of Variation	P value	P value summary	Significant?
Interaction	0.3346	ns	No
CCA	0.0221	*	Yes
TUDCA	0.3591	ns	No

Bonferroni Post Hoc Test – MULTIPLE COMPARISONS				
Comparison	Difference	t	P value	Summary
CON:Vehicle vs. CON:TUDCA	0.005502	0.03658	P > 0.05	ns
CON:Vehicle vs. CCA:Vehicle	-0.1724	1.146	P > 0.05	ns
CON:Vehicle vs. CCA:TUDCA	-0.3807	2.531	P > 0.05	ns
CON:TUDCA vs. CCA:Vehicle	-0.1779	1.183	P > 0.05	ns
CON:TUDCA vs. CCA:TUDCA	-0.3862	2.568	P > 0.05	ns
CCA:Vehicle vs. CCA:TUDCA	-0.2083	1.385	P > 0.05	ns

Table 6C. UPR^{MT} marker CPN10 protein after 4 days of CCA with TUDCA or vehicle treatment.

	CPN10			
	Vehicle		TUDCA	
N	**CON**	**CCA**	**CON**	**CCA**
1	0.819	0.616	0.670	1.069
2	0.677	0.510	0.683	0.988
3	0.671	0.803	0.855	1.670
4	0.780	1.026	0.877	1.338
X	0.737	0.739	0.771	1.266
SEM	0.037	0.113	0.055	0.154

2-Way ANOVA			
Source of Variation	P value	P value summary	Significant?
Interaction	0.0314	*	Yes
CCA	0.0302	*	Yes
TUDCA	0.0167	*	Yes

Bonferroni Post Hoc Test – MULTIPLE COMPARISONS				
Comparison	Difference	t	P value	Summary
CON:Vehicle vs. CON:TUDCA	-0.03457	0.2417	P > 0.05	ns
CON:Vehicle vs. CCA:Vehicle	-0.002185	0.01528	P > 0.05	ns
CON:Vehicle vs. CCA:TUDCA	-0.5296	3.702	P < 0.05	*
CON:TUDCA vs. CCA:Vehicle	0.03239	0.2264	P > 0.05	ns
CON:TUDCA vs. CCA:TUDCA	-0.4951	3.46	P < 0.05	*
CCA:Vehicle vs. CCA:TUDCA	-0.5275	3.687	P < 0.05	*

Table 6D. UPR^{MT} marker Sirt3 protein after 4 days of CCA with TUDCA or vehicle treatment.

	Sirt3			
	Vehicle		TUDCA	
N	**CON**	**CCA**	**CON**	**CCA**
1	0.941	1.451	1.526	2.139
2	1.236	1.835	1.582	1.880
3	0.926	1.015	1.063	2.262
4	0.855	1.034	1.178	1.575
5	1.213	1.520	1.338	2.005
X	1.034	1.371	1.338	1.972
SEM	0.079	0.156	0.099	0.118

2-Way ANOVA			
Source of Variation	P value	P value summary	Significant?
Interaction	0.2197	ns	No
CCA	0.0007	***	Yes
TUDCA	0.0013	**	Yes

Bonferroni Post Hoc Test – MULTIPLE COMPARISONS				
Comparison	Difference	t	P value	Summary
CON:Vehicle vs. CON:TUDCA	-0.3035	1.842	P > 0.05	ns
CON:Vehicle vs. CCA:Vehicle	-0.3369	2.045	P > 0.05	ns
CON:Vehicle vs. CCA:TUDCA	-0.9381	5.693	P < 0.05	***
CON:TUDCA vs. CCA:Vehicle	-0.03343	0.2029	P > 0.05	ns
CON:TUDCA vs. CCA:TUDCA	-0.6346	3.851	P < 0.05	**
CCA:Vehicle vs. CCA:TUDCA	-0.6012	3.648	P < 0.05	*

Table 7A. UPR^{ER} marker CHOP protein after 4 days of CCA with TUDCA or vehicle treatment.

	CHOP							
	Day 2				Day 4			
	Vehicle		TUDCA		Vehicle		TUDCA	
N	**CON**	**CCA**	**CON**	**CCA**	**CON**	**CCA**	**CON**	**CCA**
1	0.231	0.709	0.741	0.244	0.583	0.699	0.699	0.444
2	0.443	0.521	0.398	0.208	0.383	0.751	0.432	0.426
3	0.619	0.484	0.542	0.179	0.560	0.792	0.644	0.132
4	0.464	0.329	0.329	0.085	0.349	0.763	0.531	0.586
X	0.337	0.615	0.569	0.226	0.483	0.725	0.565	0.435
SEM	0.106	0.094	0.172	0.018	0.100	0.026	0.134	0.009

2-Way ANOVA			
Source of Variation	P value	P value summary	Significant?
Interaction	0.0024	**	Yes
CCA	0.0189	*	Yes
TUDCA	0.0148	*	Yes

Bonferroni Post Hoc Test – MULTIPLE COMPARISONS Vehicle-TUDCA				
Comparison	Difference	t	P value	Summary
Day 2: CON	-0.06312	0.6297	P > 0.05	ns
Day 2: CCA	0.3319	3.311	P < 0.05	*
Day 4: CON	-0.1079	1.076	P > 0.05	ns
Day 4: CCA	0.3545	3.274	P < 0.05	*

Table 7B. UPR^{ER} marker ATF4 protein after 4 days of CCA with TUDCA or vehicle treatment.

	ATF4			
	Vehicle		TUDCA	
N	**CON**	**CCA**	**CON**	**CCA**
1	0.819	0.616	0.670	1.069
2	0.677	0.510	0.683	0.988
3	0.671	0.803	0.855	1.670
4	0.780	1.026	0.877	1.338
X	0.748	0.563	0.677	1.029
SEM	0.071	0.053	0.007	0.040

2-Way ANOVA			
Source of Variation	P value	P value summary	Significant?
Interaction	0.9993	ns	No
CCA	0.0003	***	Yes
TUDCA	0.4513	ns	No

Bonferroni Post Hoc Test – MULTIPLE COMPARISONS				
Comparison	Difference	t	P value	Summary
CON:Vehicle vs. CON:TUDCA	-0.04759	0.5454	P > 0.05	ns
CON:Vehicle vs. CCA:Vehicle	-0.2791	3.199	P < 0.05	*
CON:Vehicle vs. CCA:TUDCA	-0.3268	3.745	P < 0.05	*
CON:TUDCA vs. CCA:Vehicle	-0.2315	2.653	P > 0.05	ns
CON:TUDCA vs. CCA:TUDCA	-0.2792	3.2	P < 0.05	*
CCA:Vehicle vs. CCA:TUDCA	-0.0477	0.5466	P > 0.05	ns

Table 7C. UPR^{ER} marker BiP protein after 4 days of CCA with TUDCA or vehicle treatment.

	BiP			
	Vehicle		TUDCA	
N	CON	CCA	CON	CCA
1	0.792	0.925	1.048	0.946
2	0.941	2.077	1.234	0.802
3	0.997	1.459	0.984	1.900
4	0.737		0.830	0.853
5	0.872	1.426	0.979	1.064
6	0.912	1.408	1.237	1.240
X	0.875	1.459	1.052	1.134
SEM	0.039	0.183	0.065	0.166

2-Way ANOVA			
Source of Variation	P value	P value summary	Significant?
Interaction	0.0576	ns	No
CCA	0.0147	*	Yes
TUDCA	0.5581	ns	No

Bonferroni Post Hoc Test – MULTIPLE COMPARISONS				
Comparison	Difference	t	P value	Summary
CON:Vehicle vs. CON:TUDCA	-0.1767	1.032	P > 0.05	ns
CON:Vehicle vs. CCA:Vehicle	-0.5836	3.25	P < 0.05	*
CON:Vehicle vs. CCA:TUDCA	-0.259	1.513	P > 0.05	ns
CON:TUDCA vs. CCA:Vehicle	-0.4069	2.266	P > 0.05	ns
CON:TUDCA vs. CCA:TUDCA	-0.08222	0.4802	P > 0.05	ns
CCA:Vehicle vs. CCA:TUDCA	0.3247	1.808	P > 0.05	ns

Table 8A. COX-I protein levels after 4 days of CCA with CHOP siRNA transfection.

	COX-I Protein			
	Scrambled		si-CHOP	
N	CON	CCA	CON	CCA
1	0.949	1.026	0.481	0.950
2	1.186	1.723	1.332	2.551
3	0.812	1.257	0.835	1.185
4	0.993	1.221	1.076	1.238
5	0.611	1.157	1.102	1.297
6	0.594	1.525	0.974	1.563
7	0.934	1.370	0.832	1.635
8	0.619	0.652	1.041	1.832
9	1.191	0.694	1.865	1.636
X	0.876	1.180	1.060	1.543
SEM	0.078	0.118	0.127	0.156

2-Way ANOVA			
Source of Variation	P value	P value summary	Significant?
Interaction	0.4721	ns	No
CCA	0.0031	**	Yes
siRNA	0.0337	*	Yes

Bonferroni Post Hoc Test – MULTIPLE COMPARISONS				
Comparison	Difference	t	P value	Summary
CON: Scrambled vs. CON: si-CHOP	-0.1834	1.055	P > 0.05	ns
CON: Scrambled vs. CCA: Scrambled	-0.304	1.748	P > 0.05	ns
CON: Scrambled vs. CCA: si-CHOP	-0.6664	3.832	P < 0.05	**
CON: si-CHOP vs. CCA: Scrambled	-0.1206	0.6933	P > 0.05	ns
CON: si-CHOP vs. CCA: si-CHOP	-0.483	2.777	P > 0.05	ns
CCA :Scrambled vs. CCA: si-CHOP	-0.3624	2.084	P > 0.05	ns

Table 8B. COX-IV protein levels after 4 days of CCA with CHOP siRNA transfection.

	COX-IV Protein			
	Scrambled		si-CHOP	
N	CON	CCA	CON	CCA
1	0.533	1.313	0.536	1.442
2	0.804	1.162	0.476	1.255
3	0.732	1.555	0.496	1.265
4	0.779	1.470	0.448	1.576
5	1.010	0.827	0.569	1.293
6	0.727	1.079	0.295	1.226
7	0.691	1.160	0.719	0.883
8	0.642	1.059	0.661	1.657
9	0.319	1.238	0.291	1.343
10	0.639	0.983	0.574	1.003
11	0.729	1.478	0.589	1.282
X	0.691	1.211	0.514	1.293
SEM	0.052	0.068	0.040	0.067

2-Way ANOVA			
Source of Variation	P value	P value summary	Significant?
Interaction	0.0314	*	Yes
CCA	<0.0001	****	Yes
siRNA	0.4155	ns	No

Bonferroni Post Hoc Test – MULTIPLE COMPARISONS				
Comparison	Difference	t	P value	Summary
CON: Scrambled vs. CON: si-CHOP	0.1774	2.159	P > 0.05	ns
CON: Scrambled vs. CCA: Scrambled	-0.5201	6.331	P < 0.05	****
CON: Scrambled vs. CCA: si-CHOP	-0.6019	7.327	P < 0.05	****
CON: si-CHOP vs. CCA: Scrambled	-0.6975	8.491	P < 0.05	****
CON: si-CHOP vs. CCA: si-CHOP	-0.7793	9.487	P < 0.05	****
CCA :Scrambled vs. CCA: si-CHOP	-0.0818	0.9958	P > 0.05	ns

Table 8C. Tfam protein levels after 4 days of CCA with CHOP siRNA transfection.

	Tfam Protein			
	Scrambled		si-CHOP	
N	CON	CCA	CON	CCA
1	0.590	0.569	0.518	0.560
2	0.548	0.755	0.551	0.847
3	0.581	0.984	0.998	0.925
4	0.442	0.886	0.523	0.919
5	0.647	0.966	0.600	0.715
6	0.712	0.537	0.671	0.883
7	0.843	1.235	0.747	1.389
X	0.623	0.848	0.658	0.891
SEM	0.048	0.093	0.065	0.097

2-Way ANOVA			
Source of Variation	P value	P value summary	Significant?
Interaction	0.9580	ns	No
CCA	0.0076	**	Yes
siRNA	0.6200	ns	No

Bonferroni Post Hoc Test – MULTIPLE COMPARISONS				
Comparison	Difference	t	P value	Summary
CON: Scrambled vs. CON: si-CHOP	-0.03523	0.3176	P > 0.05	ns
CON: Scrambled vs. CCA: Scrambled	-0.2244	2.022	P > 0.05	ns
CON: Scrambled vs. CCA: si-CHOP	-0.2679	2.415	P > 0.05	ns
CON: si-CHOP vs. CCA: Scrambled	-0.1891	1.705	P > 0.05	ns
CON: si-CHOP vs. CCA: si-CHOP	-0.2327	2.098	P > 0.05	ns
CCA :Scrambled vs. CCA: si-CHOP	-0.04358	0.3928	P > 0.05	ns

Table 9A. CHOP protein levels after 4 days of CCA with CHOP siRNA transfection.

	CHOP Protein			
	Scrambled		si-CHOP	
N	CON	CCA	CON	CCA
1	0.025	0.282	0.063	0.043
2	0.023	0.177	0.022	0.074
3	0.019	0.095	0.001	0.078
4	0.250	0.350	0.093	0.113
5	0.018	0.068	0.016	0.060
6	0.040	0.088	0.025	0.080
7	0.027	0.283	0.010	0.064
X	0.057	0.192	0.033	0.073
SEM	0.032	0.043	0.012	0.008

2-Way ANOVA			
Source of Variation	P value	P value summary	Significant?
Interaction	0.1040	ns	No
CCA	0.0044	**	Yes
siRNA	0.0166	*	Yes

Bonferroni Post Hoc Test – MULTIPLE COMPARISONS				
Comparison	Difference	t	P value	Summary
CON: Scrambled vs. CON: si-CHOP	0.02462	0.6259	P > 0.05	ns
CON: Scrambled vs. CCA: Scrambled	-0.1345	3.419	P < 0.05	*
CON: Scrambled vs. CCA: si-CHOP	-0.01589	0.4038	P > 0.05	ns
CON: si-CHOP vs. CCA: Scrambled	-0.1592	4.045	P < 0.05	**
CON: si-CHOP vs. CCA: si-CHOP	-0.04051	1.03	P > 0.05	ns
CCA :Scrambled vs. CCA: si-CHOP	0.1186	3.016	P < 0.05	*

Table 9B. ATF4 protein levels after 4 days of CCA with CHOP siRNA transfection.

	ATF4 Protein			
	Scrambled		si-CHOP	
N	CON	CCA	CON	CCA
1	1.276	2.178	2.408	2.305
2	1.846	2.837	1.848	1.702
3	1.881	1.465	1.526	3.934
4	1.495	1.631	1.590	2.129
5	1.197	1.533	1.153	1.597
6	1.619	2.187	1.495	2.013
7	1.277	1.475	1.111	2.452
X	1.513	1.901	1.590	2.305
SEM	0.106	0.196	0.167	0.295

2-Way ANOVA			
Source of Variation	P value	P value summary	Significant?
Interaction	0.4289	ns	No
CCA	0.0120	*	Yes
siRNA	0.2475	ns	No

Bonferroni Post Hoc Test – MULTIPLE COMPARISONS				
Comparison	Difference	t	P value	Summary
CON: Scrambled vs. CON: si-CHOP	-0.07718	0.2692	P > 0.05	ns
CON: Scrambled vs. CCA: Scrambled	-0.3879	1.353	P > 0.05	ns
CON: Scrambled vs. CCA: si-CHOP	-0.7914	2.76	P > 0.05	ns
CON: si-CHOP vs. CCA: Scrambled	-0.3107	1.084	P > 0.05	ns
CON: si-CHOP vs. CCA: si-CHOP	-0.7142	2.491	P > 0.05	ns
CCA :Scrambled vs. CCA: si-CHOP	-0.4035	1.407	P > 0.05	ns

Table 9C. BiP protein levels after 4 days of CCA with CHOP siRNA transfection.

	BiP Protein			
	Scrambled		si-CHOP	
N	CON	CCA	CON	CCA
1	0.729	1.463	1.203	0.678
2	1.632	2.877	1.136	1.737
3	1.107	1.544	0.861	3.057
4	1.662	2.634	1.356	1.885
5	0.902	1.442	0.736	1.617
6	1.126	1.706	1.214	2.482
7	1.482	2.520	1.177	1.739
X	1.235	2.027	1.098	1.885
SEM	0.138	0.236	0.083	0.280

2-Way ANOVA			
Source of Variation	P value	P value summary	Significant?
Interaction	0.9909	ns	No
CCA	0.0006	***	Yes
siRNA	0.4926	ns	No

Bonferroni Post Hoc Test – MULTIPLE COMPARISONS				
Comparison	Difference	t	P value	Summary
CON: Scrambled vs. CON: si-CHOP	0.137	0.4846	P > 0.05	ns
CON: Scrambled vs. CCA: Scrambled	-0.7921	2.802	P > 0.05	ns
CON: Scrambled vs. CCA: si-CHOP	-0.6505	2.301	P > 0.05	ns
CON: si-CHOP vs. CCA: Scrambled	-0.929	3.286	P < 0.05	*
CON: si-CHOP vs. CCA: si-CHOP	-0.7874	2.785	P > 0.05	ns
CCA :Scrambled vs. CCA: si-CHOP	0.1416	0.5009	P > 0.05	ns

Table 10A. UPR^{MT} marker mtHSP70 protein levels after 4 days of CCA with CHOP siRNA transfection.

	mtHSP70 Protein			
	Scrambled		si-CHOP	
N	**CON**	**CCA**	**CON**	**CCA**
1	0.290	0.754	0.474	0.505
2	0.260	0.409	0.206	0.619
3	0.422	0.619	0.437	0.454
4	0.414	0.695	0.542	0.607
X	0.347	0.619	0.415	0.546
SEM	0.042	0.075	0.073	0.040

2-Way ANOVA			
Source of Variation	P value	P value summary	Significant?
Interaction	0.2589	ns	No
CCA	0.0056	**	Yes
siRNA	0.9694	ns	No

Bonferroni Post Hoc Test – MULTIPLE COMPARISONS				
Comparison	Difference	t	P value	Summary
CON: Scrambled vs. CON: si-CHOP	-0.06856	0.8103	P > 0.05	ns
CON: Scrambled vs. CCA: Scrambled	-0.2726	3.222	P < 0.05	*
CON: Scrambled vs. CCA: si-CHOP	-0.1994	2.356	P > 0.05	ns
CON: si-CHOP vs. CCA: Scrambled	-0.2041	2.412	P > 0.05	ns
CON: si-CHOP vs. CCA: si-CHOP	-0.1308	1.546	P > 0.05	ns
CCA :Scrambled vs. CCA: si-CHOP	0.07324	0.8657	P > 0.05	ns

Table 10B. UPR^{MT} marker mtHSP60 protein levels after 4 days of CCA with CHOP siRNA transfection.

	mtHSP60 Protein			
	Scrambled		si-CHOP	
N	**CON**	**CCA**	**CON**	**CCA**
1	0.683	0.867	0.630	0.644
2	0.505	0.841	0.541	0.786
3	0.608	0.777	0.682	0.744
4	0.742	0.601	0.655	0.605
5	0.650	0.722	0.541	0.911
6	0.763	0.937	0.531	0.841
7	0.829	0.631	0.830	0.832
X	0.683	0.768	0.630	0.766
SEM	0.041	0.047	0.041	0.042

2-Way ANOVA			
Source of Variation	P value	P value summary	Significant?
Interaction	0.5533	ns	No
CCA	0.0156	*	Yes
siRNA	0.5251	ns	No

Bonferroni Post Hoc Test – MULTIPLE COMPARISONS				
Comparison	Difference	t	P value	Summary
CON: Scrambled vs. CON: si-CHOP	0.05301	0.8812	P > 0.05	ns
CON: Scrambled vs. CCA: Scrambled	-0.0851	1.415	P > 0.05	ns
CON: Scrambled vs. CCA: si-CHOP	-0.08325	1.384	P > 0.05	ns
CON: si-CHOP vs. CCA: Scrambled	-0.1381	2.296	P > 0.05	ns
CON: si-CHOP vs. CCA: si-CHOP	-0.1363	2.265	P > 0.05	ns
CCA :Scrambled vs. CCA: si-CHOP	0.001856	0.03086	P > 0.05	ns

Table 10C. UPR^{MT} marker Sirt3 protein levels after 4 days of CCA with CHOP siRNA transfection.

	Sirt3 Protein			
	Scrambled		si-CHOP	
N	CON	CCA	CON	CCA
1	0.665	0.889	0.503	0.679
2	0.439	0.984	0.494	0.688
3	0.657	0.782	0.741	0.969
4	0.874	1.127	1.143	0.821
5	1.129	1.015	0.720	0.831
6	0.453	0.850	0.499	0.926
7	0.452	0.578	0.382	0.836
X	0.667	0.889	0.640	0.821
SEM	0.098	0.068	0.097	0.041

2-Way ANOVA			
Source of Variation	P value	P value summary	Significant?
Interaction	0.7978	ns	No
CCA	0.0180	*	Yes
siRNA	0.5579	ns	No

Bonferroni Post Hoc Test – MULTIPLE COMPARISONS				
Comparison	Difference	t	P value	Summary
CON: Scrambled vs. CON: si-CHOP	0.02661	0.237	P > 0.05	ns
CON: Scrambled vs. CCA: Scrambled	-0.2222	1.979	P > 0.05	ns
CON: Scrambled vs. CCA: si-CHOP	-0.1544	1.375	P > 0.05	ns
CON: si-CHOP vs. CCA: Scrambled	-0.2488	2.216	P > 0.05	ns
CON: si-CHOP vs. CCA: si-CHOP	-0.181	1.612	P > 0.05	ns
CCA :Scrambled vs. CCA: si-CHOP	0.06775	0.6034	P > 0.05	ns

APPENDIX B - ADDITIONAL DATA

(STATISTICAL TABLES NOT SHOWN)

Fig. S1

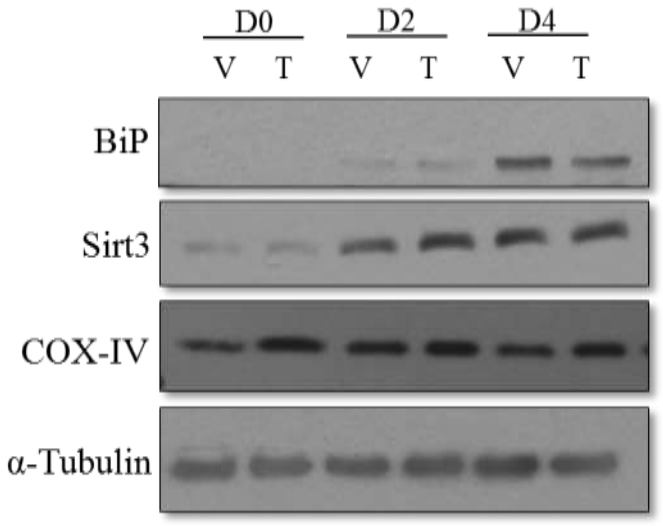

Figure S1. Representative western blots of UPR markers BiP and Sirt3, as well as mitochondrial marker COX- IV during C_2C_{12} skeletal muscle differentiation measured at days (D) 0, 2 and, 4 after 24 h vehicle (V) or TUDCA (T) treatment (500 µg/ml) prior to the onset of differentiation. BiP levels were undetectable at day 0 of differentiation but gradually increased by day 4, however less so with TUDCA-treated cells. Sirt3 levels increased during differentiation regardless of treatment. COX-IV depicted similar patterns however was consistently augmented with TUDCA. α-Tubulin serves as the loading control.

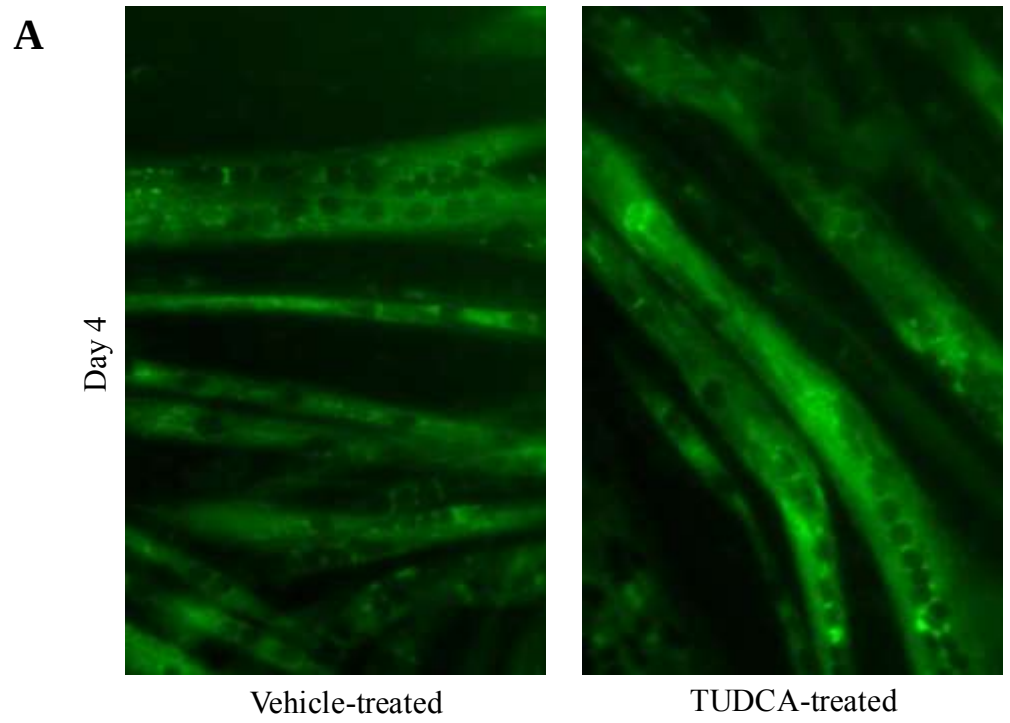

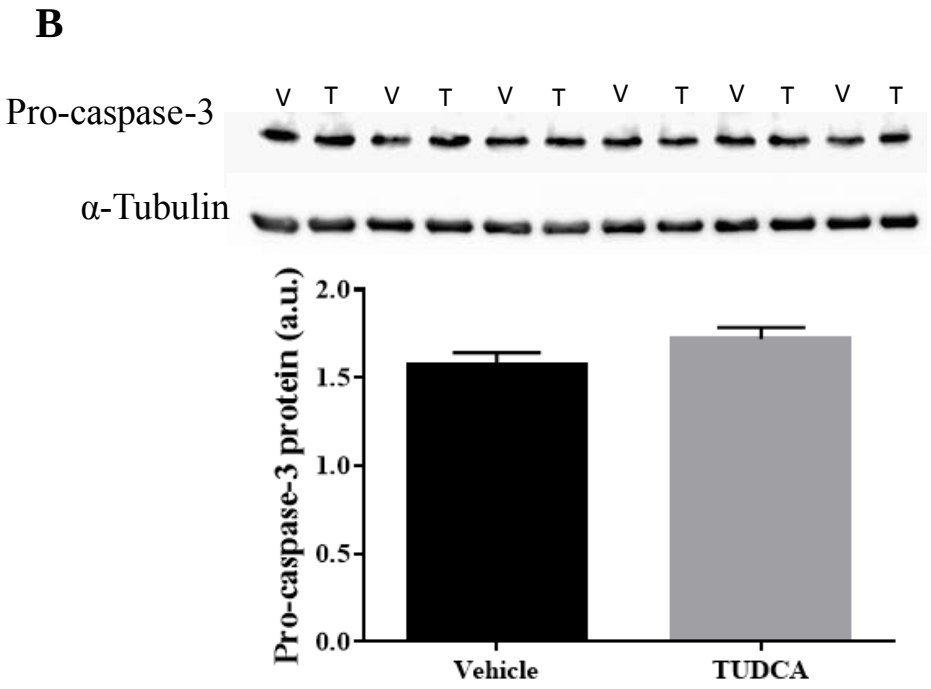

Figure S2. C_2C_{12} cells were given a one-time treatment of vehicle (V) or TUDCA (T) (500 µg/ml) prior to differentiation and *(A)* stained for mitochondria with MitoTracker green on day 4 of differentiation. Consistent with increased mitochondrial biogenesis in TUDCA-treated cells, more green fluorescence is evident in the right panel. *(B)* Representative blot and graphical representation of apoptotic marker pro-caspase-3 after 4 days of differentiation since treatment. No difference was observed between treatments.

Fig. S3

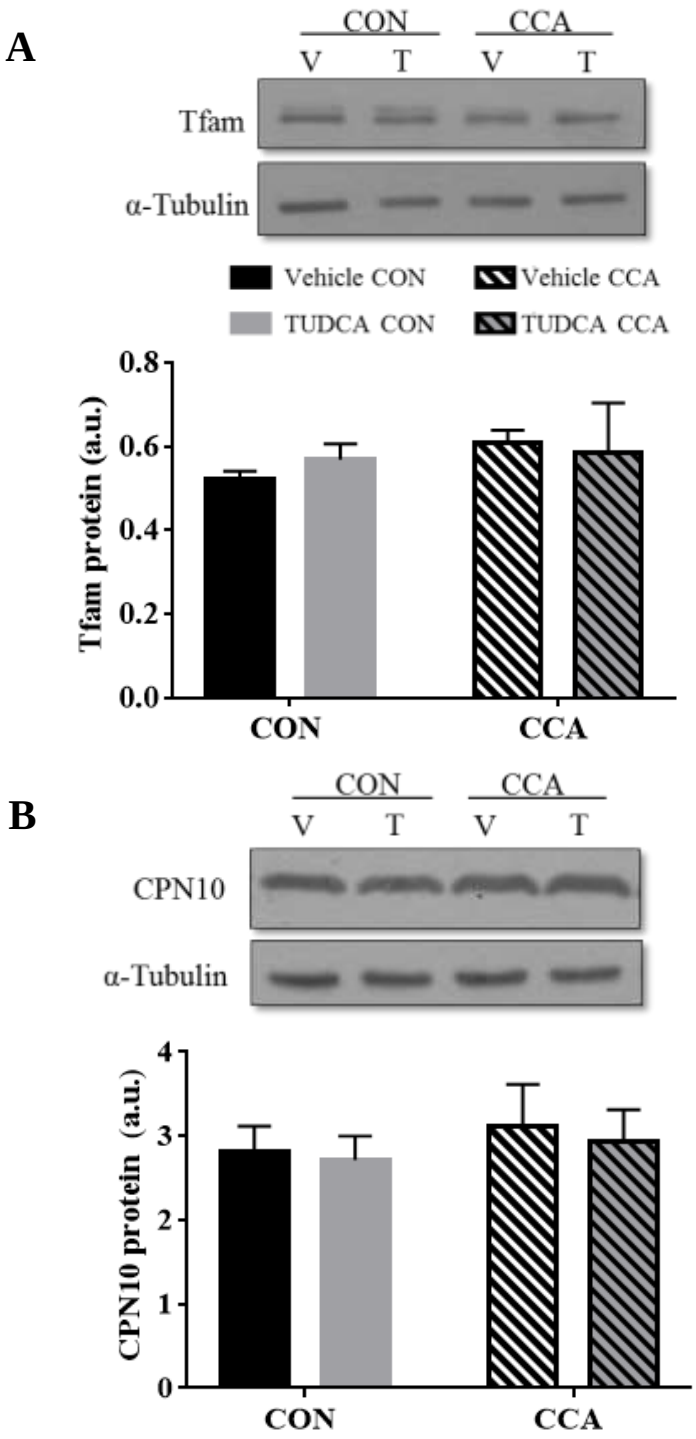

Figure S3. Murine muscle cells were subjected to 2 or 4 consecutive days of chronic contractile activity (CCA) with either vehicle (V) or TUDCA (T) treatment, commencing on day 5 of differentiation. *(A)* Representative blot and graphical quantification of mitochondrial marker TFAM after 4 days of CCA. *(B)* Protein expression of CPN10 and graphical representation after 2 days of CCA. No significant difference was observed between treatments.

Fig. S4

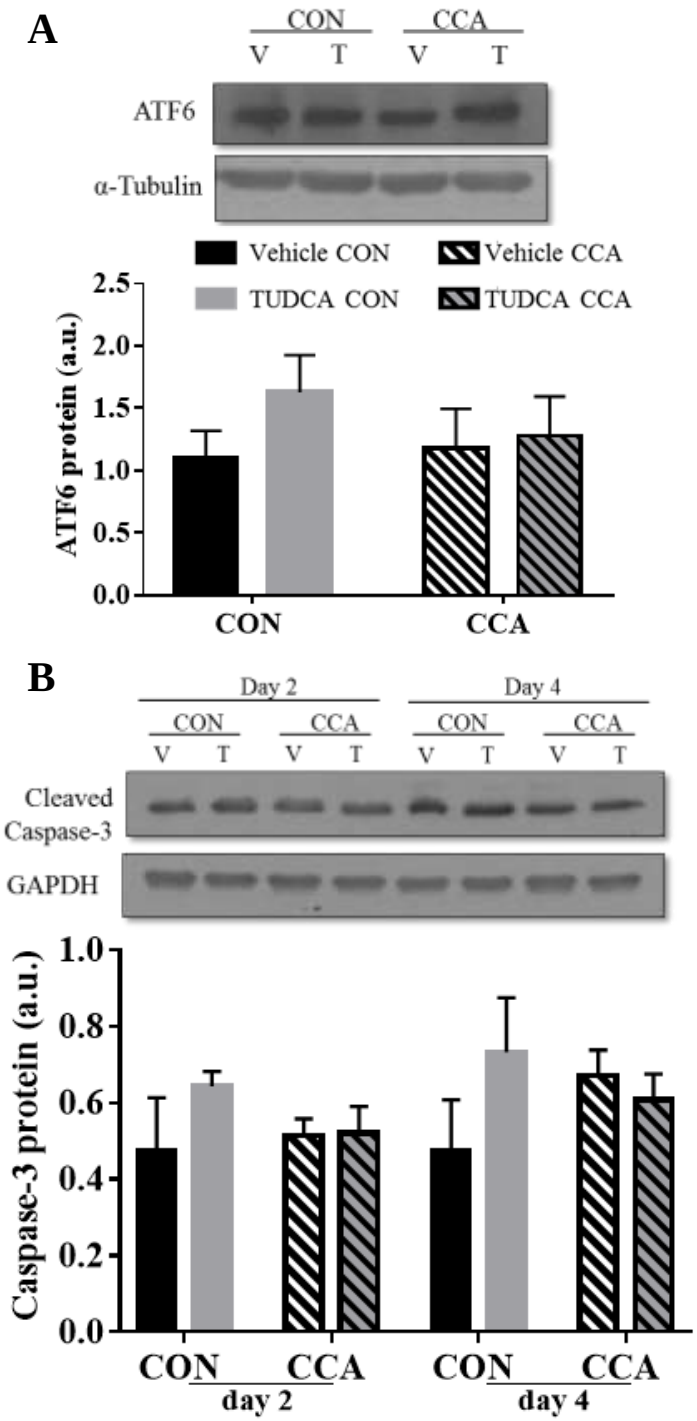

Figure S4. C_2C_{12} muscle cells were subjected to 2 or 4 consecutive days of chronic contractile activity (CCA) with either vehicle (V) or TUDCA (T) treatment, commencing on day 5 of differentiation. Representative blot and graphical quantification of *(A)* UPR^{ER} marker ATF6 (full length) at ~90 kDa after 4 days of CCA and *(B)* cleaved caspase-3 at ~17 kDa after 2 or 4 days of CCA. Both proteins showed no significant difference between treatments.

APPENDIX C – LABORATORY METHODS AND PROTOCOLS

CELL CULTURE

Cells

1. C2C12 murine skeletal muscle cells (ATCC, CRL-1772)

Materials

1. Dulbecco's Modified Eagle's Medium (DMEM; Wisent 319-015/500 ml)
2. Fetal Bovine Serum (FBS; Fisher Scientific SH30396.03/500 ml)
    a. Aliquoted into 50ml sterile conical tubes and stored at -20°C
3. Penicillin/Streptomycin (P/S; Wisent 450-201-EL/100 ml)
    a. Sterile aliquots of 5.5 mls and stored at -20°C)
4. Horse Serum (HS; Invitrogen 16050-114/1000 ml)
    a. Aliquoted into 50 ml sterile conical tubes and stored at -20°C
    b. Heat-inactivated for 30 minutes at 56.0°C
5. 0.25% Trypsin-EDTA (l×), phenol red (Invitrogen 25200-072/500 ml)
    a. Sterile aliquots of 40 mls stored at -20°C
6. Dulbecco's Phosphate Buffered Saline (PBS; Wisent 311-425-CL/500 ml)
7. 15ml conical tubes, sterile (BD Falcon 352097)
8. 50ml conical tubes, sterile (BD Falcon 352098)
9. 175cm^2 canted/vented tissue cultured flasks (BD Falcon 353112)
10. 6-well sterile tissue culture dish (BioBasic SP41117)
11. Gelatin (Sigma G1890)
    a. 0.1% solution autoclaved for sterilization

Procedure

1. Allow myoblasts to proliferate in 175cm^2 flask with growth medium (GM; DMEM supplemented with 10% FBS and 1% P/S) until ~70% confluent.
2. Pre-heat GM, trypsin and PBS in 37°C water bath for 30 minutes prior to use.
3. Discard old GM from tissue culture flask and wash with 5 mls of PBS (×2) to rinse off remaining GM. (Trypsin works best if GM has been thoroughly washed off).
4. Apply 5 mls of trypsin to the flask and place in the incubator at 37°C for 3-5 minutes.
5. Remove flask from incubator and gently knock sides of the flask to ensure cells are lifted from flask bottom. Remove trypsin with the cells and place into a sterile 15 ml conical tube.
6. Rinse flask with 5mls GM and add to sterile 15 ml conical tube containing the cells.
7. Spin tube for 3 minutes at 1400 rpm at room temperature.
8. Discard the supernatant and add 1ml of GM for resuspension with 1ml pipette.
9. Add 3mls of GM to resuspended cell mixture for a total volume of 4 mls, depending on pellet size and desired concentration.
10. Fill each well of tissue culture dishes with 2 mls of GM and add 100 µl of cell mixture to each well of the 6-well plate.

11. Rotate plate slowly in an 8-motion for 30 secs and subsequently place into 37°C incubator overnight.
12. The following day remove GM from cells and replace with differentiation medium (DM; DMEM supplemented with 5% heat-inactivated HS and 1% P/S) once myoblasts are ~100% confluent.
13. Refresh DM every day after day 1 of differentiation. Mature myotubes will form after five days and be ready for contractile activity.

ELECTRICAL STIMULATION OF MYOTUBES IN CULTURE

Cells

1. C_2C_{12} murine myocytes (ATCC)

Materials

1. Electrical Stimulator
   Gange bipolar output (+ /- amplitude adjustable using one knob)
   Output voltage range = 0 to +/- 30V
   Maximum Output current = 1A
   Adjustable output pulse duration from 0.001 to 0.1 seconds (10-1 kHz)
   Adjustable output pulse repetition from 0.0005 to 0.01 seconds (100-2 kHz)
   Adjustable polarity duration range from 1 to 100 seconds (0.01 to 1 Hz)
   Polarity duration range = time duration for the output "pulse burst" to be positive before switching to a similar negative (amplitude) pulse burst. Positive and negative duration are of equal value except for the amplitude.

2. 6-well sterile plastic culture dishes with modified covers for electrical stimulation (see below). Coat 6-well plates with 0.1% gelatin and leave to dry in the hood.

Procedures

1. Before each stimulation protocol, electrodes are wiped with 70% ethanol and left in the flow hood with UV light on for 1 hour for sterilization purposes.
2. Myotubes (on day 5 of differentiation) are stimulated in a parallel circuit (up to 4 6-well dishes at a time/ protocol) at 5 Hz, 9V for 3 hours in 4 ml of DM.
3. The following day (after 21 hours), differentiation medium is replenished 1 hour prior to the next stimulation. The total stimulation protocol lasts for 4 days and 21 hours after the 4_{th} stimulation day cell are harvested.

Electrical Stimulation of myocytes in culture.
(Left: picture of electrical stimulator; Right: Modified cover of a 6-well dish for stimulation)

MITOTRACKER GREEN FM STAINING

Reagents

1. Pre-warmed PBS
2. MitoTracker Green FM (Molecular Probes, M-7514)
3. DMSO (Dimethyl sulfoxide, D8418-100ML)

Procedure

1. Grow cells on custom-made glass bottom 6-well dishes.
2. Once experimental protocol is complete, wash cells 3X 2 ml using pre-warmed PBS.
3. Dilute MitoTracker Green FM in 74.5 ul of DMSO and add to differentiation medium to make a working concentration of 100 nM (total volume 27 ml). Add 2 ml of this 100 nM stock to each well.
4. Incubate the cells at 37℃ and 5% C02 for 45 minutes.
5. Following incubation, briefly wash cells with PBS once again to remove any residual MitoTracker Green FM and add differentiation medium.
6. Examine mitochondrial content using the Nikon Eclipse TE2000-U microscope and take all images using the same exposure to allow for adequate comparison between conditions.

FUSION INDEX

Materials and reagents:

1. Sodium Phosphate Na_2HPO_4
2. Phosphoric acid NaH_2PO_4
3. dH_20
4. Phosphate Buffered Saline (PBS)
5. 100 % methanol
6. Giemsa stain (EMS, 15940/100mL)
7. Inverted light microscope
8. Canon G5 PowerShot digital camera with microscope attachments
9. Computer with ImageJ software

Procedure

1. **Make 1 mM of sodium phosphate buffer (pH 5.6):**
    a. Make 1 mM solution of Na_2HPO_4 by mixing 14.2 mg of Na_2HPO_4 in 100 ml of dH_20 and have it stir in a beaker.
    b. In another beaker, weight out 13.8 mg of NaH_2PO_4 and add ~80 mL of dH_20 and have it stir.
    c. pH the NaH_2PO_4 solution with Na2HPO4 to get a final pH of 5.6.
    d. Once final pH is reached, volume up to 100 mL of dH_20. Do not go over 100 mL.
    e. Place in a bottle and store at room temperature.

2. **Stain C_2C_{12} myotubes:**
    a. Place pre-aliquoted 100% methanol in -20°C freezer to cool for 10 minutes.
    b. Wash cells with cold-PBS twice.
    c. Fix cells with cold methanol for 5 min by adding 1 mL/well.
    d. Meanwhile, dilute 1part Giemsa stain stock to 20 parts of 1 mM sodium phosphate buffer made in step 1 (1:20 ratio) to make a working solution.
    e. Aspirate the methanol and let plates air dry for 10 min under laminar hood. Leave lids to the cells plates off.
    f. Add 1 ml of Geimsa stain solution to each well, gently shake plates to ensure even distribution. Incubate for 10 min.
    g. Aspirate the solution and wash twice with dH_20.
    h. Proceed to capturing phase-contrast images (slide filter of microscope) using a Canon Powershot G5 camera adapted to a light microscope at a 10× magnification.
    i. Take at least 10 pictures per condition.
    j. Have the pictures labeled in an investigator-blind manner by a second unbiased individual.

3. **Calculate Fusion Index:**
    a. Choose three randomly selected photos per experimental group and open the images with ImageJ software.

b. Click on Plugins/Analyze/Cell counter to assist in manually counting the % nuclei within myotubes as indication of Fusion Index.
c. Choose a specified coloured pointer and mark all the nuclei found within the myotubes. Myotubes are defined as cells with two or more nuclei
d. As you click on the nuclei, a coloured dot appears over it and a tallied count is kept by the software.
e. Choose another coloured pointer and click on all the nuclei lying outside of the myotubes.
f. Fusion index is calculated by determining the fraction of total nuclei (calculated by adding the total marked/coloured nuclei together) found in myotubes.

$$Fusion\ index = \frac{nuclei\ within\ myotubes}{total\ number\ of\ nuclei}$$

g. Determine the experimental conditions of each photo after all images are quantified from the unbiased individual who labeled the photos.
h. Average the fusion index of the images per condition.

TUDCA TREATMENT IN C_2C_{12} CELLS

Reagents

1. Differentiation media (DMEM supplemented with 5% HS and 1% P/S)
2. Growth media (DMEM supplemented with 10% FBS and 1% P/S)
3. Dulbecco's Phosphate Buffered Saline (PBS; Wisent 311-425-CL/500 ml)
4. Growth medium (GM; DMEM supplemented with 10% FBS and 1% P/S)
5. Tauroursodeoxycholic acid sodium salt (TUDCA; Millipore 580549-5GM)
6. Sterile water (Wisent 809-115-CL/500 ml)
7. Sterile 10 ml syringe and 0.2 µM filter

Procedure

To make 100× TUDCA stock solution (50 mg/ml):

1. For a 10 ml stock, weight out 500 mg of TUDCA and dilute in 10 ml of sterile water under a sterile hood.
2. Vortex until fully diluted.
3. Filter stock solution under a sterile hood for purity using 10 ml syringe and 0.2 µM filter.
4. Store at 4°C for up to 2 months.

To treat myoblasts prior to differentiation:

1. Plate C2C12 cells in 6-well dishes to be ready at ~50-60 % confluency for the next day.
2. Make a working concentration of 500 µg/ml of TUDCA for 2 ml of GM per well.
3. Leave cells to be treated with TUDCA or water (vehicle) for 24 h.
4. Rinse cells with PBS and switch media to DM (cells should be at 100% confluency to be ready for subsequent differentiation).
5. Replenish media with DM daily after day 1 of differentiation.

To treat myotubes for chronic contractile activity (CCA):

1. Differentiate C2C12 cells for up to 5 days as described previously.
2. Make a working concentration of 500 µg/ml of TUDCA for 4 ml of DM per well. Do the same for water-treated cells.
3. On day 5 of differentiation, 1 h prior to stimulation, change the media to DM supplemented with either TUDCA or water and stimulate cells in the same media.
4. After 3 h of stimulation, replenish cells again with DM supplemented with either TUDCA or water.
5. For the entire CCA protocol which commences on day 5 of differentiation, myotubes will be treated with TUDCA or vehicle as described above in steps 3 and 4.

siRNA TRANSFECTION OF C_2C_{12} MYOTUBES

Materials

1. Lipofectamine 2000 (Invitrogen, 11668-019)
2. Dulbecco's Modified Eagle's Medium (DMEM)
3. Pre-transfection medium (PTM; DMEM supplemented with 5% HS)
4. Differentiation medium (DMEM supplemented with 5% HS and 1% P/S)
5. CHOP siRNA oligonucleotide (Life Technologies)
    a. CHOP siRNA IDs: s201245 and s64888
6. Scrambled siRNA oligonucleotide (Life Technologies)
    a. Silencer Select Negative control #2 ID: 4390846
7. RNase free sterile water

Procedure

To make 20 µM siRNA stock solution:

1. Spin down dried oligonucleotide pellet in an ultracentrifuge.
2. For a 5 nmole siRNA, dilute 250 µl of RNase free water with pellet and gently resuspend to make a 20 µM stock. For a 20 nmole siRNA, dilute in 1000 µl of RNase free water.
3. Aliquot and store in -20°C.

Transfecting cells:

1. Switch medium from DM to pre-transfection medium on the evening of the 3rd day of differentiation.
2. The following morning dilute desired amount of siRNA (30 nM) into DMEM and mix (tube 1).
3. Aliquot Lipofectamine (10 µl*)* into DMEM and mix gently (tube 1A).
4. Incubate at room temperature for 5 minutes.
5. Combine contents of tube 1 and 1A and mix by tapping gently.
6. Incubate at room temperature for 20 minutes.
7. During the 20 minute incubation period, remove medium from wells and replace with 1.5 ml of serum-free DMEM.
8. Following the incubation, add 500 µl of siRNA/Lipofectamine complexes to each well and swirl gently.
9. Incubate at 37°C at 5% CO_2 for 6 hours.
10. Briefly wash cells with pre-warmed PBS and add 2 ml of DM to each well.
    a. If cells are to be subjected to contractile activity, incubate at 37°C at 5% CO2 for 1hour. Sterilize electrodes during this time. Following incubation, attach dishes to electrical stimulator and stimulate for 3 hours (5 Hz, 9V), as previously described.
11. To prolong knockdown, transfect cells on day 7of stimulation by changing media to pre-transfection media on day 6 after the 2nd round of stimulation.
12. Seven h prior to stimulation on day 7 (3rd day of stimulation), transfect cells with the siRNA as described in steps 2 through 10.

PROTEIN COLLECTION AND EXTRACTION FROM CELL CULTURE

Reagents

1. 5× Passive Lysis Buffer, dilute to 1× using ddH_20 (Promega, E194A)
2. Dulbecco's Phosphate Buffered Saline (PBS; Wisent 311-425-CL/500 ml)
3. Growth medium (GM; DMEM supplemented with 10% FBS and 1% P/S)
4. 0.25% Trypsin-EDTA (lx), phenol red (Invitrogen 25200-072/500ml)
5. 100× Phosphatase Inhibitor Cocktails 2 and 3 dilute to 1× (Sigma-Aldridch, P0044-5ML; P5726-5ML)
6. 100× Protease Inhibitor Cocktail tablets dilute to 1× (Complete, 11697 498 001)

Procedure

Cell harvesting:

1. Remove media and wash cells 3× using 2 ml of cold-PBS. Aspirate last wash.
2. Add 500 µl of trypsin to each well and place in incubator for 3-5 minutes at 37℃.
3. Add equal amount of GM, 500 µl to each well to inactivate trypsin. Collect with 1000 µl and transfer to 15 ml sterile conical tubes.
4. Centrifuge for 3 min at 1400 rpm and proceed to aspirate the GM.
5. Add 1 ml of PBS and transfer to labeled 1.5 ml Eppendorf tube. Place in ultra-centrifuge for 3 min at 3000 rpm.
6. Aspirate the PBS and flash freeze pellet in liquid nitrogen and store at -80℃ for later analysis or refer to the following steps for protein extraction.

Protein extraction:

1. Prepare fresh lysis buffer by mixing passive lysis buffer, phosphatase inhibitor cocktails 2 and 3, and protease inhibitor cocktail tablet together after diluting reagents to 1× concentrations.
2. Add equal to twice the pellet size of extraction buffer to pellet. Vigorously vortex each sample for 5 seconds and freeze-thaw cells for 3 cycles in liquid nitrogen.
3. Spin samples for 10 minutes at maximum speed, 16.1 rcf at 4℃.
4. Collect supernatant and add into newly labeled Eppendorf tube.
5. Measure total protein concentrations using Bradford assay.
6. Store at -80℃.

SDS POLYACRYLAMIDE GEL ELECTROPHORESIS (SDS-PAGE)
PROTEAN BIO-RAD SYSTEM

Reagents

1. Acrylamide/Bis-Acrylamide, 30% Solution 37.5:1 (BioShop 10.502)
    a. Store at 4°C
2. Under Tris Buffer
    a. 1M Tris-HCl, pH 8.8 (60.5g/500ml)
    b. Store at 4°C
3. Over Tris Buffer
    a. 1M Tris-HCl, pH 6.8 (12.1g/100ml)
    b. Bromophenol Blue (for colour)
    c. Store at 4°C
4. Ammonium Persulfate (APS)
    a. 10% (w/v) APS in ddH_20 (1g/10ml)
    b. Stored at 4°C
5. Sodium Dodecyl Sulfate (SDS)
    a. 10% (w/v) in ddH_20 (1g/10ml)
    b. Store at room temperature
6. TEMED (Sigma T-9281)
7. Electrophoresis Buffer, pH 8.3 (10L)
    a. 25mM Tris 30.34g, 192mM Glycine 144g, 0.1% SDS 10g
    b. Volume to 10L with ddH_20
    c. Store at room temperature
8. 6X SDS
    a. Warm 100% glycerol in water bath at 65°C for 30 minutes
    b. Combine 1.2g SDS, 0.06g Bromophenol Blue, 3mls of 1M Tris, pH 6.8 and 1ml of ddH_20 and stir at 4°C for 5 minutes
    c. Add 3mls of 100% glycerol, stir and aliquot mixture.
    d. Store at -20°C
    e. Add 5% (v/v) ß-mercaptoethanol (Sigma M6250) to 6X SDS <u>just prior</u> to use
9. *tert*-Amyl alcohol ReagentPLus, 99% (Sigma 152463)

Procedure

1. **Prepare electrophoresis rack:**
    a. Clean glass plates thoroughly with soap followed by 95% ethanol then ddH_20.
    b. Dry carefully with a kimwipe.
    c. Assemble glass plates as shown below:

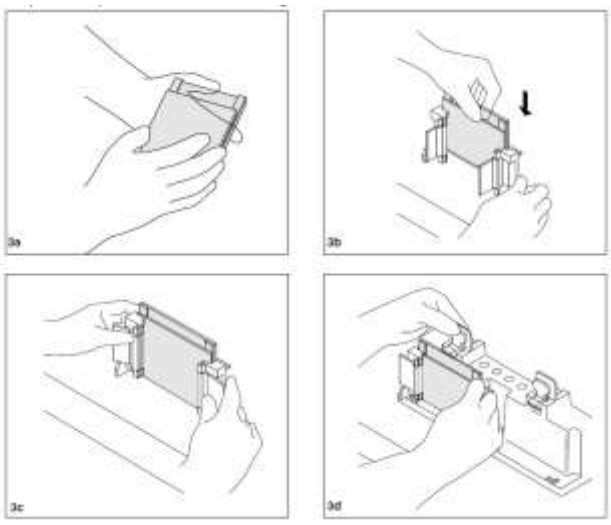

d. Check the seal by adding a small volume of ddH_20 then pour off and let dry.

2. Prepare separating gels:

a. Mini Protean 3 Bio-Rad System volumes:

	8%	**10%**	**12%**	**15%**	**18%**
Acrylamide	2.7 ml	3.3 ml	4.0 ml	5.0 ml	6.0 ml
ddH_20	4.1 ml	3.5 ml	2.8 ml	1.8 ml	0.8 ml
Under Tris	3.0 ml	3.0 ml	3.0 ml	3.0 ml	3.0 ml
SDS	100µl	100µl	100µl	100µl	100µl
APS	100µl	100µl	100µl	100µl	100µl
TEMED	10µl	10µl	10µl	10µl	10µl

b. Mix the contents of the separating gel without adding APS or TEMED. Stir.
c. Add APS and TEMED. Stir.
d. Slowly pour the entire volume of the solution into the space between the two plates while keeping plates tilted to prevent bubble formation.
e. Add *tert*-Amyl alcohol to coat top surface of gel solution.
f. Allow 30 minutes for gel polymerization.
g. Remove *tert*-Amyl alcohol by pouring it off and remove any remainder with a kimwipe. Rinse with ddH_20.

3. Prepare stacking gel:

a. For a single mini gel use the following volumes:

Acrylamide	500 µl
Over Tris	625 µl
ddH_20	3.75 ml
SDS	50 µl
APS	50 µl
TEMED	20 µl

b. Mix the contents of the stacking gel without adding APS or TEMED. Stir.
c. Add APS and TEMED. Stir.
d. Using a Pasteur pipette slowly add the entire volume from the beaker in between the plates.
e. Add comb for desired number of wells.
f. Allow 30 minutes for gel polymerization.

4. Prepare samples:

a. Turn on the block heater to 95ºC.
b. Pipette required volume of sample into new eppendorf with 2X SDS (or passive lysis buffer; 1 volume of sample to 1 volume of 2X SDS). Keep samples on ice until all samples are prepared.
c. Briefly spin each sample to bring volume to the bottom of the eppendorf.
d. Incubate each sample at 95 ºC for 5 minutes in the heating block to denature the proteins.
e. Briefly spin again to return volume to the bottom of the eppendorf.

5. Assemble Mini-PROTEAN gel caster system:

a. See images below:

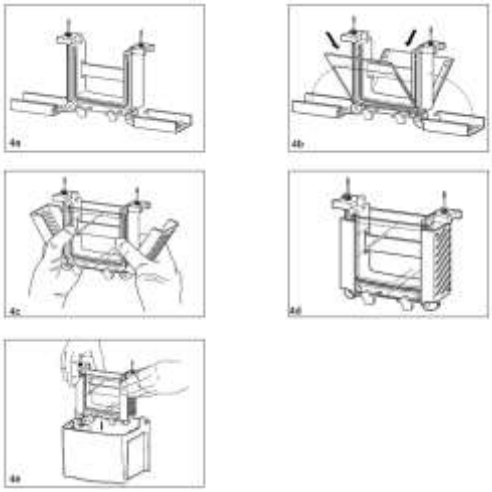

b. If you are only running one gel a plastic rectangular pseudo plate must be clamped on the other side of the caster.
c. Fill with electrophoresis buffer between the plates and outside of the plates in the chamber.
d. Slowly remove the comb using both hands (one on each side) by pulling the comb straight upwards.
e. Fix any wells that are deformed using a small spatula.
f. Clean out the wells using a syringe filled with electrophoresis buffer.
g. Withdraw the entire volume of the sample using a Hamilton syringe. Inject volume slowly into the bottom of the well.

6. Gel electrophoresis

a. Immediately after all samples are loaded place the lid on the gel chamber.
b. Place positive and negative plugs into the power supply and turn on power supply.
c. Set power supply to 120V. Gel will run for ~2 hours depending on percent gel made.
d. When the bromophenol blue has run off the bottom of the gel turn off the power supply. Remove plugs from power supply and remove lid.
e. Prepare for electrotransfer of proteins from the gel to nitrocellulose membrane.

WESTERN BLOTTING AND IMMUNODETECTION

Reagents

1. Transfer Buffer
    a. 0.025M Tris-HCl pH 8.3 12.14g
    b. 0.15M Glycine 45.05g
    c. 20% Methanol 800ml
    d. make up to 4L with ddH_20
    e. store at 4°C
2. Ponceau S stain
    a. 0.1% (w/v) Ponceau S
    b. 0.5% (v/v) Acetic Acid
    c. Store at room temperature
3. Wash Buffer
    a. Tris-HCl pH 7.5 12g
    b. NaCl 58.5g
    c. 0.1% Tween 10ml
    d. Store at room temperature
4. Blocking Solution
    a. 5% (w/v) skim milk power in wash buffer OR
    b. 5% (w/v) BSA in wash buffer
5. Enhanced Chemiluminescence Fluid (ECL; Santa Cruz sc-2048)
6. Film/Developer/Fixer

Procedure

1. Transfer Procedure

a. Remove electrophoresis plates from chamber and separate the plates.
b. Cut away unnecessary parts of the gel using a spatula and measure remaining gel size.
c. Using a paper cutter cut 6 pieces of Whatman paper per gel to the same size as the gel. Wearing gloves cut nitrocellulose membrane (GE Healthcare RPN303D) to the dimensions of the gel.
d. Assemble Whatman paper, nitrocellulose memebrane and gel as shown below:

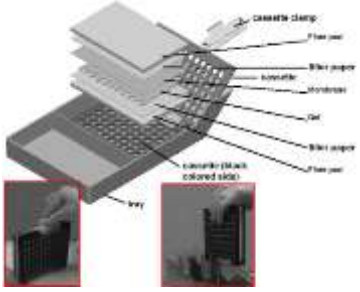

e. Close the cassette and place in the transfer chamber with the black side of the cassette facing the back side of the chamber.
f. Place ice pack in the chamber.
g. Place lid on the chamber and connect the leads to the power supply.

h. Turn on the power supply and run at 120V for 2 hours. This can vary depending on the size of the protein of interest.

2. Removal of transfer membrane:

a. Turn off the power supply and disconnect leads from the power supply then remove the lid from the chamber.
b. Remove the cassette from the chamber.
c. With gloves on, remove the Whatman paper and gel and place the nitrocellulose membrane in a plastic dish.
d. Add Ponceau S stain on the membrane and gently swirl.
e. Drain off the remaining Ponceau S and save for reuse.
f. Rinse the membrane with ddH_20 to reduce the red background. Wrap membrane in saran wrap and scan image.
g. Cut the membrane while protein bands are still visible at the desired molecular weight.
h. Rotate membrane at room temperature in wash buffer until remaining Ponceau S has been removed.
i. Incubate membrane for 1 hour with rotation in blocking solution.
j. Incubate membrane with desired antibody diluted in blocking solution overnight at 4ºC. Membrane is placed face down into the solution on a glass plate covered in parafilm. To maintain a moist environment overnight, wet a small kimwipe and form it into a ball and place in each corner of the dish. Cover the dish with saran wrap.

3. Immunodetection

a. Wash the blots in wash buffer with gentle rotation for 5 minutes 3X.
b. Incubate the blots for 1-2 hours with the appropriate secondary antibody diluted in blocking solution.
c. Membrane is placed face down in solution on a glass plate covered with parafilm. Place moist kimwipes in each corner of the dish and cover the dish with saran wrap.
d. Following the incubation, wash the membrane 3X for 5 minutes with wash buffer.

4. Enhanced Chemiluminescence Detection

a. Mix ECl fluids "A" and "B" in a 1:1 ratio in a disposable Rohr tube.
b. Place blots on saran wrap face up and apply ECL solution for 2 minutes.
c. Dab off excess ECL on a kimwipe and place blots face down on a fresh piece of saran wrap and wrap tightly.
d. Expose blot to film (time will vary depending on protein and antibody).
e. Place film into developer (time will vary).
f. Once image appears place film into fixer for 2 minutes. Wash with fresh water when complete.

APPENDIX D – OTHER CONTRIBUTIONS TO LITERATURE

Published refereed contributions

1. Erlich AT, Tryon LD, Crilly MJ, Memme JM, **Mesbah Moosavi ZS**, Oliveira AN, Beyfuss K, Hood DA. Function of specialized regulatory proteins and signaling pathways in exercise-induced muscle mitochondrial biogenesis. *Integr Med Res* 5: 187-197, 2016.

Published Abstracts

1. **Moosavi Z** and Hood DA. Modulation of the UPR in relation to mitochondrial biogenesis adaptations in muscle cells. *Proc Muscle Health Awareness Day*. p. 26, 2016.

Oral Presentations

1. **Mesbah Moosavi ZS** and Hood DA. Modulation of the UPR in relation to mitochondrial biogenesis adaptations in muscle cells. KAHS Graduate Student seminar, York University, Toronto, ON. March 11, 2016.